GEOLOGICAL SURVEY OF CANADA

OPEN FILE 4085

Focal mechanisms for eastern canadian earthquakes of 1999

Allison L. Bent, Janet Drysdale

2001

Natural Resources Canada Ressources naturelles Canada

Canada

Geological Survey of Canada
601 Booth St.
Ottawa, ON, Canada, K1A 0E8
Price subject to change without notice

ABSTRACT

Although earthquake focal mechanism solutions provide information about the faults on which the earthquakes occur and on local stress field orientations and seismotectonics, they were not routinely determined in the past. We have begun to systematically attempt to determine focal mechanisms for all eastern Canadian earthquakes of magnitude 4.0 or greater and intend to publish the results annually in an Open File. This report covers the year 1999. We analyzed nine earthquakes. Two did not strictly meet our selection criteria but are included because they are of interest. We were able to determine focal mechanisms for six of the events. As has been the case in previous efforts, those events for which we could not obtain solutions were in offshore or northern regions where seismograph coverage is sparse.

RÉSUMÉ

Les mécanismes au foyer des tremblements de terre nous fournissent de l'information sur les failles sur lesquelles les tremblements de terre se produisent, et sur l'orientation des contraintes régionales et séismotectoniques mais auparavant on ne les déterminait pas régulièrement dans l'est du Canada. Nous avons commencé à essayer systématiquement de déterminer les mécanismes au foyer pour tous les tremblements de terre de magnitude 4,0 ou plus dans l'est du Canada. On a l'intention de publier les résultats tous les ans. Ce rapport-ci traite l'année 1999. On a analysé neuf tremblements de terre dont deux n'ont pas satisfait parfaitement nos critères mais ont attiré notre attention. On a obtenu des solutions pour six de ces tremblement de terre. Comme c'était le cas dans nos études précédents, les séismes pour lesquels on n'a pas pu obtenir des solutions se sont produits dans le nord ou des régions côtières où la couverture du réseau séismographique n'est pas suffisante.

INTRODUCTION

Earthquake focal mechanism solutions provide information about the faults on which the earthquakes occur and on local stress field orientations. If focal mechanisms can be determined for many earthquakes in a given region then we also gain insight into regional seismotectonic precesses and stress fields. In eastern Canada earthquake focal mechanisms were not routinely determined in the past, although solutions may exist for individual earthquakes that were of particular interest as well as for some time periods or regions that have been systematically studied. We have begun to routinely analyze first motion data for all eastern Canadian (roughly defined as east of 110° W) earthquakes of magnitude 4.0 or greater in an effort to determine their focal mechanisms. The data will be tabulated and mechanisms summarized annually in Geological Survey of Canada (GSC) Open Files. The years 1994 to 1998 have been completed (Bent and Perry, 1999, 2000; Bent and Drysdale, 2000). The current report covers the year 1999. Seven events met our selection criteria. We also examined two other earthquakes that were of interest although they did not strictly satisfy the criteria: one that was slightly smaller (magnitude 3.8) than our minimum magnitude but that was felt in the Toronto area and one that was just outside our area of interest (magnitude 5.7 in the western Arctic islands). Of the nine events studied we were able to determine focal mechanisms for six.

Figure Captions:

Figure 1. Map of southeastern Canadian events studied. Symbol size is scaled to magnitude. Magnitude range 3.8-5.1.

Figure 2. Map of northeastern Canadian events studied. Symbol size is scaled to magnitude. Magnitude range 4.0-5.7.

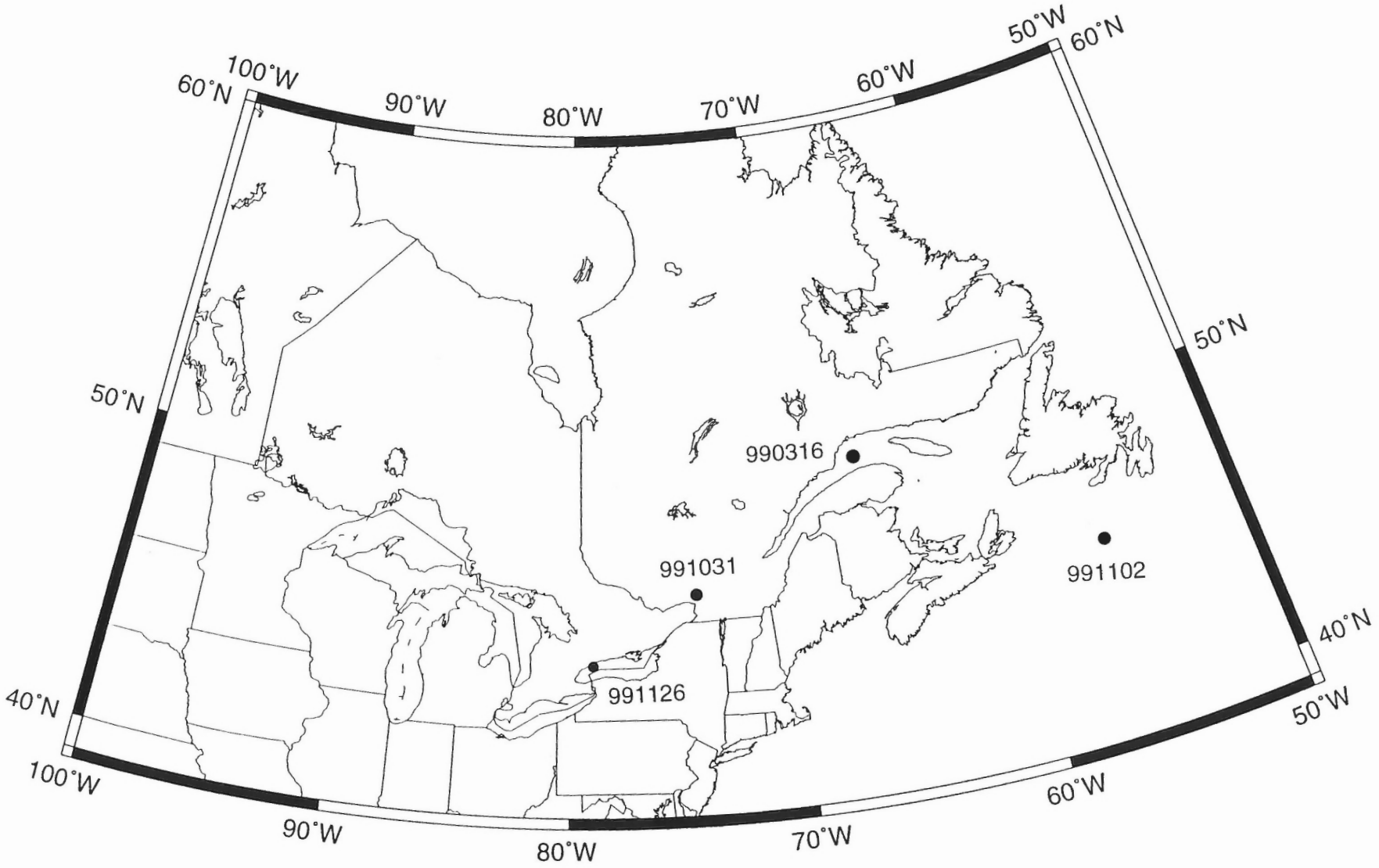
100°W
90°W
80°W
70°W
60°W
50°W
60°N
50°N
40°N
990316
991031
991102
991126

Figure 1

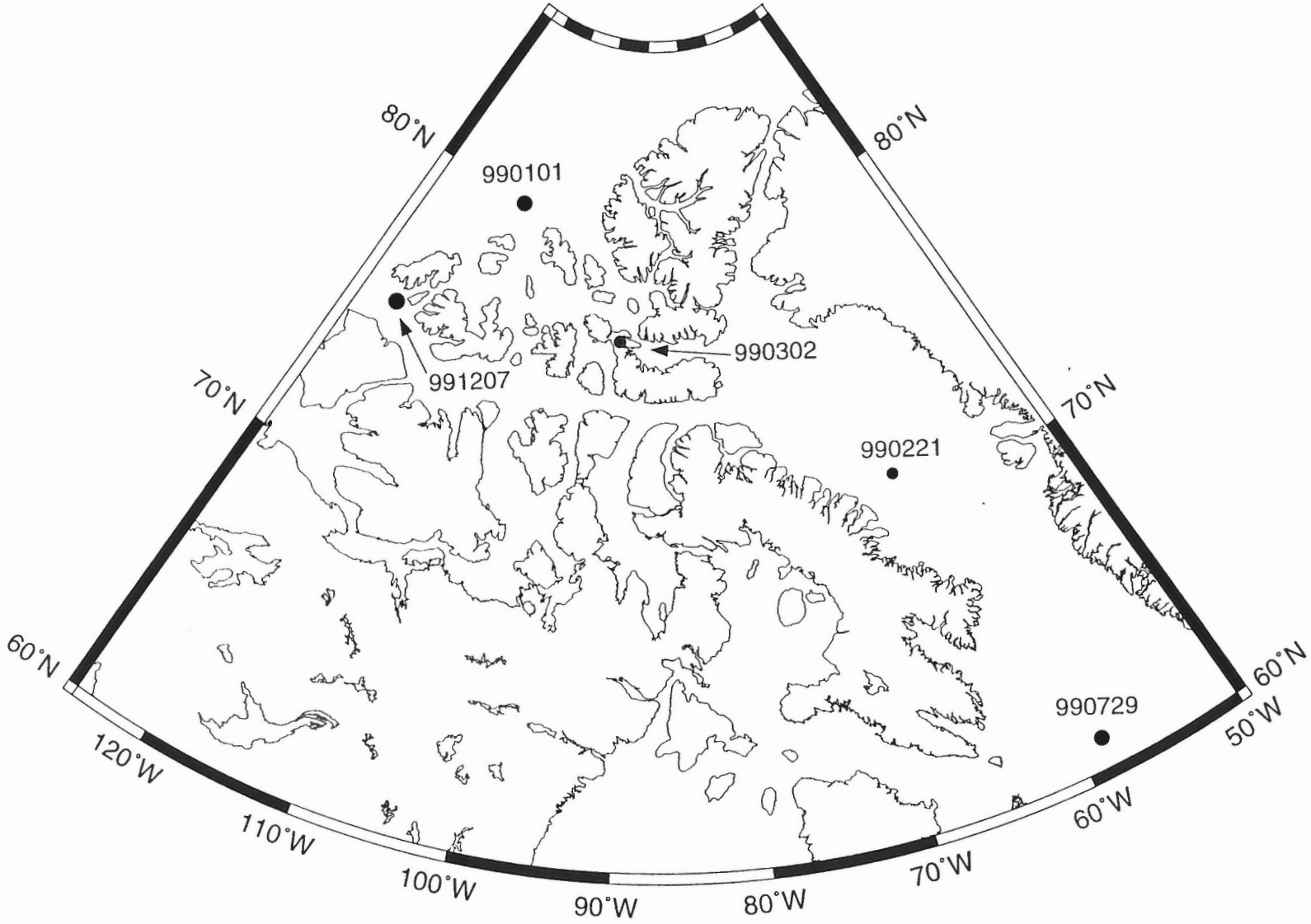
80°N
80°N
990101
991207
990302
70°N
70°N
990221
60°N
60°N
990729
120°W
110°W
100°W
90°W
80°W
70°W
60°W
50°W

Figure 2

METHOD

The focal mechanisms were determined primarily from P wave first motions. We usually only attempted to read S polarities if the P data did not provide a well-constrained solution. We looked at the vertical component of all digital seismograms of the Canadian National Seismogram Network or CNSN received in Ottawa either by continuous transmission or dial-up request. Rotated horizontal data were used as much as possible for S polarities. Note that data from some western Canadian stations, particularly from the dense array on Vancouver Island, were not routinely archived in Ottawa. However, data from enough stations in British Columbia are routinely received that we can determine whether data from the additional stations are likely to be useful, in which case the waveform data can be requested.

We also include any first motion data contained in the Canadian Earthquake Epicenter File (CEEF) database for which the seismograms were not archived. Generally these polarities were supplied by operators of regional, usually U. S., networks or single stations within a few hundred kilometers of the epicenter. In the discussions of individual earthquakes, we note any polarities not determined directly by the authors.

We attempted to obtain non-CNSN seismograms or polarity data if they were likely to better constrain the solution, but did not routinely request external data for southern Canadian events except for earthquakes in southern Ontario. For the southern Ontario events, we tried to obtain data from the Southern Ontario Network (SONT) operated by the University of Western Ontario. Data from these stations improved the azimuthal coverage and provided more data at short distances.

For events from Baffin Bay to Ellesmere Island, we routinely requested data from two stations operated by the Incorporated Research Institutions for Seismology (IRIS) : Alert (ALE) on Ellesmere Island and Sondre Stromfjord (SFJ) on Greenland. Data from SFJ were also routinely requested for earthquakes in the Labrador Sea. For events in the western Arctic or the Boothia-Ungava seismic zone, we requested data from the IRIS station at Flin Flon, Manitoba (FFC). For earthquakes occurring offshore along the southeastern margin, we consulted analog seismograms from stations in Halifax (HAL) and Guysborough, Nova Scotia (GBN) and St. John's, Newfoundland (STJN), all three of which are archived in Ottawa.

Most of the earthquakes we studied were relatively small (magnitude less than 5.0). Therefore we did not routinely attempt to acquire teleseismic data although it was obtained for some events. For readers not familiar with station locations or codes, a map of all seismograph stations operating in Canada, including those that are not part of the CNSN, may be found on the internet. The current address is

http://www.seismo.nrcan.gc.ca/cnsn/stn_map.e.html.

As much as possible we read the polarities from unfiltered data. However, given that the

earthquakes studied were generally small, it was occasionally necessary to filter some seismograms, particularly those from more distant broadband stations. Because high frequencies are attenuated more than low frequencies, there is always some danger that a first motion read from filtered data will not be the true first motion. By restricting the filtering of the broadband data to the frequency range of the short-period instruments, we should not adversely affect the data any more than a short-period instrument response would do. Unless stated otherwise, all filters were two-pole, single-pass Butterworth filters. Any filtering is noted on the seismogram traces where "hp" is used to designate a highpass filter, "lp" a lowpass filter and "bp" a bandpass filter. Corner frequencies are also noted. All filtering of data was performed using the Seismic Analysis Code (SAC) routines (Tapley and Tull, 1991), which were also used to rotate horizontal records into their radial and tangential components.

There was also some concern, particularly for broadband seismograms, that the first motions could be affected by the FIR filters applied to the data. In any case where it was suspected that what appeared to be the first motion was actually a FIR filter artifact, the data were run through a program to deconvolve the FIR filter (Scherbaum and Bouin, 1997). A small apparent first motion followed by a significantly larger arrival of opposite polarity was the principal reason for de-FIR-ring the data. In the end, we found that these small first motions did not appear to be filter related.

As far as we have been able to ascertain polarities for CNSN instruments were correct during 1999. Instrument polarities are checked approximately once a year using large teleseismic events with known focal mechanisms. Polarities for stations of the Southern Ontario Network were confirmed by staff of the University of Western Ontario, who operate the network.

The first motions were read independently by the two authors. In case of disagreement, the seismograms in question were re-evaluated. If we could not reach a consensus, data from that particular station were not used to determine the focal mechanism.

To determine the focal mechanism, the grid search algorithm of Snoke *et al.* (1984) was employed. The search is based on the orientation of the B axis. Normal procedure was to initially search the focal sphere at 5° intervals. If no solutions were found to satisfy all the data, the search increment was gradually decreased. If with a 1° search no solutions were found, we returned to the 5° search, but allowed 1 polarity error. The procedure of alternately decreasing the search interval and increasing the number of allowed polarity misfits was repeated until at least one solution was found. If the initial 5° no error search resulted in a large number of solutions or if there were large differences among the solutions, we attempted to find more polarity data by reading S wave polarities and/or looking for data from additional seismograph stations. For many of the offshore and northern events, the solutions could not always be further constrained.

The inversion procedure normally ignores emergent polarities. If the inversion resulted in a large number of potential solutions or a small number of very different solutions, we reran the program using a weighting scheme by which emergent stations were treated

as impulsive and each impulsive arrival was entered twice, effectively half-weighting the emergent phases. Focal mechanisms resulting from the weighted inversion were assumed to be more probable solutions than those which satisfied the impulsive data only.

Earthquake epicenters were taken from the CEEF. With a few exceptions, depths for eastern Canadian earthquakes are fixed, usually at 18 km (roughly the midpoint of the crust). Only one of the events selected (991126 in southern Ontario) had a calculated depth in the database. Bent and Perry (2000) determined the depths of two additional earthquakes as part of a study of earthquake depths. Since take-off angle is depth dependent, using an assumed depth may influence on the focal mechanism to some degree. Having said that, in most cases the effect will be minimal. As long as the hypocenter is within the crust, the take-off angle for Pn and teleseismic P will not be greatly influenced by the depth. At closer distances, the depth will have a greater effect on take-off angle and can also affect the Pg-Pn cross-over distance. However, the close stations are usually few in number, except in the Charlevoix region, where the depths are usually reliably calculated and not fixed. In any case, it is possible to determine how dependent the solution is on these stations by running the inversion using take-off angles appropriate for different depths.

FOCAL MECHANISMS

The epicenters for events included in this study are shown in Figures 1 (southeastern Canada) and 2 (northeastern Canada) where they are identified by date of occurrence. In the tables that follow for each earthquake, we include a list of polarities used to determine the fault plane solution(s). C's and D's indicate compressional and dilatational P polarities respectively. If the P polarity is emergent, a + indicates compression and a - indicates dilatation. SV waves are indicated by an F for motion toward the station or a B for motion toward the source. For SH waves, a < indicates counterclockwise motion (or to the left if one is facing the station with one's back to the source) and > indicates clockwise motion. Emergent S waves were not used as their polarities are difficult to pick with confidence. We also include portions of all seismograms from which we picked the first motions as well as focal mechanism solutions plotted in terms of both stress axes and P nodal planes. Unless it is explicitly stated that data from a particular station could not be obtained (based on the station selection criteria discussed in the previous section), it should be assumed that the authors evaluated the data but could not determine the first motion.

In the seismogram figures that follow, the velocity records are shown. In an effort to be consistent, we have plotted a constant time window (4 sec) for each seismogram shown. This window is normally adequate to clearly illustrate the preceding noise and first motion, but we note that there may be occasions where showing a longer time segment or the displacement record might have provided stronger evidence for our choice of first motion.

All azimuths and strikes are measured in degrees clockwise from north. Take-off or incidence angles are measured from the vertical. Dip angles are measured from the horizontal. Rake is also known as slip angle. A rake of 0° implies pure left lateral strike-slip motion, 90° pure thrust motion, 180° pure right lateral strike-slip motion, and -90° (or 270°) pure normal faulting. Seismic source zones are as defined by Basham *et al.* (1982)

Quality rankings of A, B, C or D are assigned to each preferred focal mechanism. The quality should be taken not as an indication of how well the solution fits the data but rather as a comment on the quality and quantity of the data used to determine the solution. Azimuthal distribution, redundancy of coverage, number of misfits and total number of observations are the principal criteria considered. The availability of S polarity data can help compensate for poor azimuthal coverage as the S and P radiation patterns are different.

The Northwest Territories were partitioned to become two territories - Nunavut and the Northwest Territories - on 1 April 1999. For simplification, we use the new names for the entire calendar year.

1 JANUARY 1999: ARCTIC OCEAN

Seismic Zone: outside zones defined in 1982
Latitude: 79.79° N
Longitude: 110.24° W
Depth: 18 km (fixed)
Magnitude: 5.3 (m_b)
Origin Time: 09:28:11 (UT)
Comments:

Polarity Data

Station	Distance (km)	Azimuth (°)	Take-off Angle (°)	First Motion
RES	680	138.7	49.1	+
ALE	847	47.2	49.1	D
IGL	1407	129.6	49.1	D
INK	1446	220.8	49.1	+
YKW3	1931	186.8	49.6	D
DAWY	1973	244.6	43.8	C
FRB	2208	119.4	42.8	+
WHY	2287	215.8	40.5	C
HYT	2297	219.3	38.9	C
FCC	2413	156.9	38.7	C
DLBC	2476	208.0	35.0	C
KUQ	2807	123.9	34.5	D
EDM	2964	183.9	30.8	C
LLLB	3283	195.1	30.0	C
ULM	3344	161.5	32.7	C
SOLO	3399	156.7	32.6	C
PNT	3416	192	29.7	+
WALA	3426	184.7	29.7	+

Station	Distance (km)	Azimuth (°)	Take-off Angle (°)	First Motion
PGC	3509	196.8	29.6	C
TBO	3570	153.7	32.4	C
EEO	3901	141.7	31.8	-
LMQ	3915	131.2	28.9	-
CRLO	3988	139.8	31.5	C
SADO	4105	142.2	31.2	+

Focal Mechanism Solutions

Strike	Dip	Rake
101.65	42.06	31.11
107.73	44.81	35.53
107.75	42.06	31.11
113.83	44.81	35.53
119.93	44.81	35.53
125.42	47.85	39.32
131.52	47.85	39.32
76.63	42.27	17.14
83.53	43.96	22.18
89.96	46.03	26.73
90.07	43.96	22.18
96.5	46.03	26.73
102.48	48.44	30.79
109.02	48.44	30.79
84.58	50.14	22.91
90.41	52.24	26.57

Strike	Dip	Rake
85.47	48.36	18.88
91.64	22.91	50.14
97.47	52.24	26.57

total number solutions: 19
grid search: 5°
misfits: 0
comments:

Preferred solution: take solution from above list that fits highest number of emergent stations using weighting scheme discussed previously; solution below fits all except FRB and EEO

Plane 1:
- Strike: 85°
- Dip: 48°
- Rake: 19°

Plane 2:
- Strike: 343°
- Dip: 76°
- Rake: 137°

P-axis:
- Trend: 40°
- Plunge: 17°

T-axis:
- Trend: 295°
- Plunge: 40°

B-axis:
- Trend: 148°
- Plunge: 45°

Quality: B; poor azimuthal coverage but large number of observations and high degree of redundancy at azimuths covered

Figure Captions:

Figure 3a-f. Seismograms from which polarity data were read by the authors.

Figure 4. Focal mechanism solutions. Lower hemisphere projection. The P and T axes are shown on the left and the P nodal planes on the right. Data are also plotted. Solid symbols indicate compressional first motions and open symbols dilatations.

Arctic Ocean: 1 January 1999

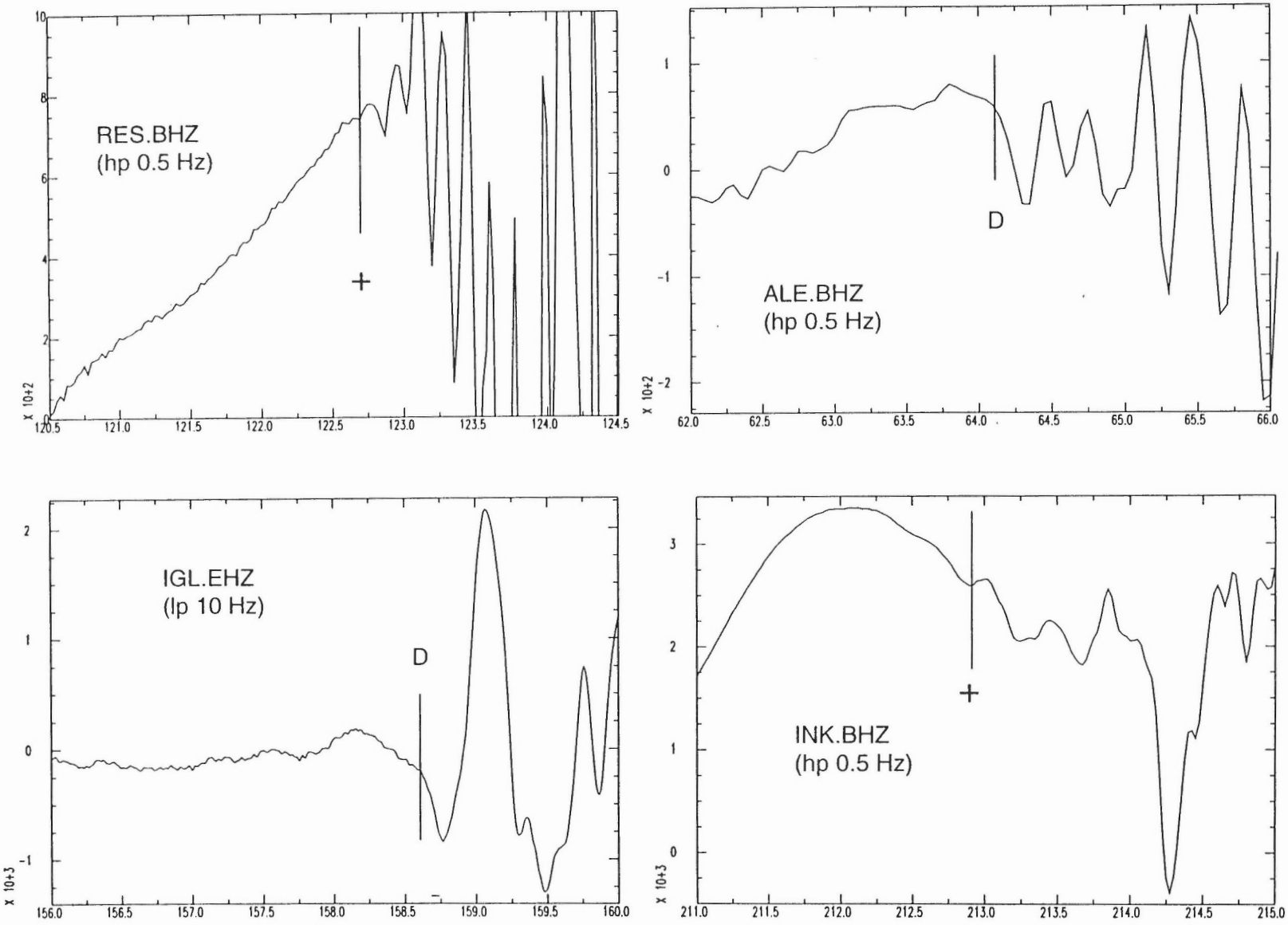

Figure 3a

Arctic Ocean: 1 January 1999

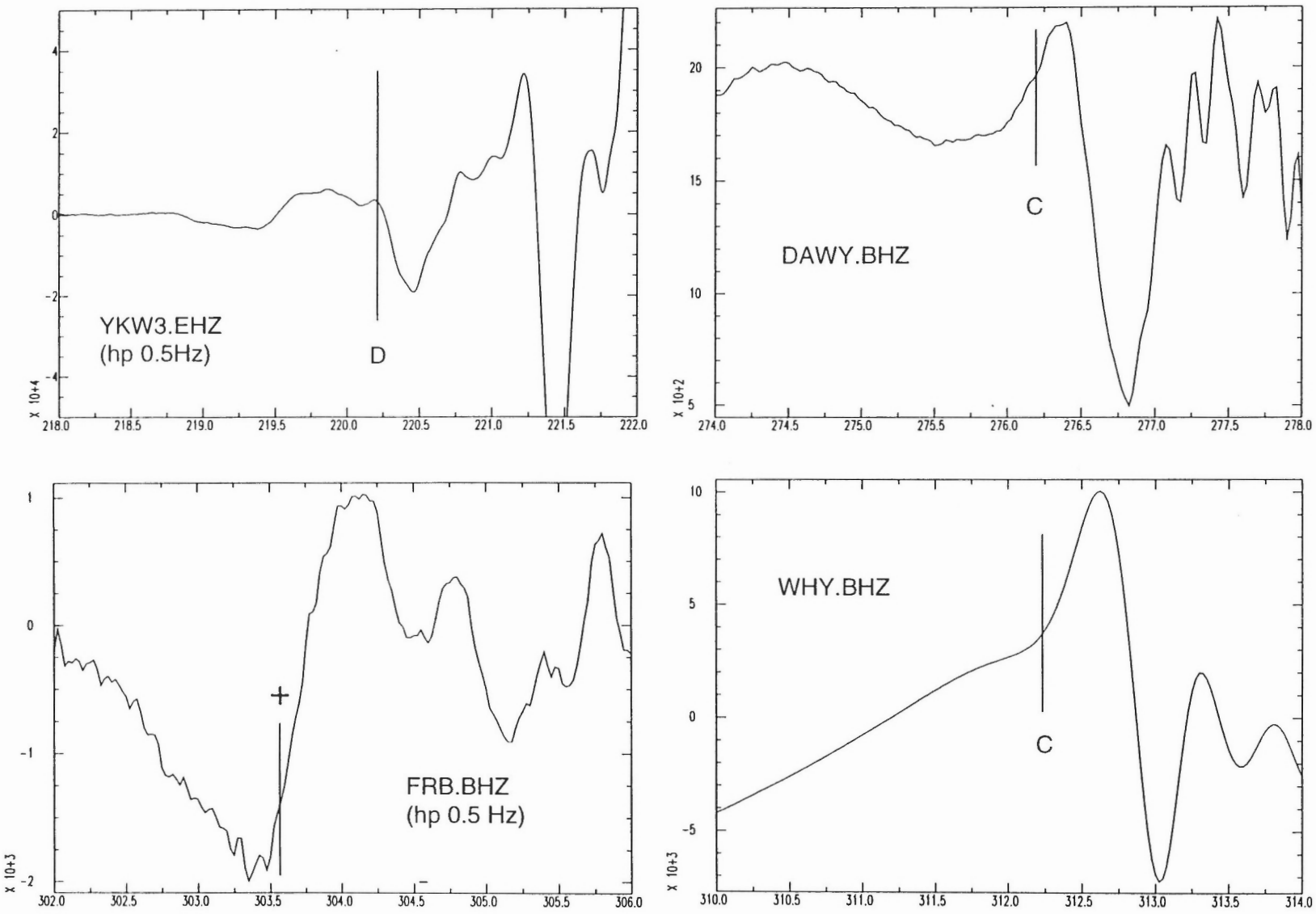

Figure 3b

Arctic Ocean: 1 January 1999

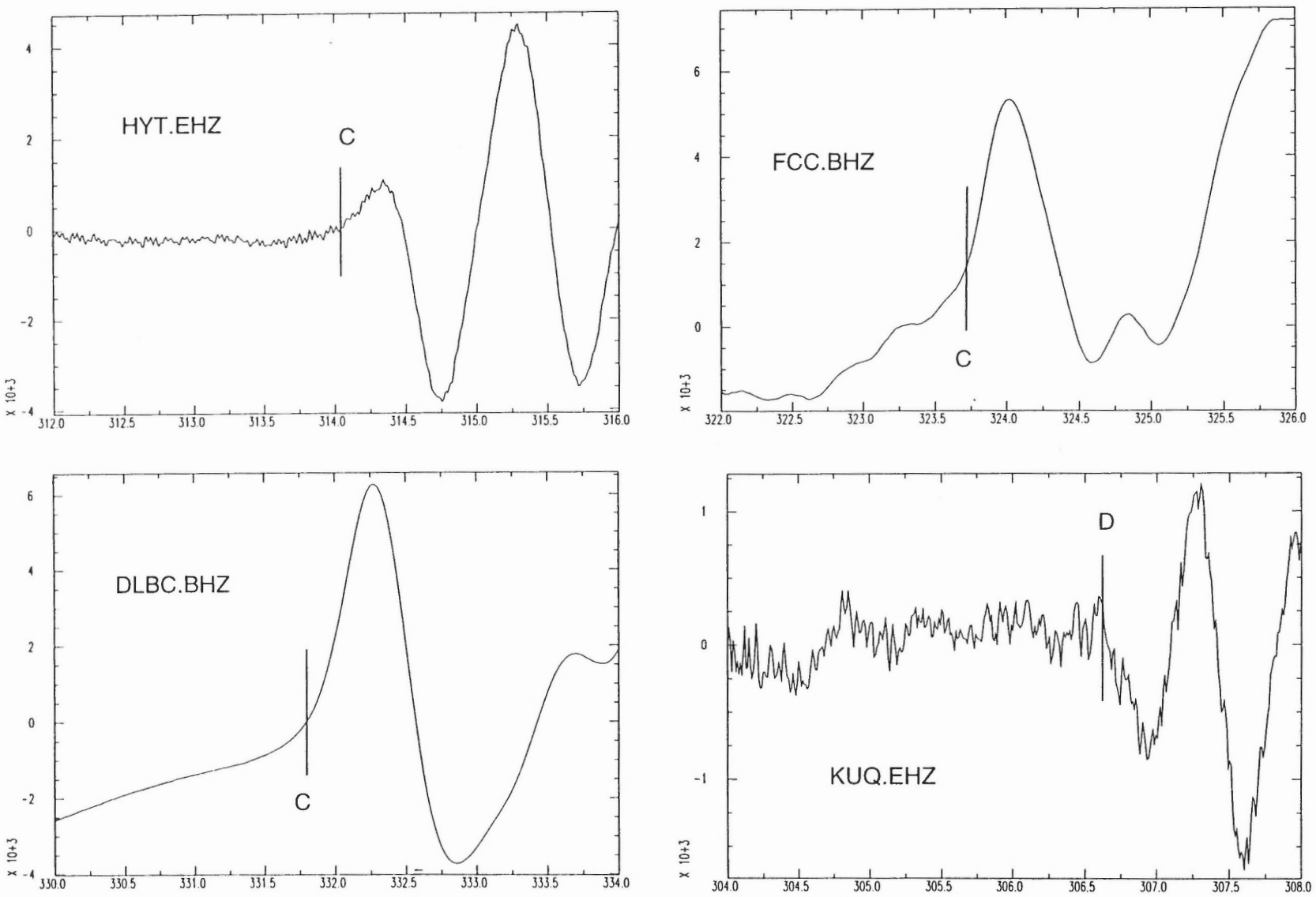

Figure 3c

Arctic Ocean: 1 January 1999

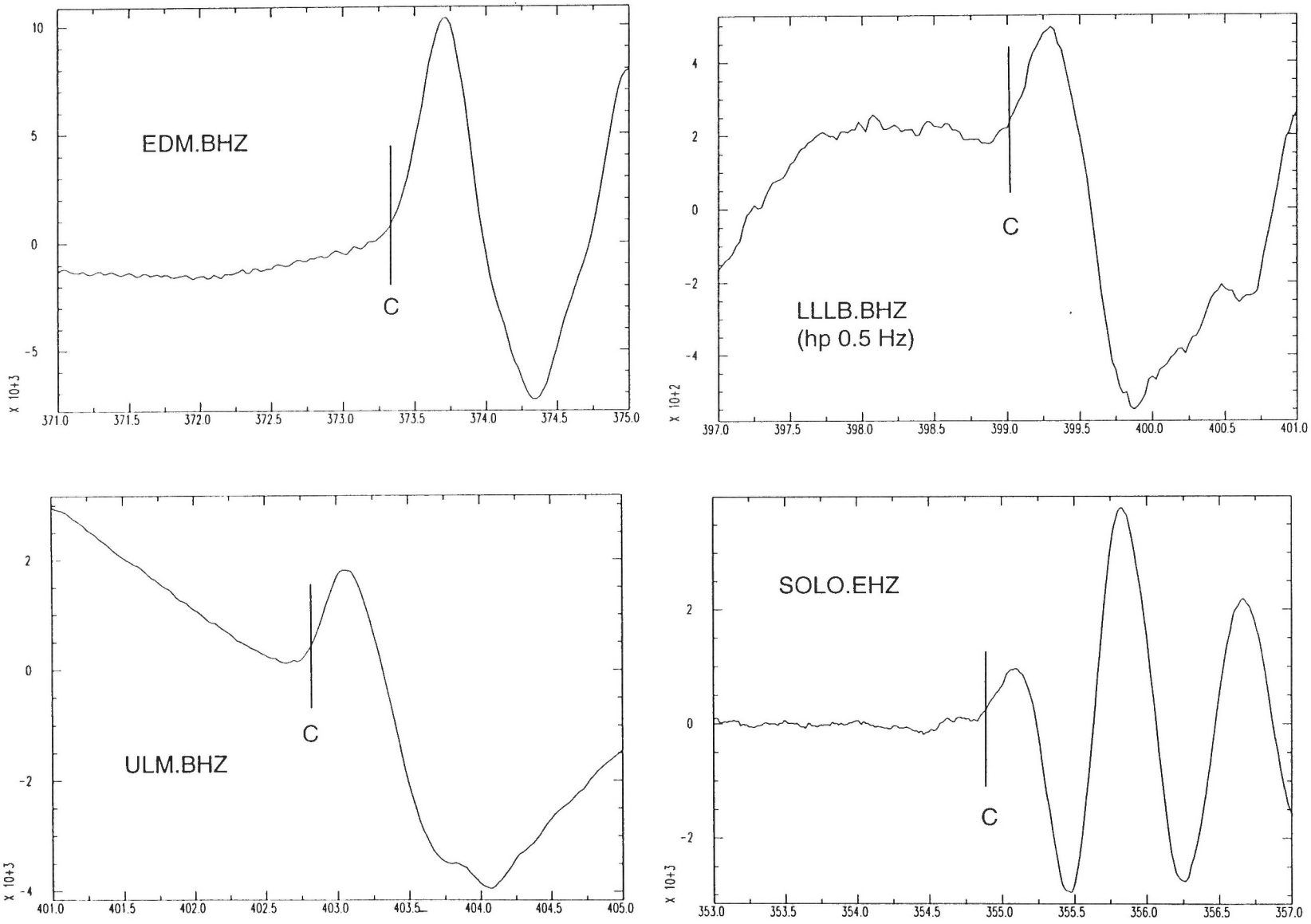

Figure 3d

Arctic Ocean: 1 January 1999

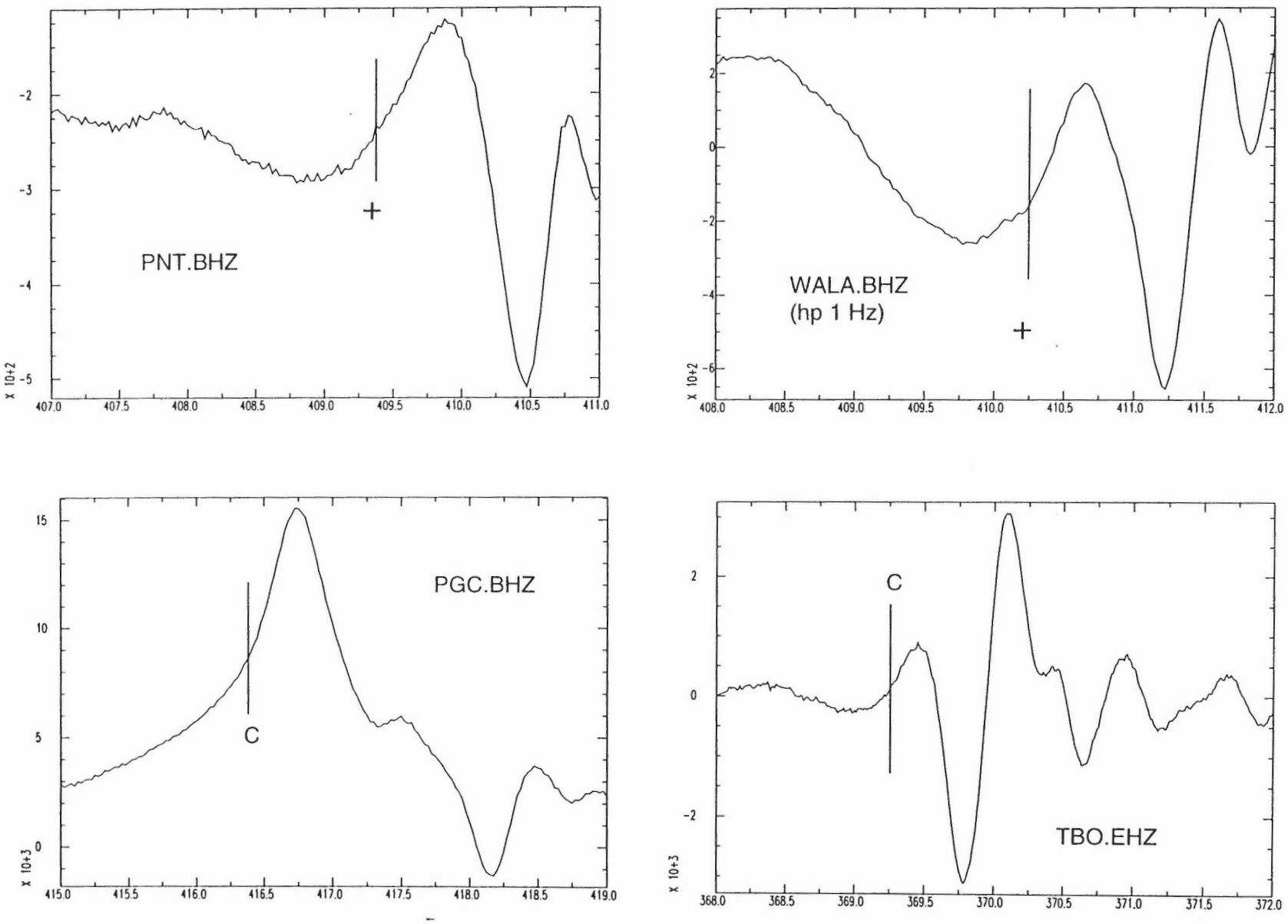

Figure 3e

Arctic Ocean: 1 January 1999

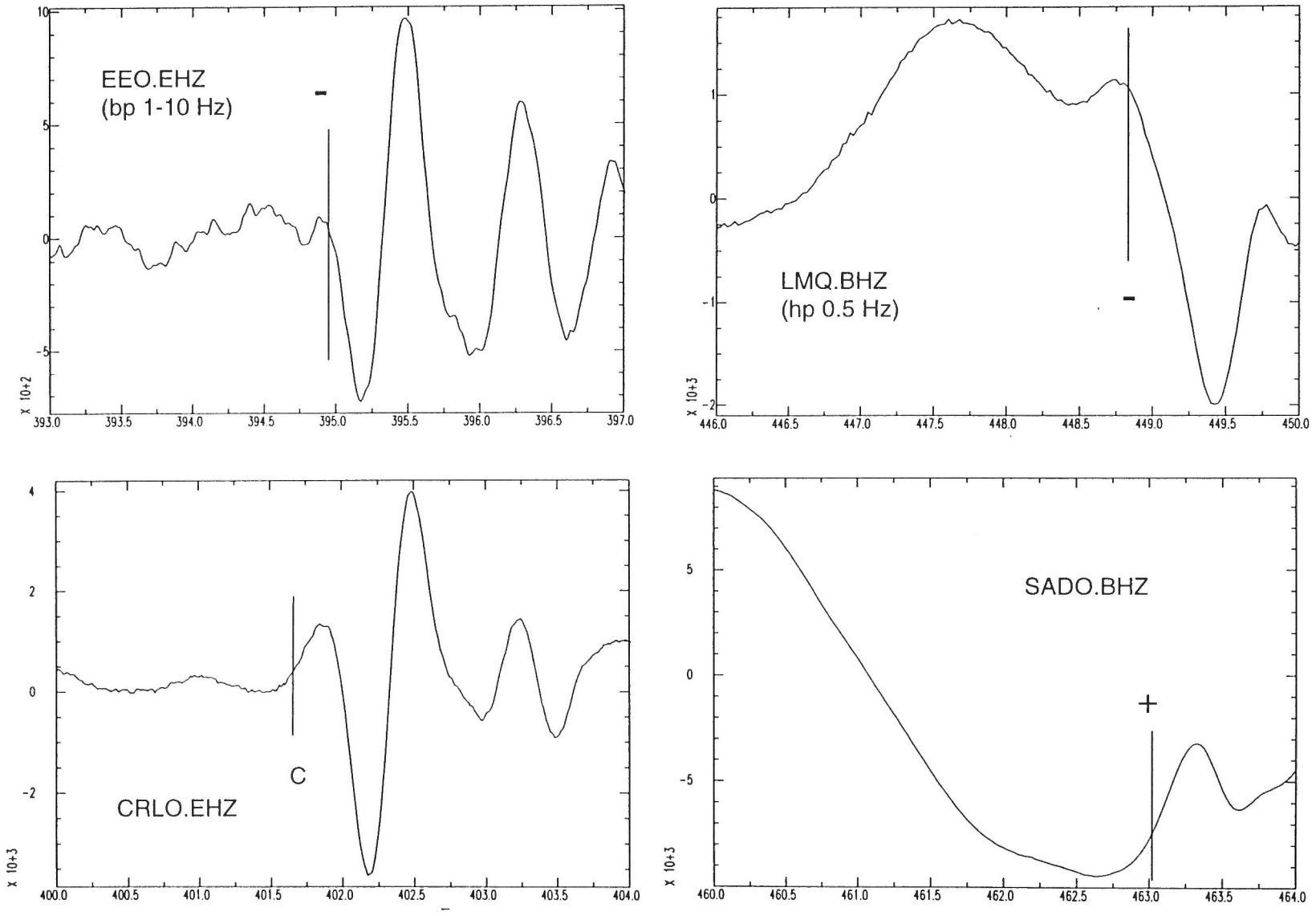

Figure 3f

Arctic Ocean: 1 January 1999

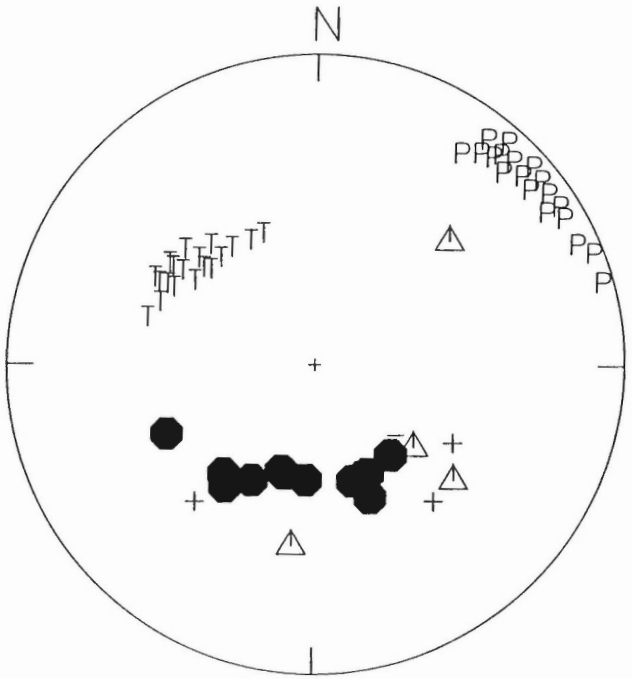

P and T axes

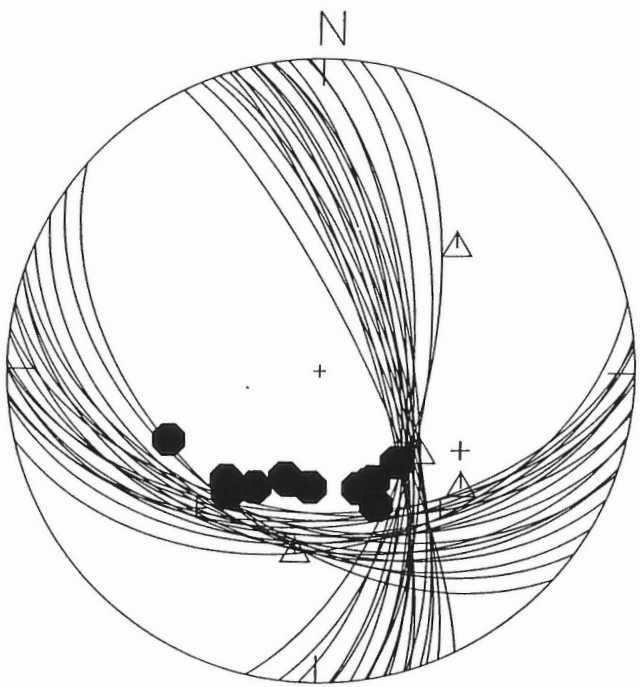

P nodal planes

Figure 4

21 FEBRUARY 1999: BAFFIN BAY

Seismic Zone: Baffin Bay
Latitude: 70.92° N
Longitude: 64.46° W
Depth: 18 km (fixed)
Magnitude: 4.1 (M_L)
Origin Time: 17:34:11 (UT)
Comments:

Polarity Data

Station	Distance (km)	Azimuth (°)	Take-off Angle (°)	First Motion
IGL	679	263.6	49.1	-
FRB	820	194.4	49.1	D
RES	1077	306.8	49.1	-
ALE	1294	1.4	49.1	+
SCHQ	1800	185.0	51.6	+
YKW3	2319	271.8	40.5	+

Focal Mechanism Solutions

total number solutions: 565
grid search: 5°
misfits: 1
comments: solutions based on weighted data; solutions misfit one of YKW3, RES, SCHQ or ALE (listed in decreasing order of number of solutions that misfit station)

Preferred solution: insufficient data to determine

Fault Plane:
Strike: undetermined
Dip: undetermined
Rake: undetermined

P-axis:		
	Trend:	most solution SW-NW auadrant but others possible; not in S-SW octant
	Plunge:	undetermined
T-axis:		
	Trend:	NW-SSE; not in S-NW range
	Plunge:	undetermined
B-axis:		
	Trend:	undetermined
	Plunge:	undetermined

Figure Captions:

Figure 5a-b. Seismograms from which polarity data were read by the authors.

Figure 6. Focal mechanism solutions. Lower hemisphere projection. The P axes are on the left, T axes on the right and B axes below. Data are also plotted. Solid symbols indicate compressional first motions and open symbols dilatations. Solutions based on weighted data.

Baffin Bay: 21 February 1999

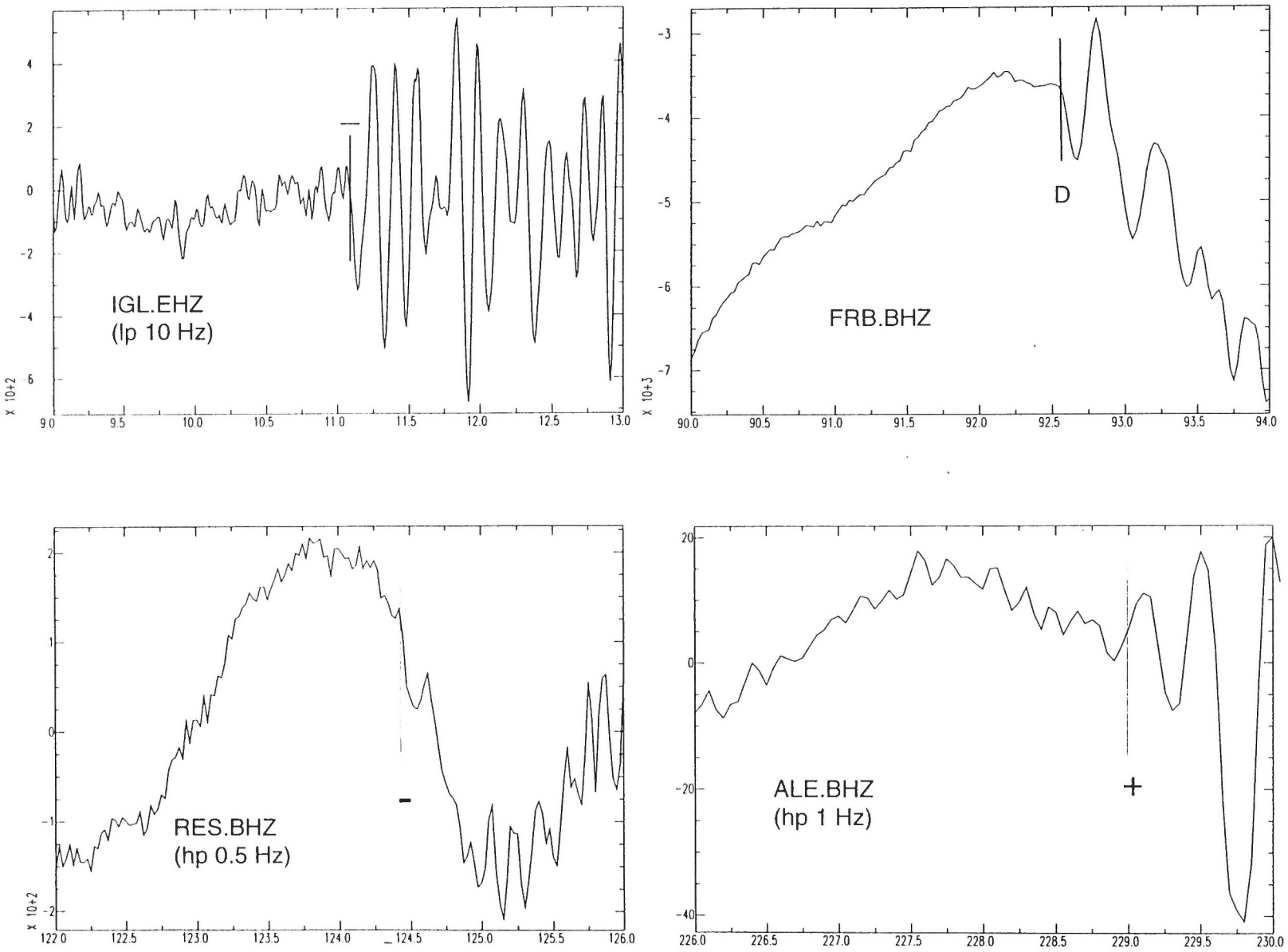

Figure 5a

Baffin Bay: 21 February 1999

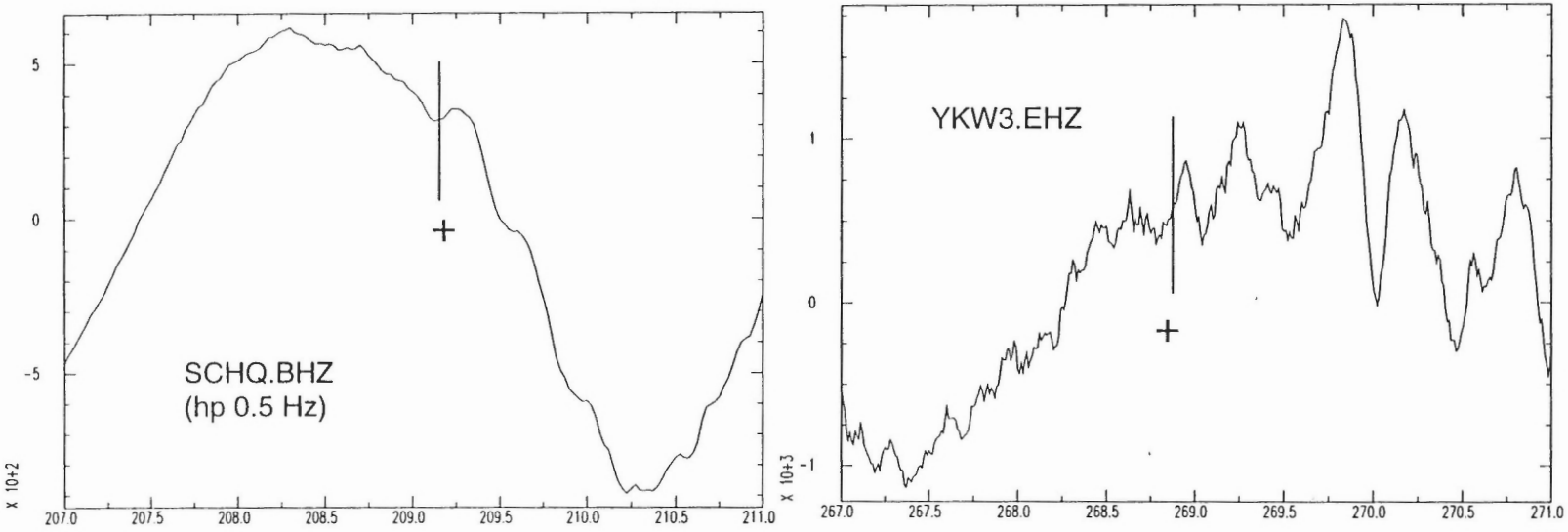

Figure 5b

Baffin Bay: 21 February 1999

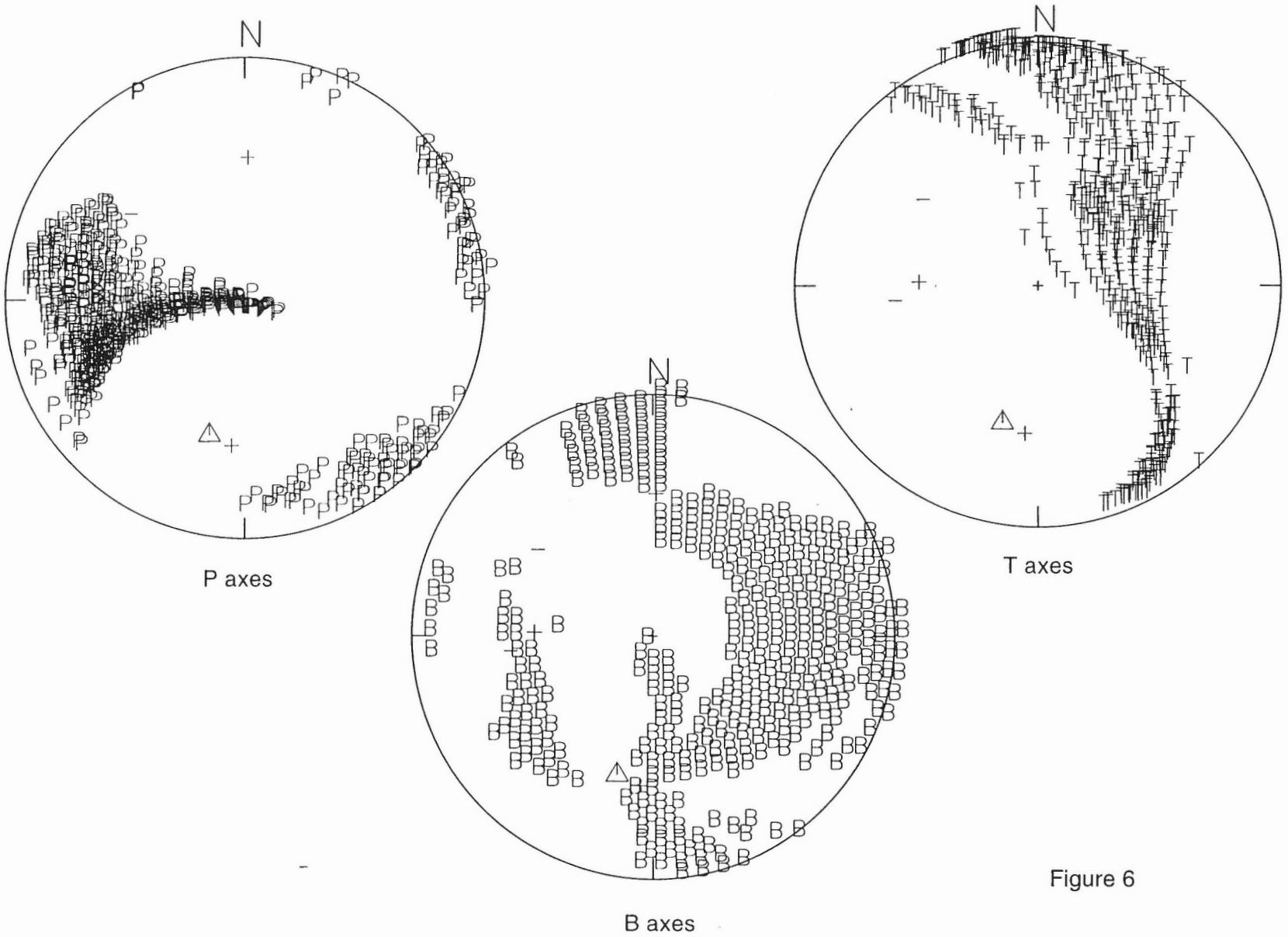

Figure 6

2 MARCH 1999: DEVON ISLAND, NUNAVUT

Seismic Zone: Eastern Arctic Background
Latitude: 76.32° N
Longitude: 91.96° W
Depth: 18 km (fixed)
Magnitude: 4.0 (m_N)
Origin Time: 07:11:13 (UT)
Comments:

Polarity Data

Station	Distance (km)	Azimuth (°)	Take-off Angle (°)	First Motion
RES	201	205.7	49.1	D
IGL	843	151.8	49.1	D
INK	1620	258.7	49.1	-
FRB	1640	136.0	49.1	+
SFJ	1731	104.1	49.1	+
YKW3	1750	221.0	49.1	D

Focal Mechanism Solutions

total number solutions: 7477 impulsive only; 1021 using weighting scheme
grid search: 5°
misfits: 0
comments: ALE unavailable

Preferred solution: insufficient data to determine; comments based on solutions from weighted data

Nodal Planes: cannot be determined

P-axis: majority of solutions in SW quadrant; some solutions in NW quadrant and SSE octant

T-axis: majority of solutions in NE quadrant; some near-horizontal solutions in ESE and NNW octants

B-axis:	not near-vertical; not near-horizontal if at NE-SE or SSW-W azimuths; almost any other orientation is possible

Figure Captions:

Figure 7a-b. Seismograms from which polarity data were read by the authors.

Figure 8. Focal mechanism solutions. Lower hemisphere projection. The P axes are shown on the left and the T axes on the right. Data are also plotted (lower). Solid symbols indicate compressional first motions and open symbols dilatations. Solutions shown are based on weighted data.

DEVON ISLAND, NUNAVUT: 2 MARCH 1999

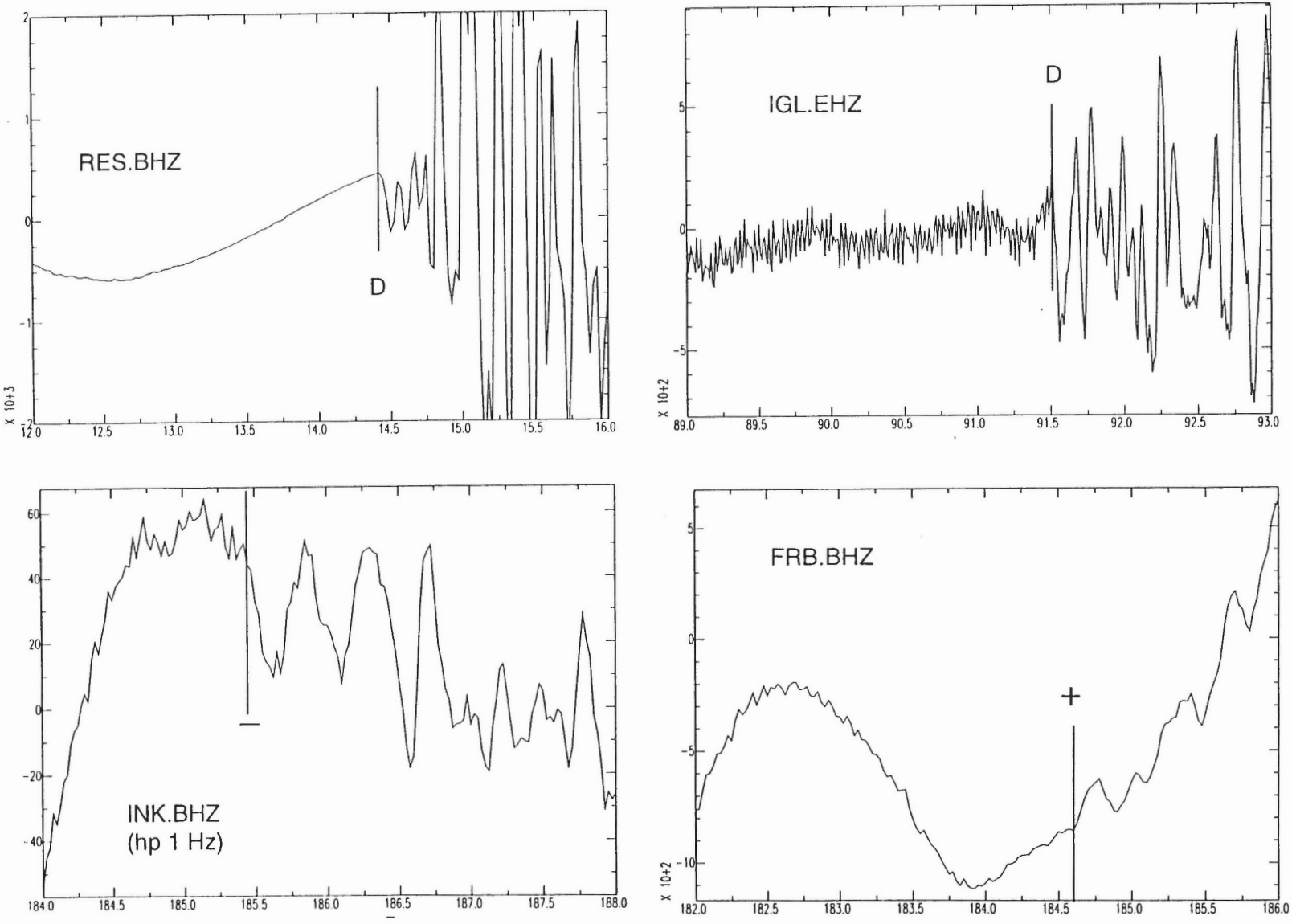

Figure 7a

DEVON ISLAND, NUNAVUT: 2 MARCH 1999

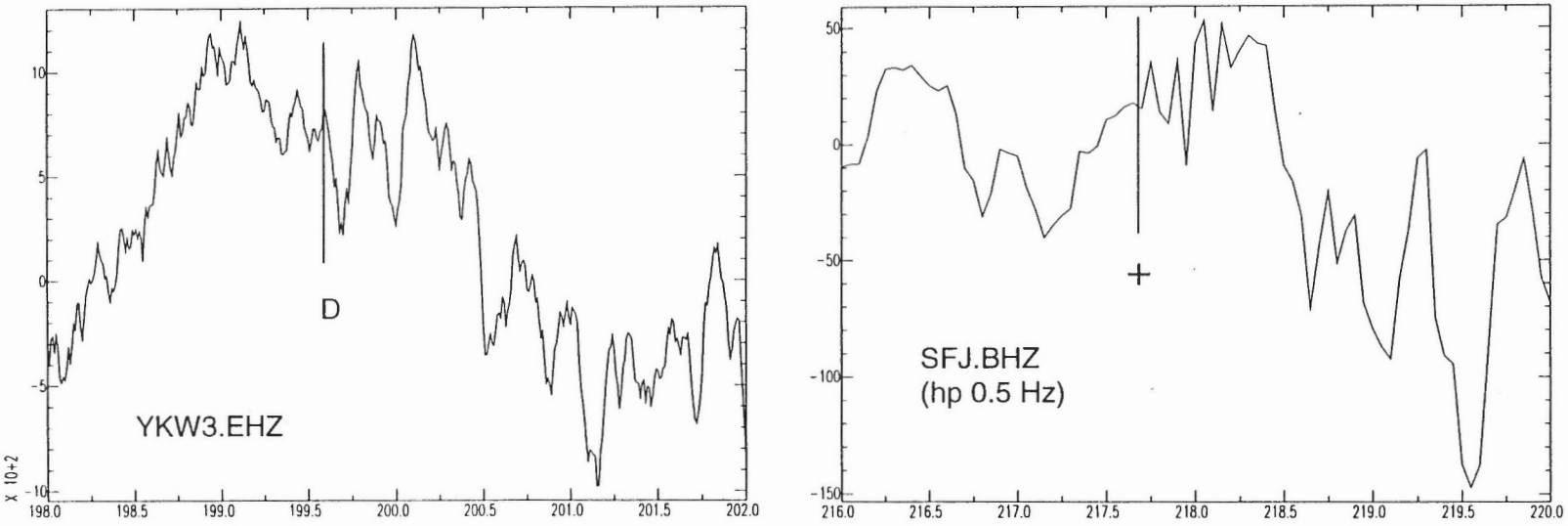

Figure 7b

DEVON ISLAND, NUNAVUT: 2 MARCH 1999

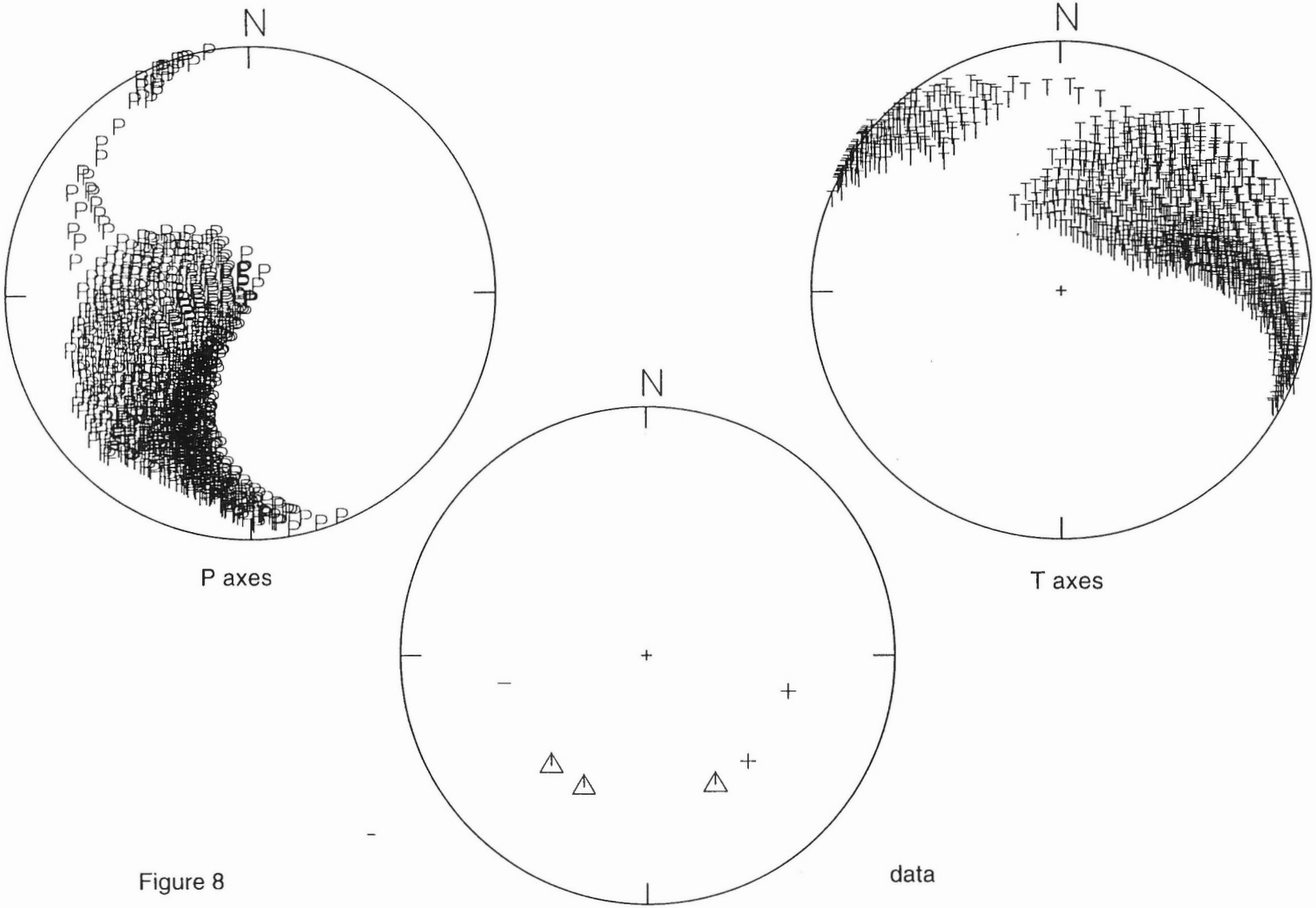

Figure 8

16 MARCH 1999: CÔTE-NORD, QUEBEC

Seismic Zone: Lower St. Lawrence
Latitude: 49.61° N
Longitude: 66.32° W
Depth: 18 km (fixed), 19.2 km (Bent and Perry, 2000)
Magnitude: 5.1 (m_N)
Origin Time: 12:50:48 (UT)
Comments: felt in eastern Quebec and northern New Brunswick; largest instrumentally recorded earthquake in Lower St. Lawrence seismic zone

Polarity Data

Station	Distance (km)	Azimuth (°)	Take-off Angle (°)	First Motion
ICQ	70	261.9	-75.5	D
SMQ	73	338.0	-76.2	D
GSQ	97	216.8	-79.5	D
CNQ	132	255.4	-82.2	D
MNQ	203	301.1	49.1	D
A21	327	230.7	49.1	C
A64	330	234.3	49.1	C
A61	351	233.9	49.1	C
A16	362	230.2	49.1	-
LMQ	375	233.7	49.1	C
A54	386	233.1	49.1	-
A11	390	228.7	49.1	C
DAQ	406	245.0	49.1	+
LMN	434	164.3	49.1	+
DPQ	581	238.3	49.1	+
SCHQ	582	356.7	49.1	C
MOQ	655	225.3	49.1	D

Station	Distance (km)	Azimuth (°)	Take-off Angle (°)	First Motion
LG4Q	700	312.6	49.1	D
MNT	715	233.0	49.1	+
OTT	849	240.0	49.1	-
WBO	849	236.2	49.1	D
CRLO	918	248.5	49.1	-
KUQ	951	352.6	49.1	D
EEO	1005	255.6	49.1	-
SADO	1110	245.8	49.1	D
KAPO	1171	275.3	49.1	-
FRB	1581	356.0	49.1	+
TBO	1683	275.2	49.1	C
SOLO	1847	281.3	49.6	+
FCC	2060	310.2	45.1	D
ULM	2111	283.2	45.1	+
RES	3089	344.2	30.4	D
EDM	3215	295.3	30.1	-
YKW1	3222	314.6	30.1	D
YKW2	3226	314.5	30.1	D
YKW3	3228	314.8	30.1	D
INK	4100	325.3	28.5	+
FINES	5410	39.3	25.3	C

Focal Mechanism Solutions

Strike	Dip	Rake
320.26	58.23	25.7

total number solutions: 1

grid search: 5°
misfits: 3
comments: misfits SMQ, MOQ and TBO

Preferred solution:

Plane 1:
- Strike: 320°
- Dip: 58°
- Rake: 26°

Plane 2:
- Strike: 216°
- Dip: 68°
- Rake: 146°

P-axis:
- Trend: 270°
- Plunge: 6°

T-axis:
- Trend: 175°
- Plunge: 39°

B-axis:
- Trend: 8°
- Plunge: 50°

Quality: B; good azimuthal coverage with redundancy; would have been an "A" except for the fact that it misfits SMQ

Figure Captions:

Figure 9a-j. Seismograms from which polarity data were read by the authors.

Figure 10. Focal mechanism solutions. Lower hemisphere projection. The P and T axes are shown on the left and the P nodal planes on the right. Data are also plotted. Solid symbols indicate compressional first motions and open symbols dilatations.

CÔTE-NORD, QUEBEC: 16 MARCH 1999

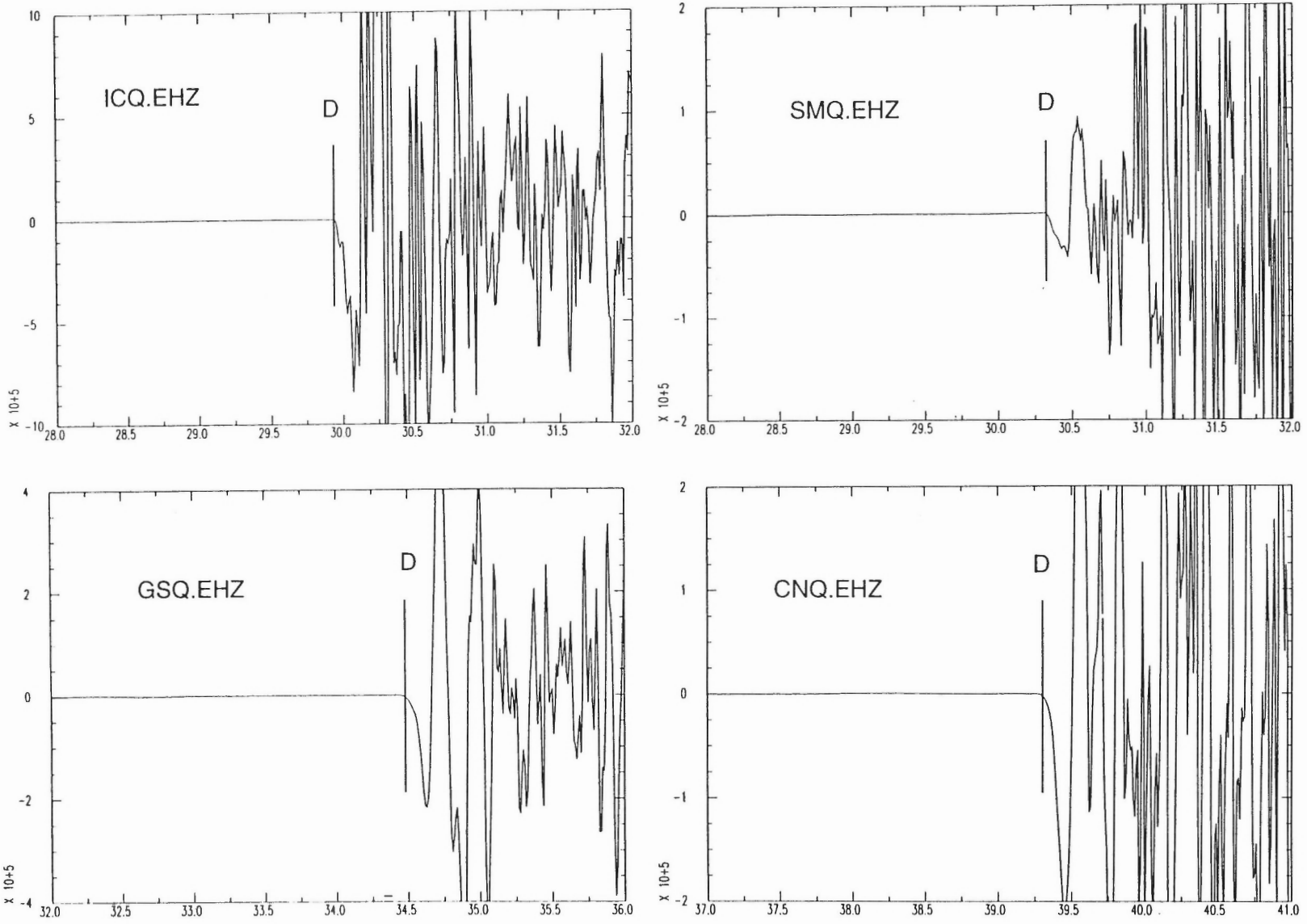

Figure 9a

CÔTE-NORD, QUEBEC: 16 MARCH 1999

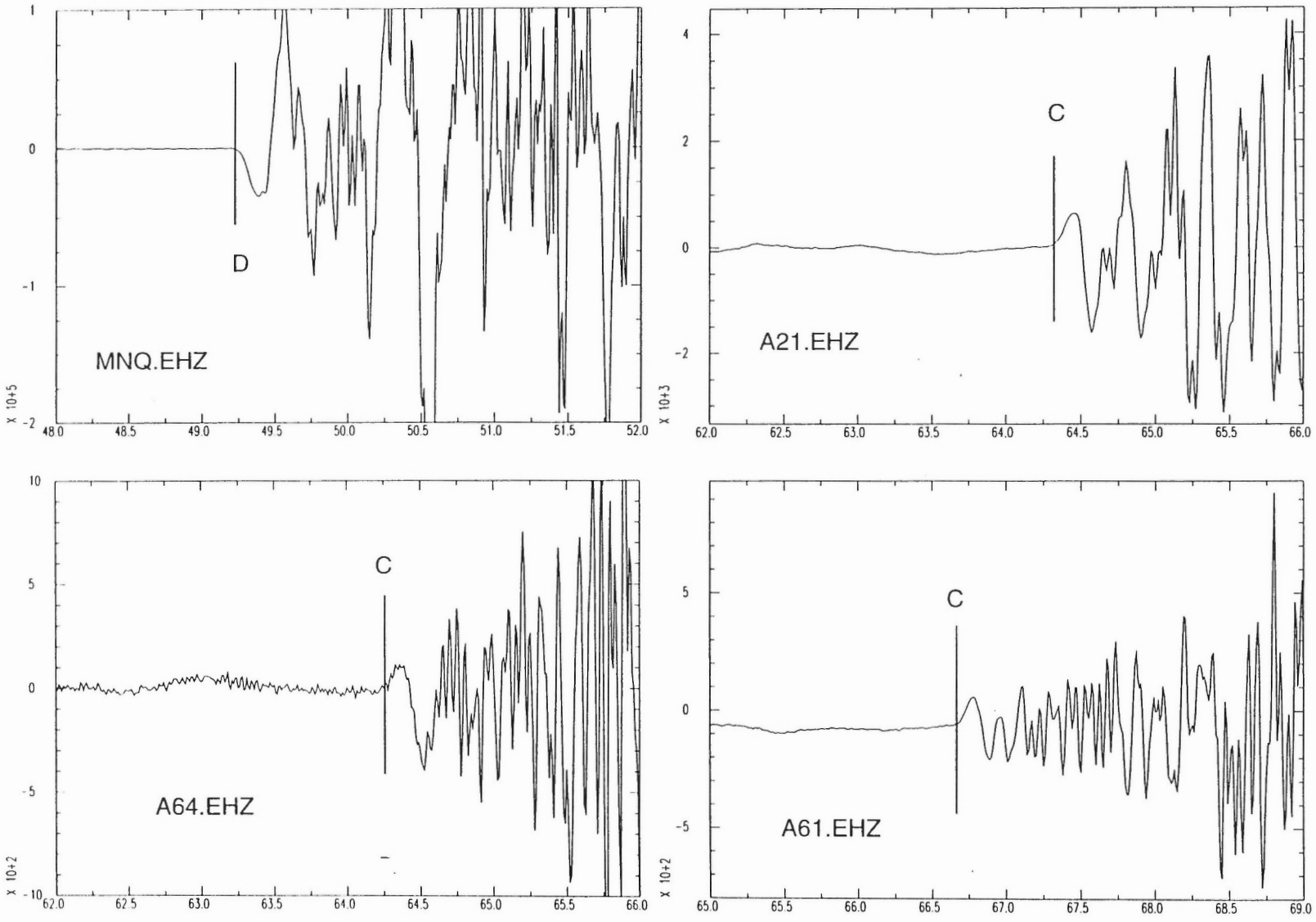

Figure 9b

CÔTE-NORD, QUEBEC: 16 MARCH 1999

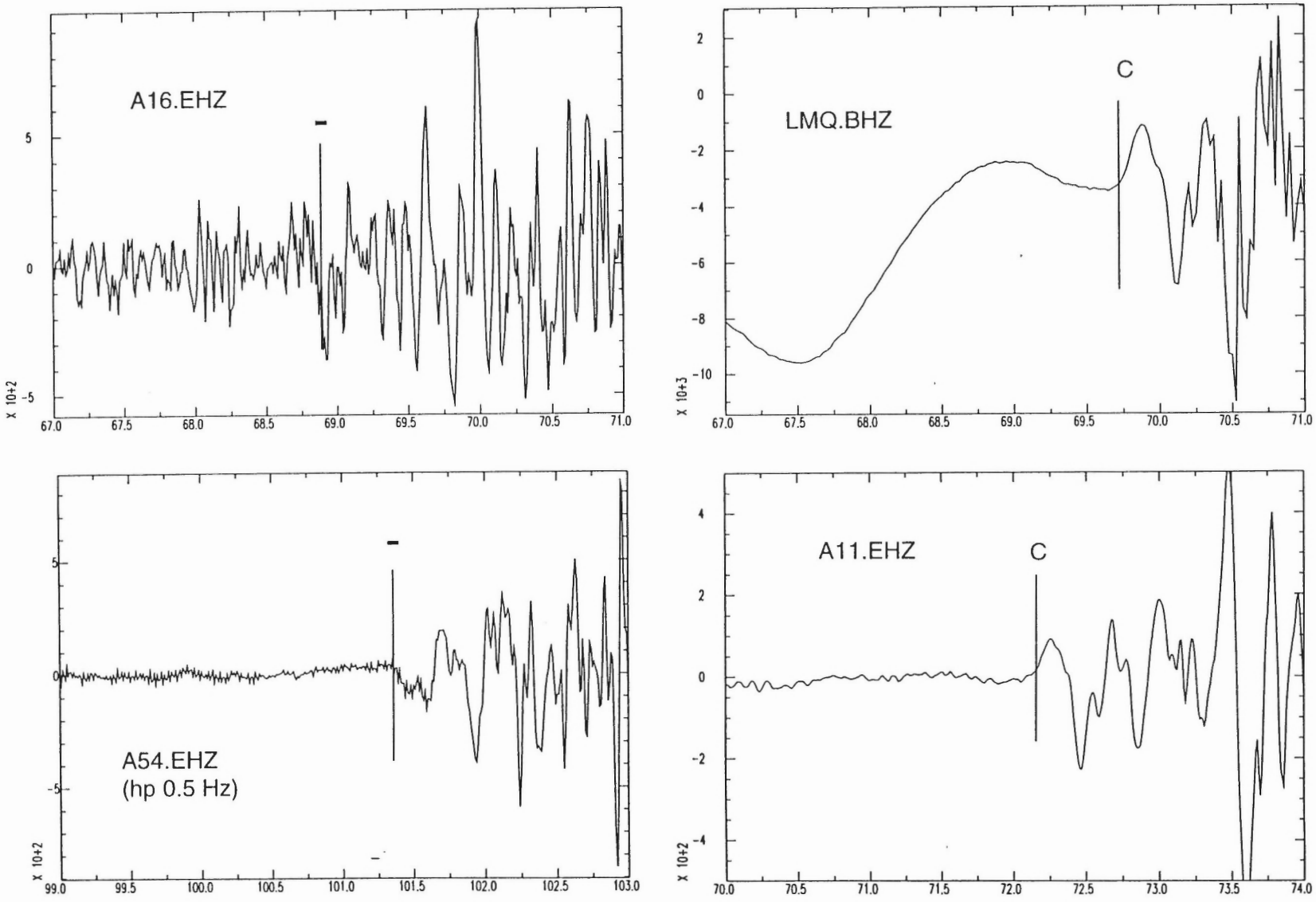

Figure 9c

CÔTE-NORD, QUEBEC: 16 MARCH 1999

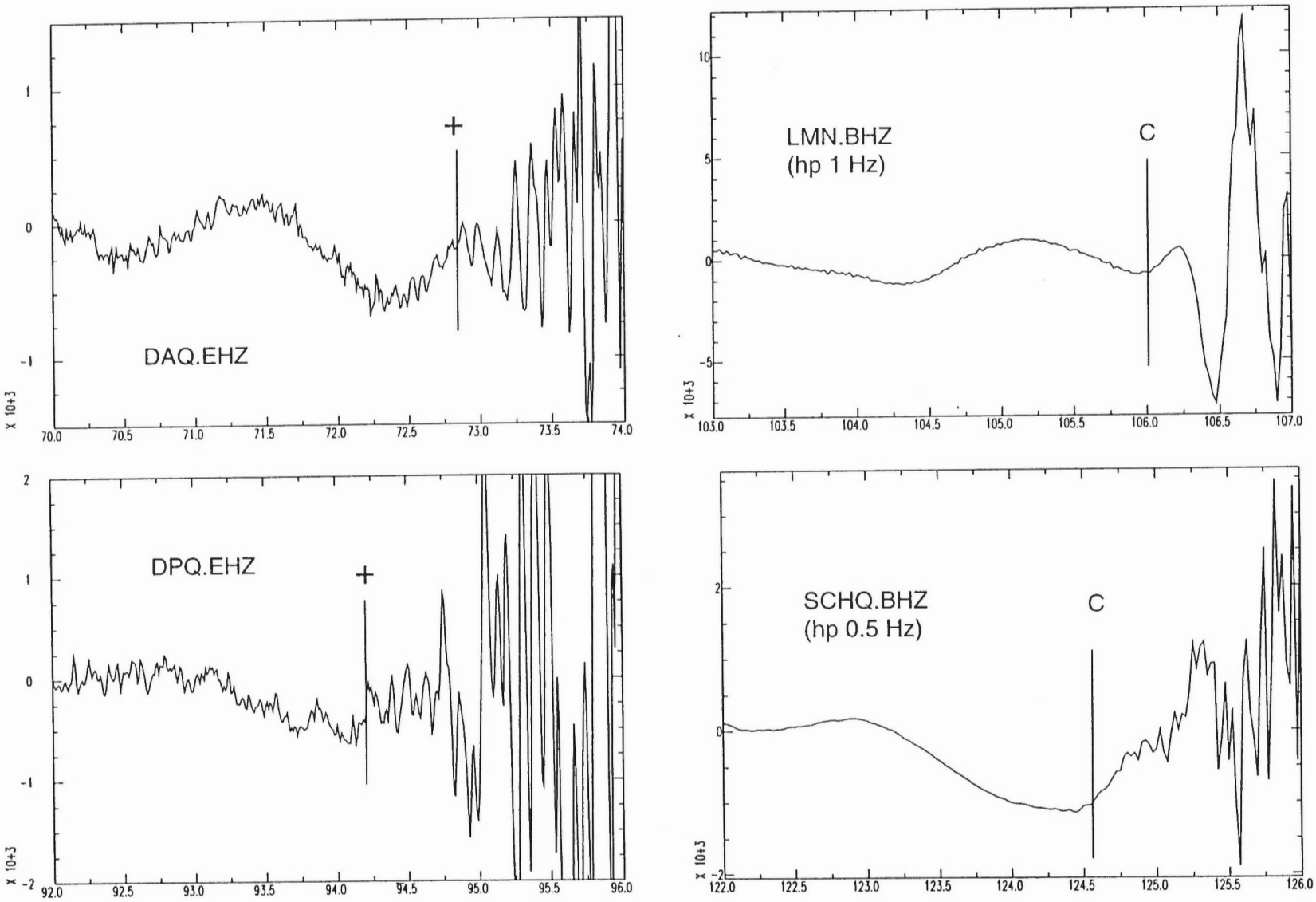

Figure 9d

CÔTE-NORD, QUEBEC: 16 MARCH 1999

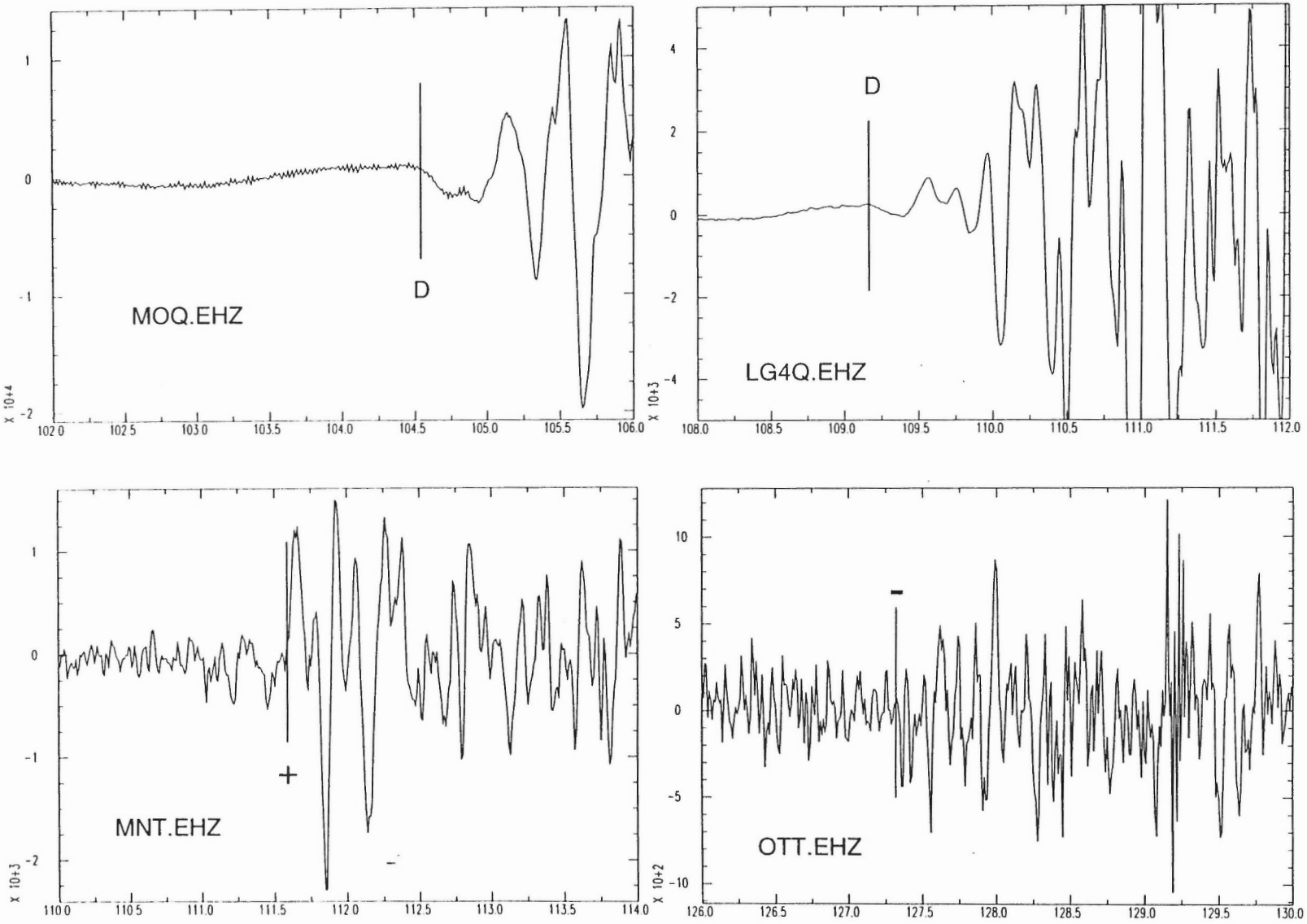

Figure 9e

CÔTE-NORD, QUEBEC: 16 MARCH 1999

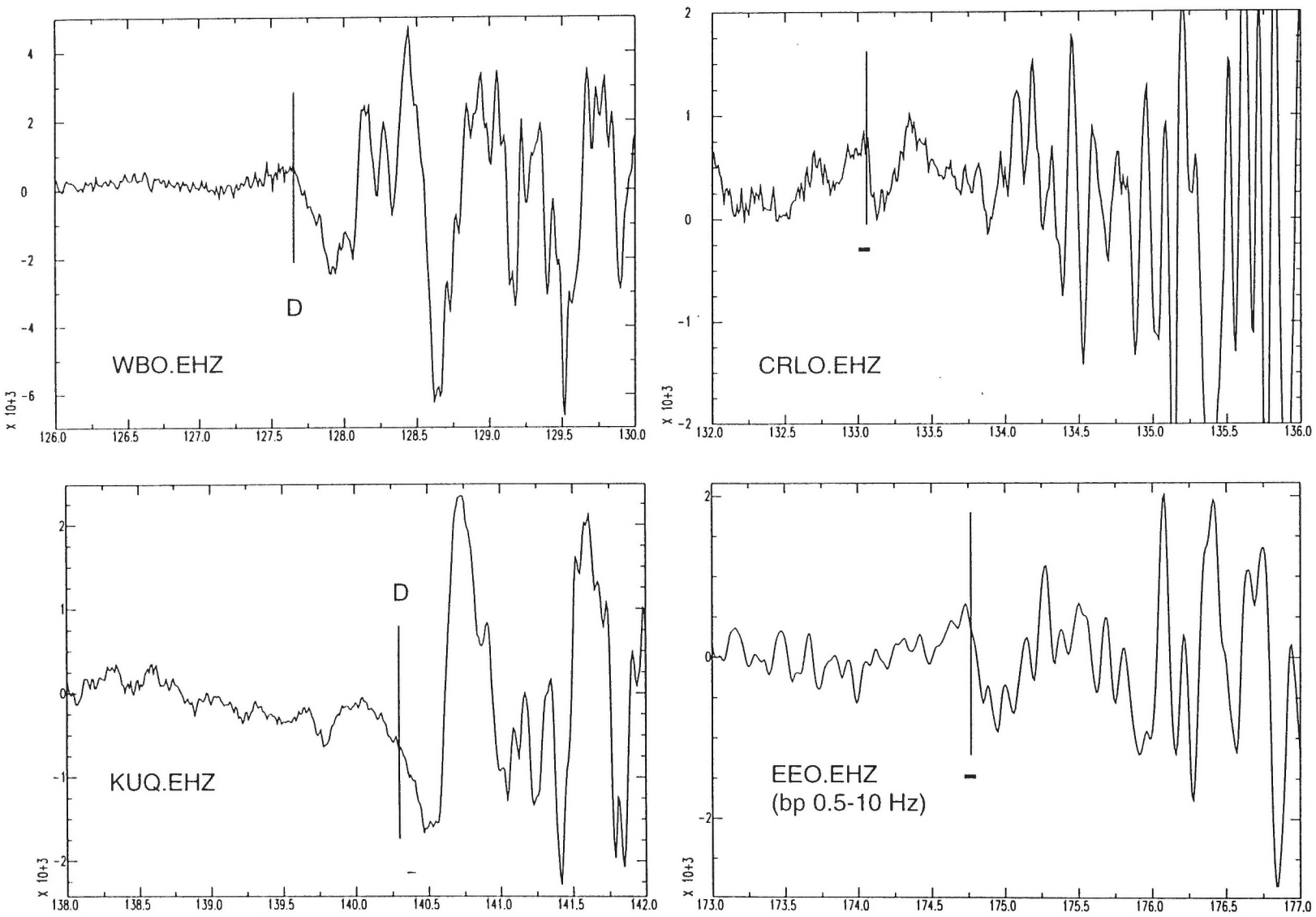

Figure 9f

CÔTE-NORD, QUEBEC: 16 MARCH 1999

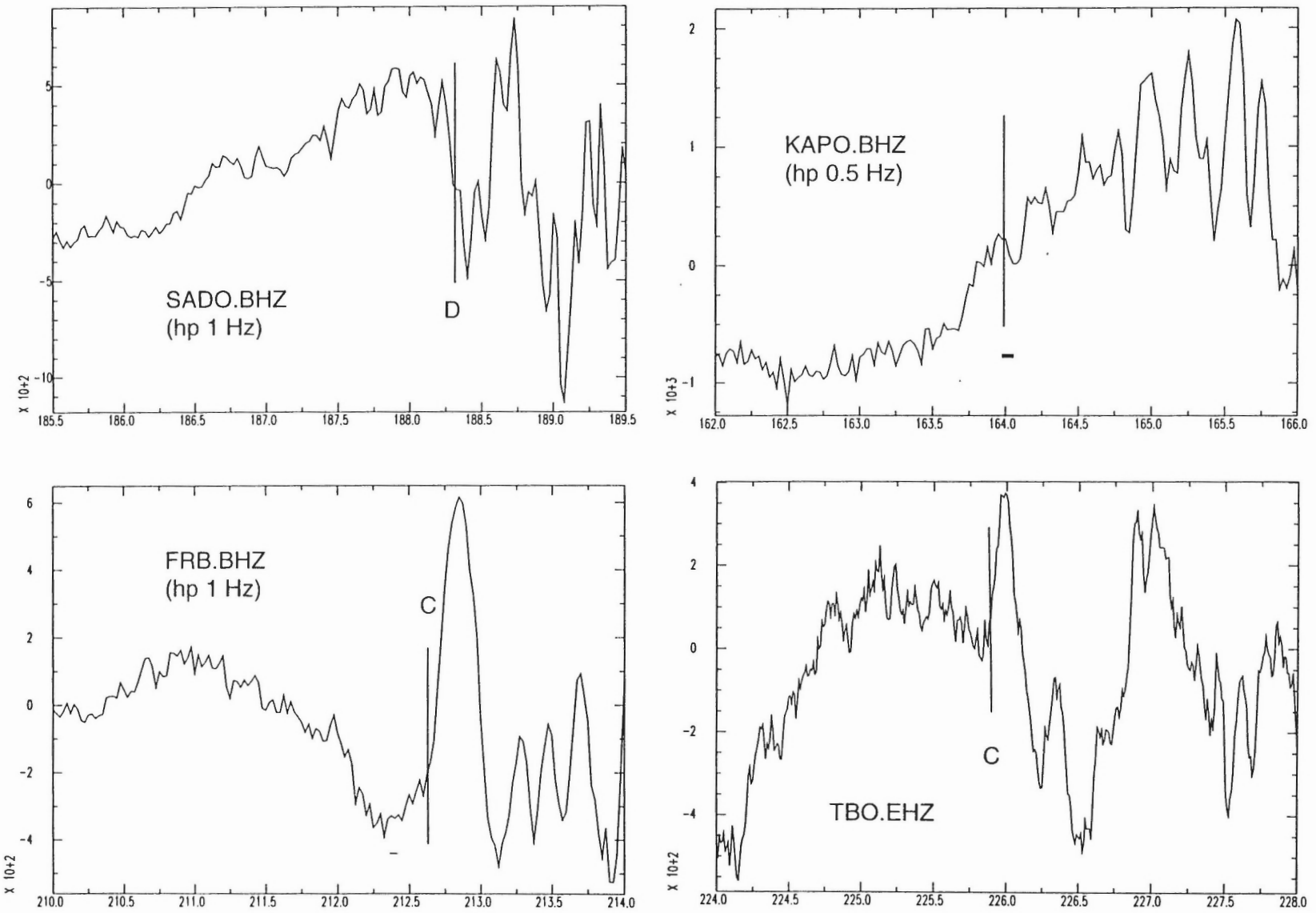

Figure 9g

CÔTE-NORD, QUEBEC: 16 MARCH 1999

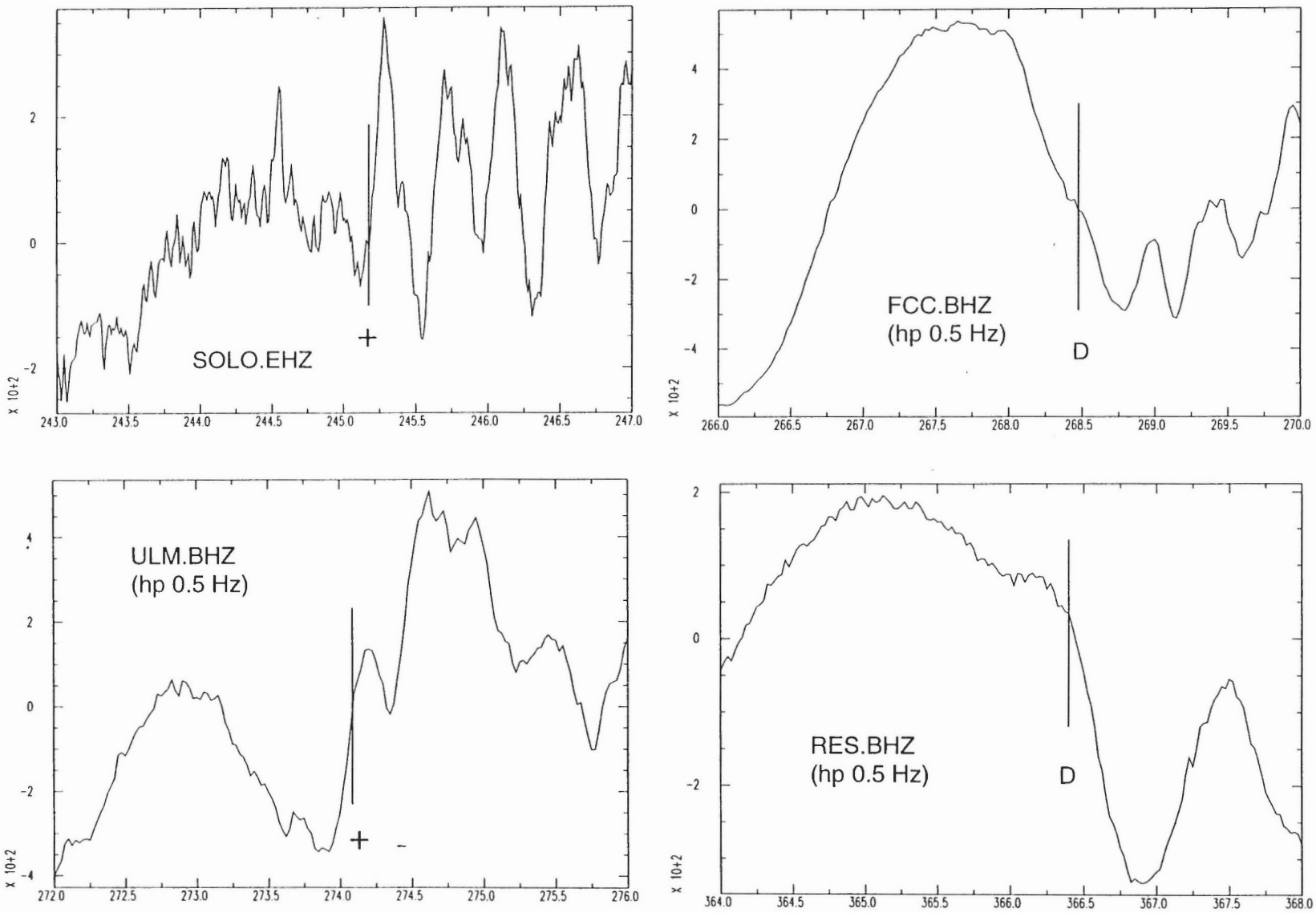

Figure 9h

CÔTE-NORD, QUEBEC: 16 MARCH 1999

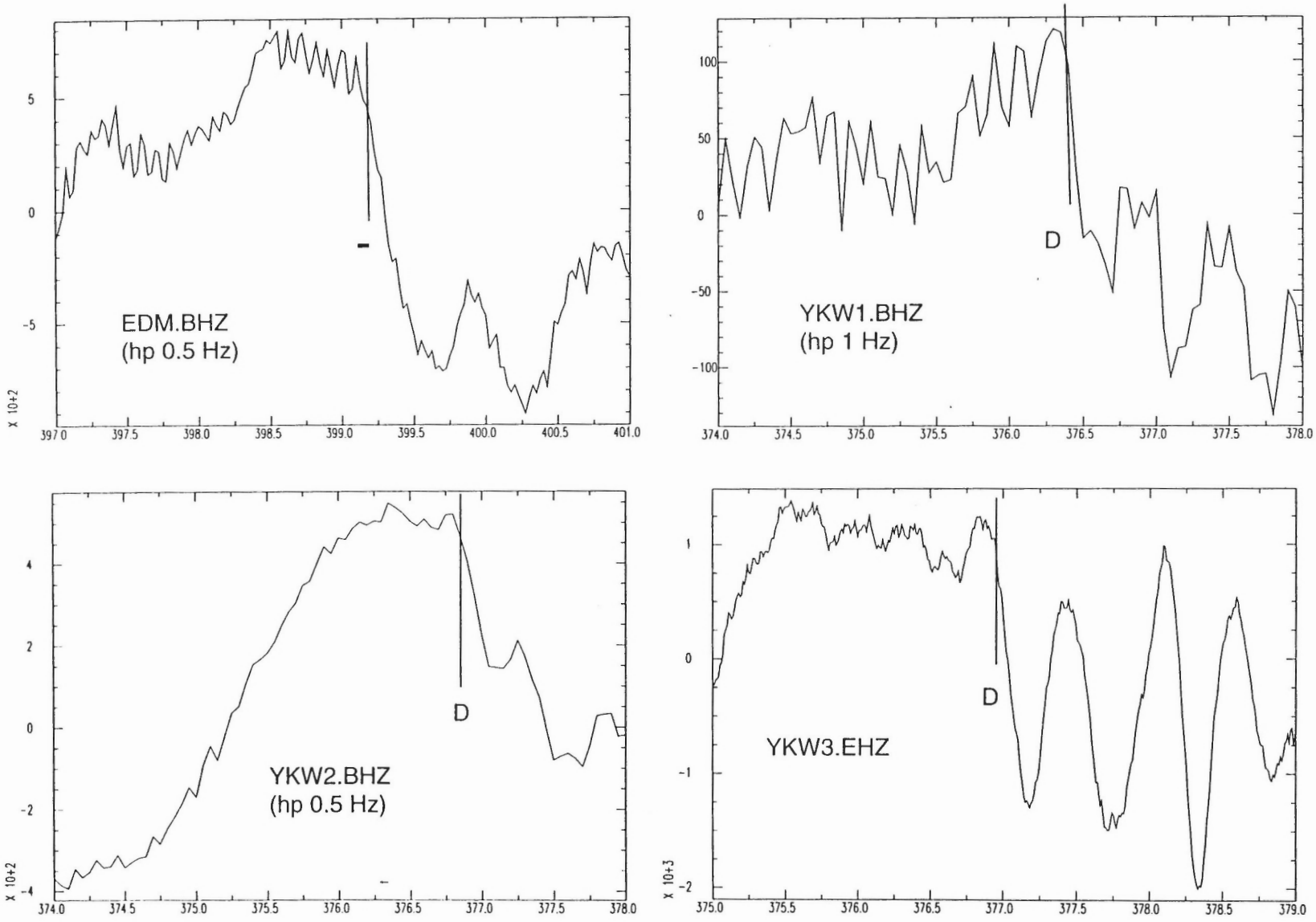

Figure 9i

CÔTE-NORD, QUEBEC: 16 MARCH 1999

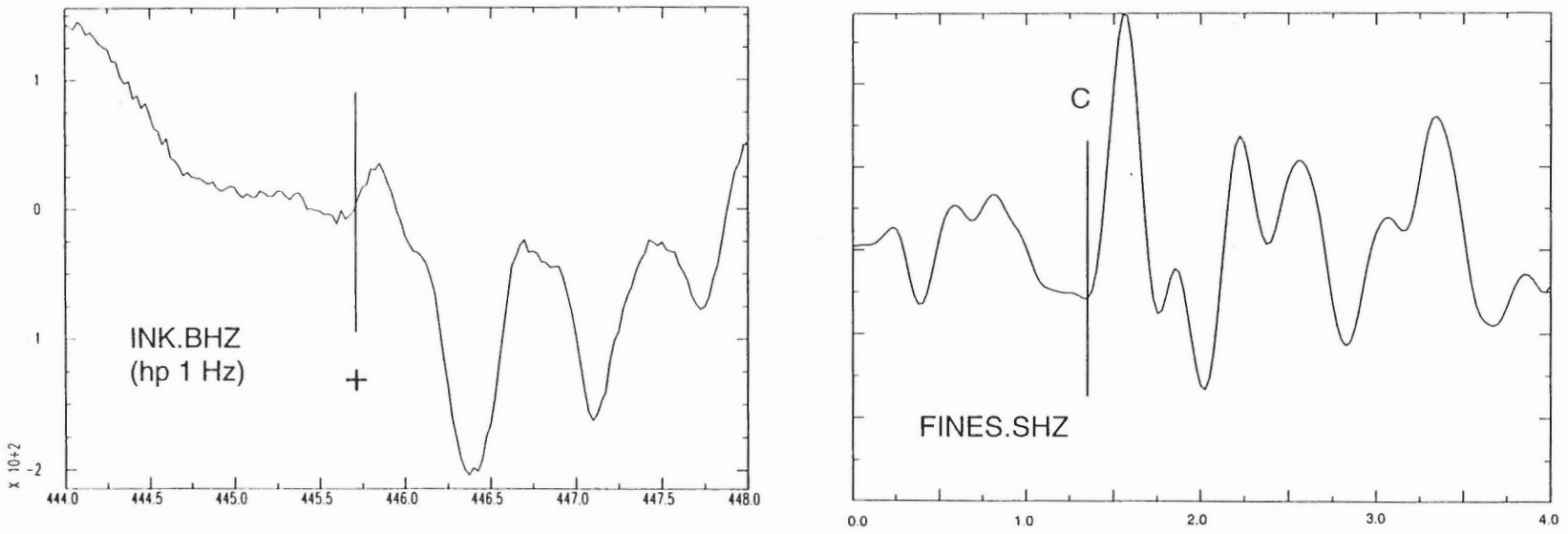

Figure 9j

Côte-Nord, Quebec: 16 March 1999

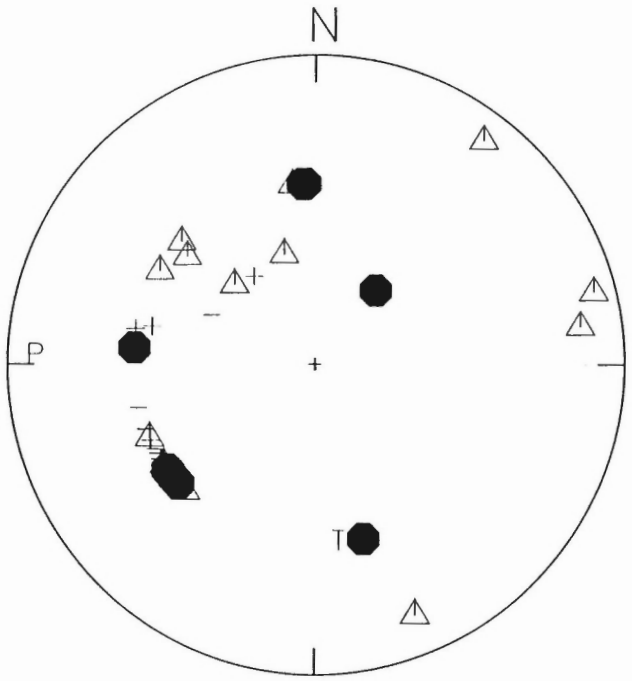

P and T axes

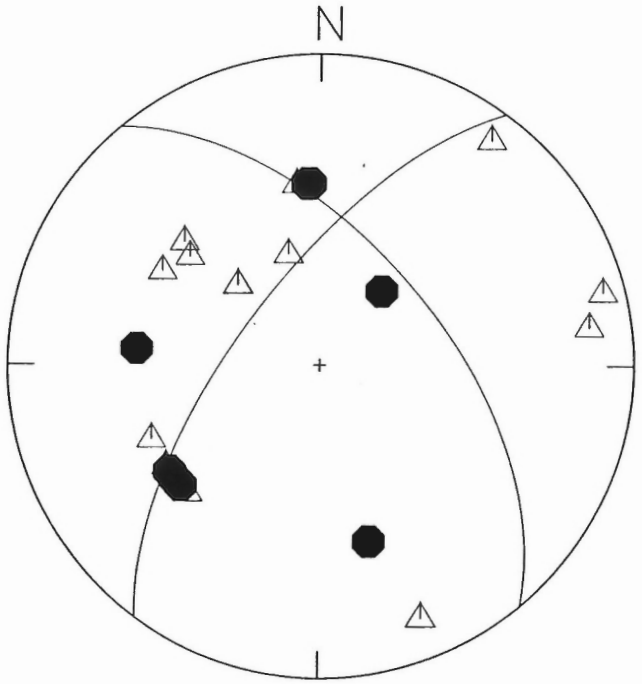

P nodal planes

Figure 10

29 JULY 1999: LABRADOR SEA

Seismic Zone: Labrador Sea
Latitude: 60.90°N
Longitude: 58.03°W
Depth: 18 km (fixed)
Magnitude: 5.3 (M_L) 4.8 (m_b)
Origin Time: 12:50:59 (UT)
Comments:

Polarity Data

Station	Distance (km)	Azimuth (°)	Take-off Angle (°)	First Motion
FRB	631	304.8	49.1	-
KUQ	665	246.7	49.1	+
SCHQ	854	221.5	49.1	-
LG4Q	1259	237.1	49.1	C
DRLN	1298	178.3	49.1	-
SMQ	1307	208.4	49.1	C
MNQ	1335	214.9	49.1	+
ICQ	1395	208.8	49.1	C
CNQ	1439	210.7	49.1	C
IGL	1449	320.7	49.1	+
GSQ	1454	207.4	49.1	+
A64	1643	212.9	49.1	+
A61	1662	213.2	49.1	D
A16	1682	212.7	49.1	D
LMQ	1684	213.5	49.1	C
A54	1696	213.6	49.1	D
A11	1711	212.8	49.1	D
LMN	1734	197.9	49.1	+
TRQ	1956	220.8	47.4	-
GRQ	1967	224.0	47.4	+

Station	Distance (km)	Azimuth (°)	Take-off Angle (°)	First Motion
KAPO	1996	214.4	47.4	+
CRLO	2080	226.0	45.1	-
EEO	2091	230.1	45.1	C
RES	2125	330.8	45.1	-
SADO	2271	227.3	42.8	+
TBO	2403	249.7	38.7	-
SOLO	2435	255.6	38.7	C
ULM	2619	260.3	35.5	D
EDM	3341	280.5	29.9	+
INK	3463	316.0	29.7	C
WALA	3679	274.9	29.3	C
DLBC	3861	298.8	29.0	+
DAWY	3923	311.3	28.9	D
PNT	3967	279.7	28.8	C
LLLB	3991	283.0	28.8	C
HYT	4048	305.9	28.6	C

Comments: FCC, DAQ and A21 not functioning

Focal Mechanism Solutions

Strike	Dip	Rake
133.30	41.41	40.89
96.48	43.96	-22.18
103.37	42.27	-17.14
117.21	41.03	-11.69
107.76	45.86	-9.85
114.71	45.22	-4.98
86.70	58.23	-25.70

total number solutions: 7
grid search: 5°
misfits: 2
comments: all solutions misfit LMQ and ULM

Preferred solution: use weighting scheme to determine whether thrust or normal component; solution 4 most consistent with emergent data

Plane 1:
- Strike: 117°
- Dip: 41°
- Rake: -12°

Plane 2:
- Strike: 216°
- Dip: 41°
- Rake: -130°

P-axis:
- Trend: 90°
- Plunge: 39°

T-axis:
- Trend: 337°
- Plunge: 26°

B-axis:
- Trend: 223°
- Plunge: 40°

Quality: D; no stations in eastern hemisphere but large number of stations and good azimuthal redundancy in western hemisphere; emergent data used to determine sign of dip-slip component

Figure Captions:

Figure 11a-i. Seismograms from which polarity data were read by the authors.

Figure 12. Focal mechanism solutions. Lower hemisphere projection. The P and T axes are shown on the left and the P nodal planes on the right. Data are also plotted. Solid symbols indicate compressional first motions and open symbols dilatations.

LABRADOR SEA: 29 JULY 1999

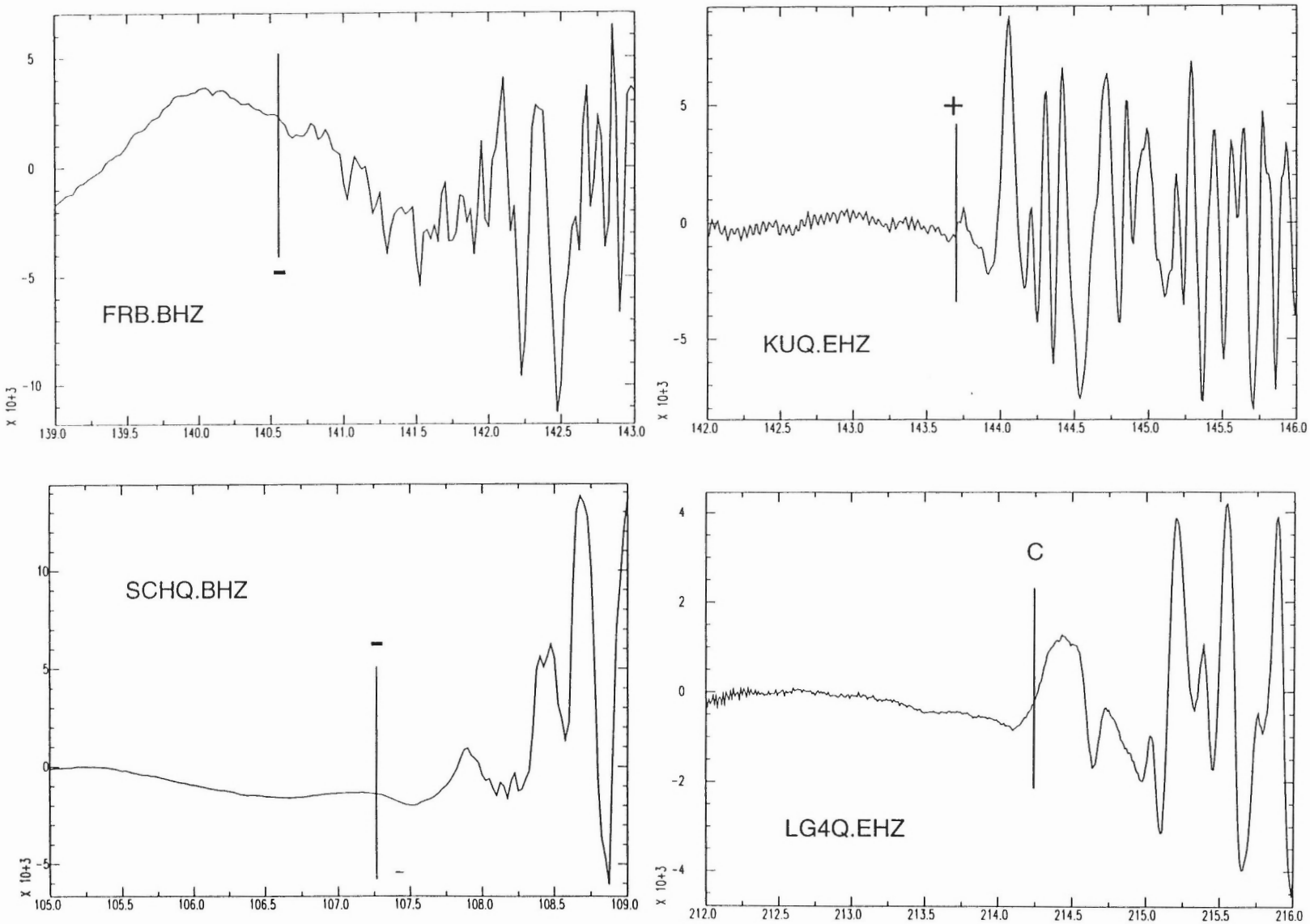

Figure 11a

LABRADOR SEA: 29 JULY 1999

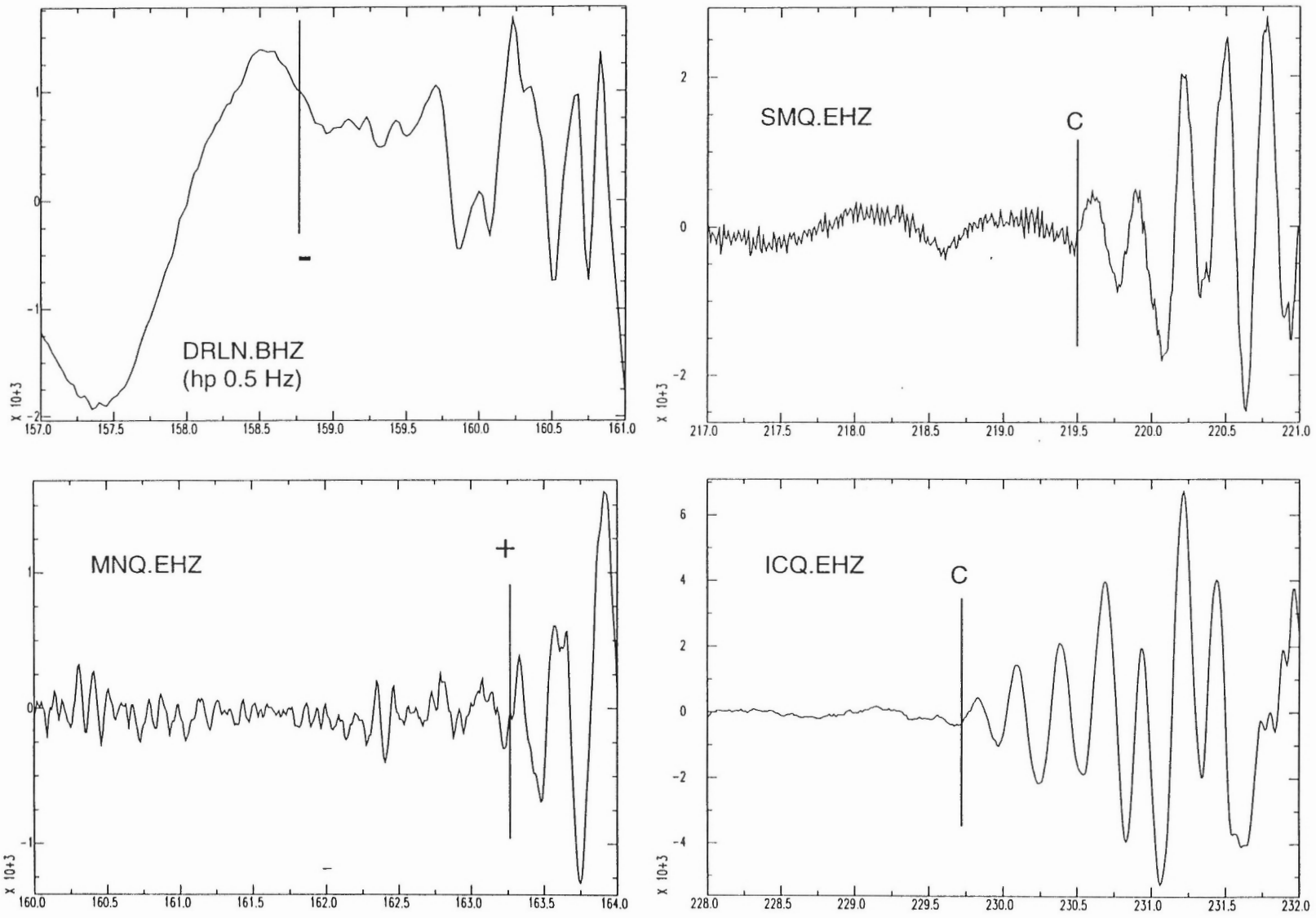

Figure 11b

LABRADOR SEA: 29 JULY 1999

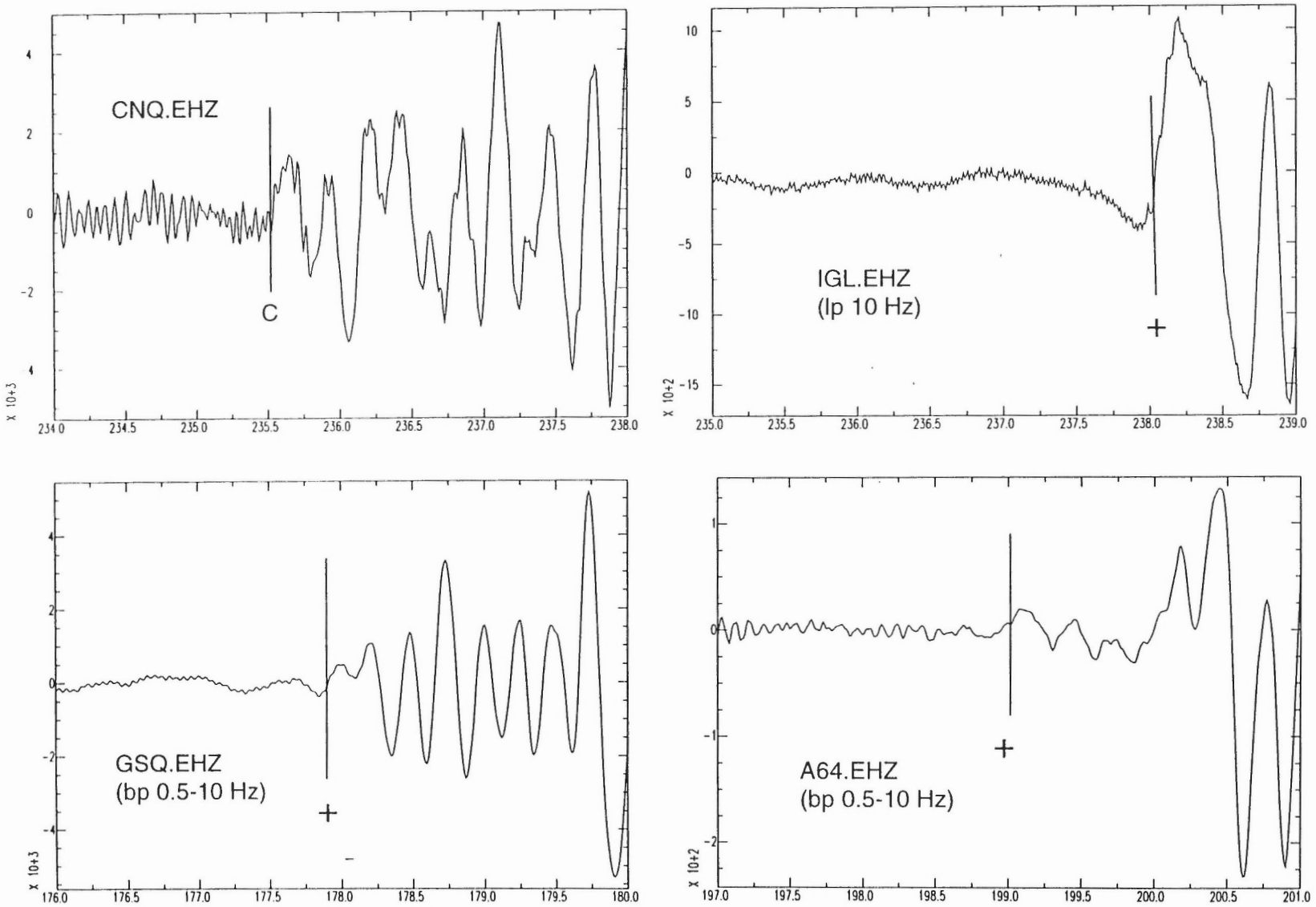

Figure 11c

LABRADOR SEA: 29 JULY 1999

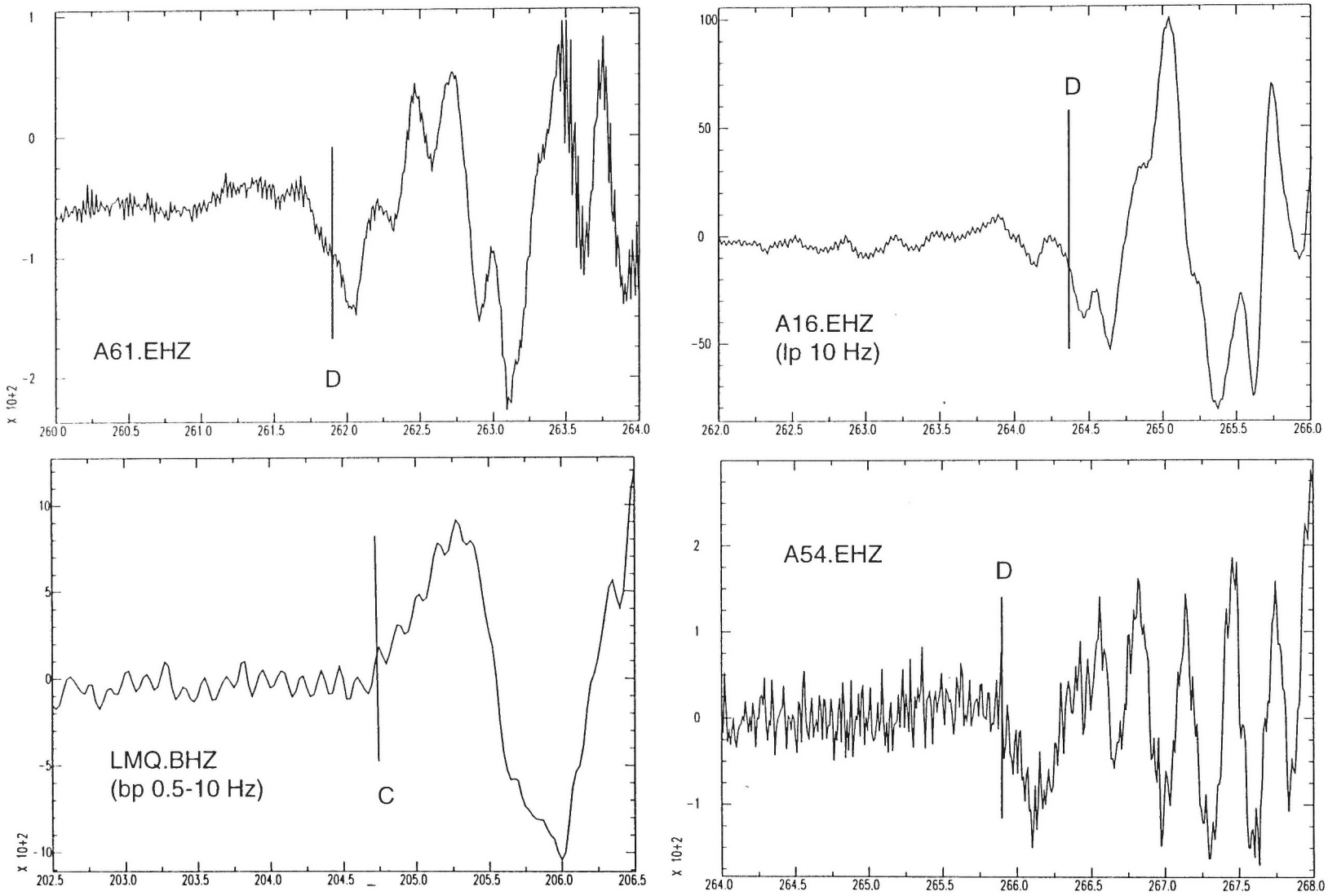

Figure 11d

LABRADOR SEA: 29 JULY 1999

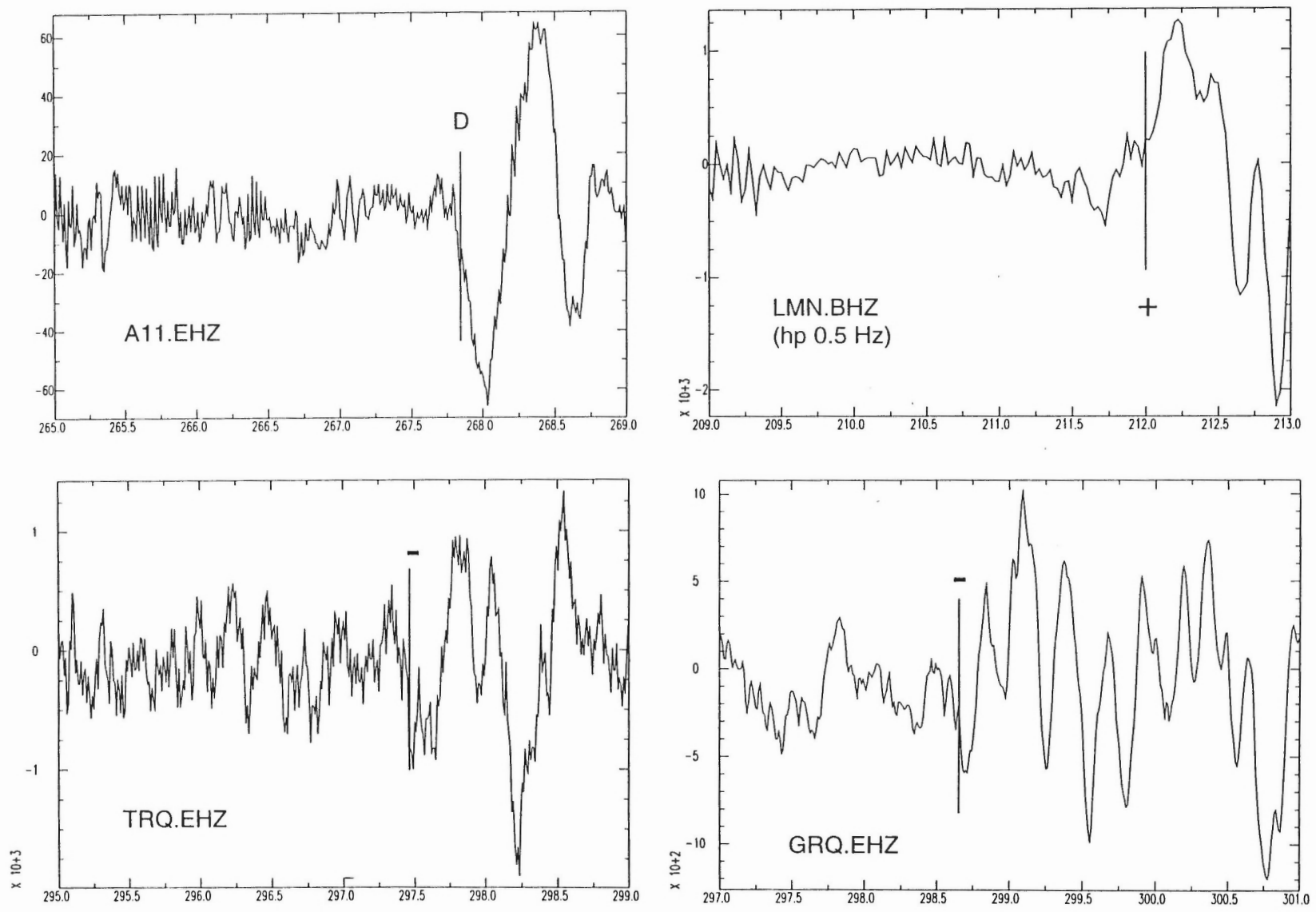

Figure 11e

LABRADOR SEA: 29 JULY 1999

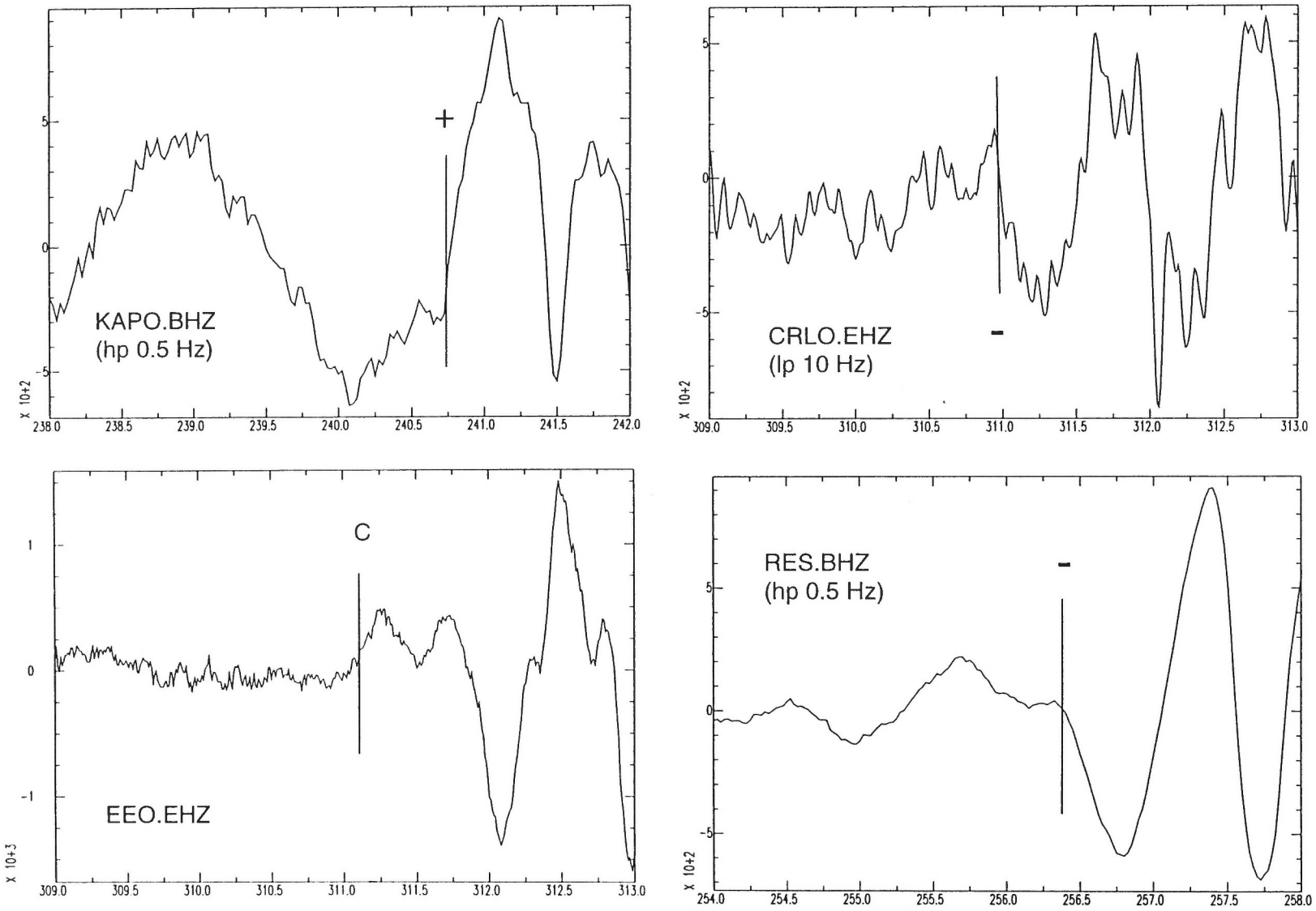

Figure 11f

LABRADOR SEA: 29 JULY 1999

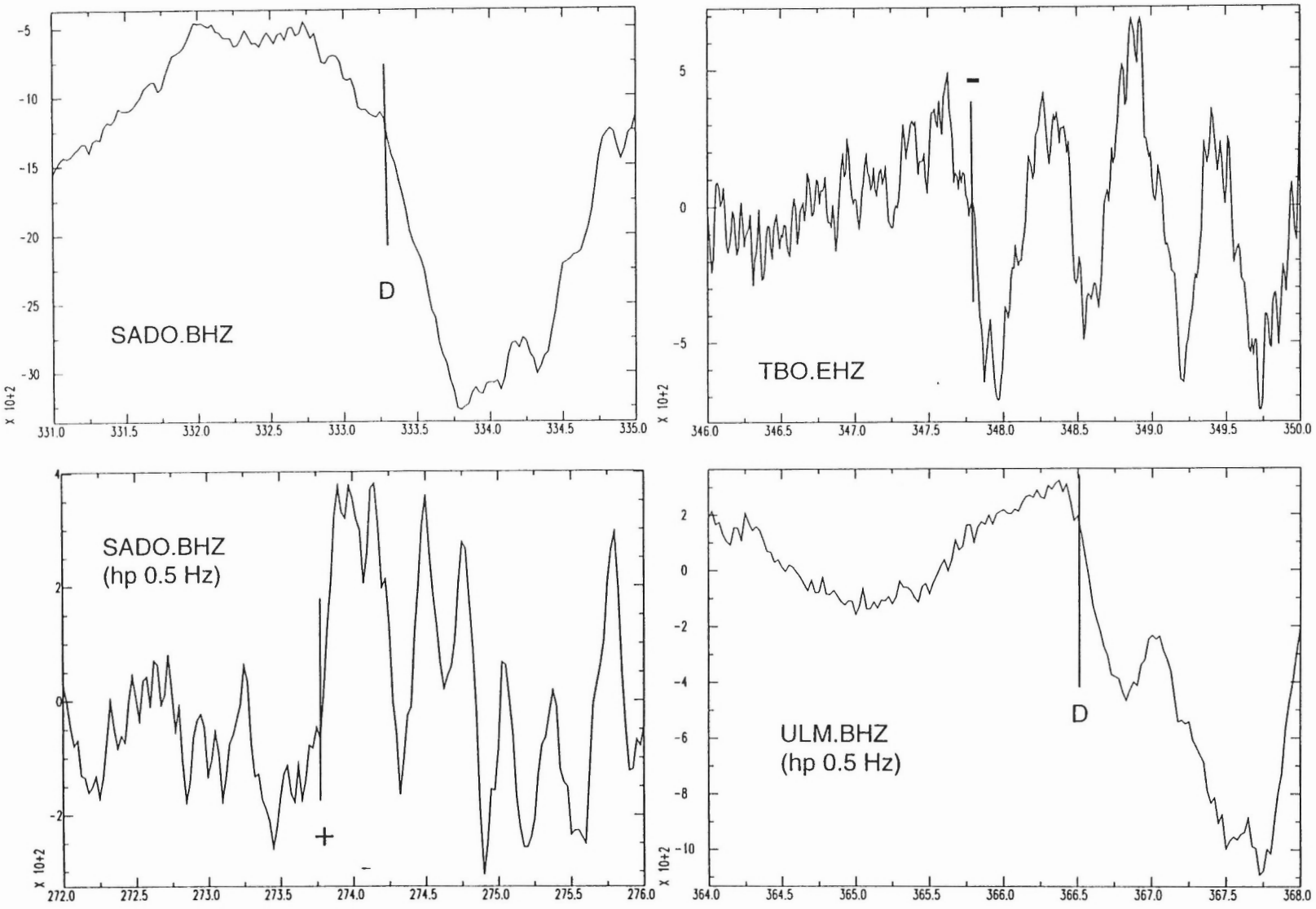

Figure 11g

LABRADOR SEA: 29 JULY 1999

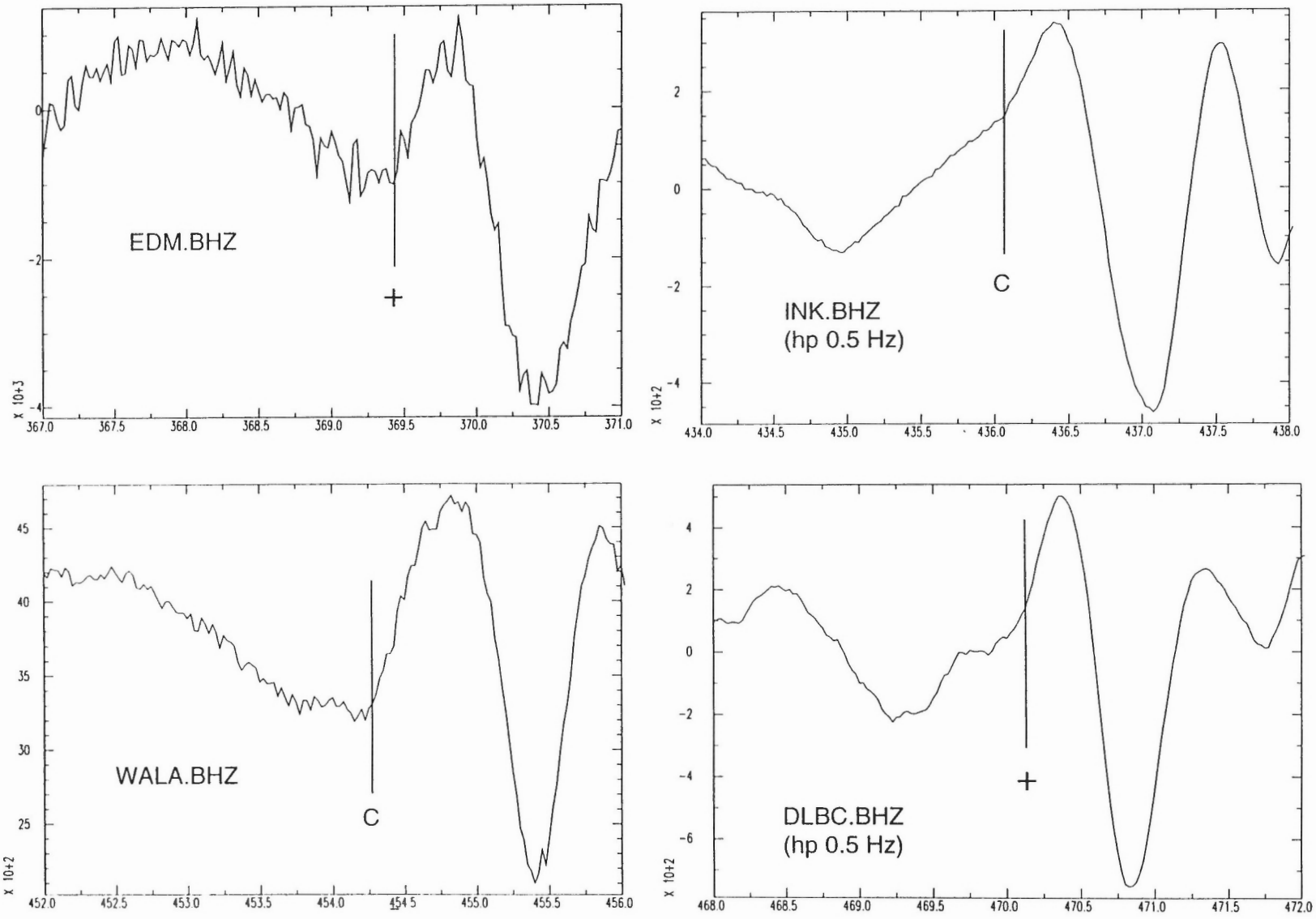

Figure 11h

LABRADOR SEA: 29 JULY 1999

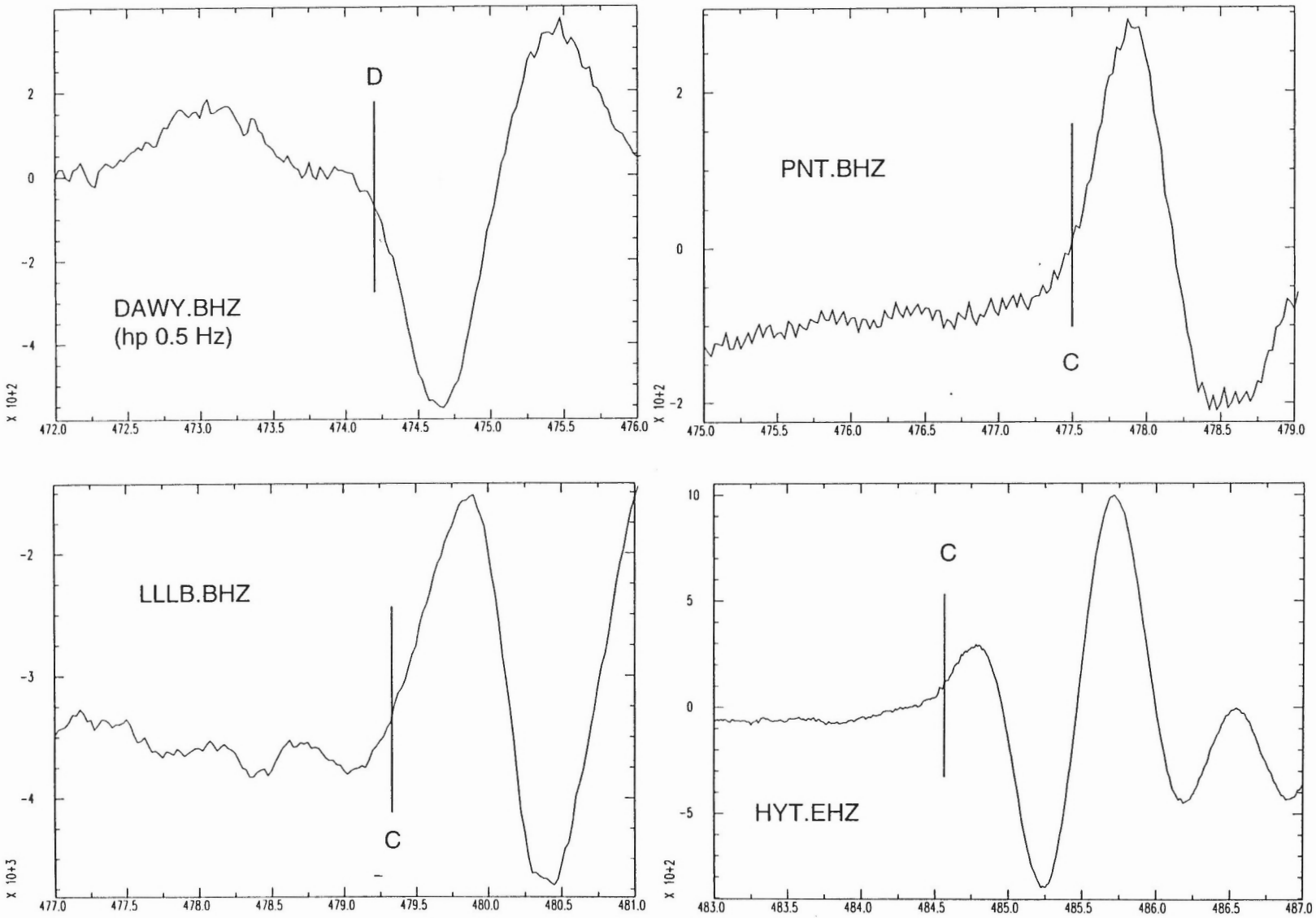

Figure 11i

LABRADOR SEA: 29 JULY 1999

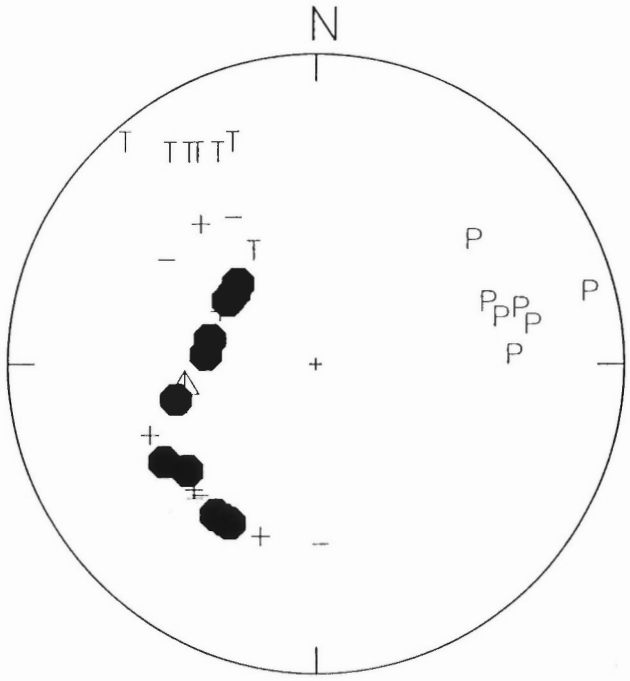

P and T axes

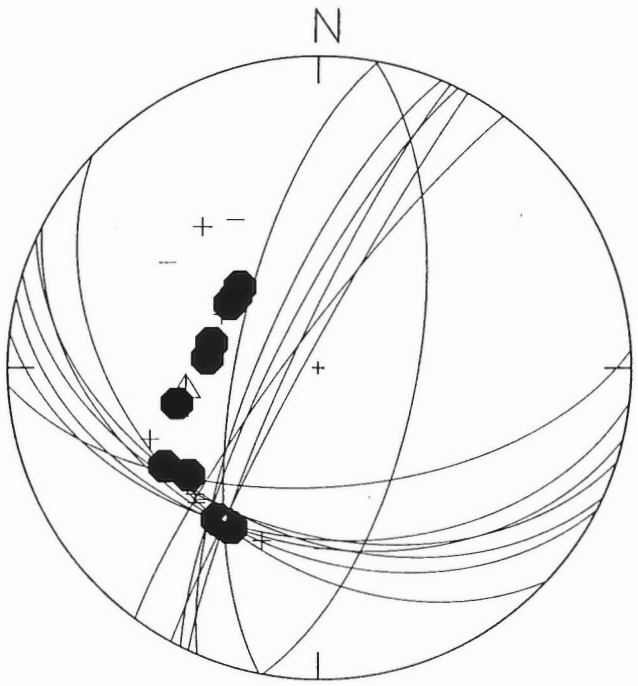

P nodal planes

Figure 12

31 OCTOBER 1999: MORIN HEIGHTS, QUEBEC

Seismic Zone: western Quebec
Latitude: 45.84° N
Longitude: 74.31° W
Depth: 18 km (fixed), 20.8 km (Bent and Perry, 2000)
Magnitude: 4.2 (m_{bLg})
Origin Time: 20:14:10 (UT)
Comments: felt in western Quebec and eastern Ontario

Polarity Data

Station	Distance (km)	Azimuth (°)	Take-off Angle (°)	First Motion
TRQ	45	334.5	–68.3	D
MNT	66	126.3	–74.7	C
GAC	93	259.9	–79.0	D
GAC	93	259.9	–79.0	B
GAC	93	259.9	–79.0	>
BGR	114	182.8	–81.0	C
OTT	122	245.5	–81.6	D
WBO	122	219.0	–81.6	D
GRQ	146	305.4	–83.0	C
DPQ	149	51.5	–83.1	D
PTN	153	200.7	–83.3	0
MOQ	171	110.0	49.1	+
BRC	188	212.8	49.1	D
FINE	190	201.3	49.1	D
CRLO	240	275.9	49.1	C
QCQ	255	65.2	49.1	+
A54	347	57.7	49.1	–
LMQ	358	56.8	49.1	D

Station	Distance (km)	Azimuth (°)	Take-off Angle (°)	First Motion
EEO	378	285.1	49.1	+
WLVO	388	237.9	49.1	+
SADO	398	254.1	49.1	–
A64	402	55.4	49.1	D
PKRO	431	242.5	49.1	–
ACTO	520	243.3	49.1	–
GPD	538	181.4	49.1	–
PAL	540	176.5	49.4	<
GSQ	641	55.4	49.1	D
MNQ	663	36.3	49.1	+
KAPO	734	305.9	49.1	C
SMQ	746	46.6	49.1	+
LG4Q	865	0.9	49.1	+

Focal Mechanism Solutions

Strike	Dip	Rake
136.49	51.13	42.55
84.71	90.00	45.00
88.22	86.47	44.89
91.72	82.95	44.56
79.45	95.15	44.01

total number solutions: 5
grid search: 5°
misfits: 1
comments: data from a large number of Southern Ontario (SONT) and

Lamont-Doherty (LDEO) Network stations were examined; those from which polarities could be picked are noted in the data table; we were unable to pick polarities from the SONT stations BRCO, LDN, STCO ,TYNO, RD01, RD02, RD03 and RD04 or the LDEO stations ARNY, CHIP, CRNY, MANY, MSNY, TBR and WCC

1st solution has misfit at GRQ; GRQ is near Pg-Pn crossover distance; if if is actually a Pn, it would fit solution but we believe it has been correctly identified as a Pg; other 4 solutions misfit SH at GAC

same 5 solutions result if we include emergent polarities using weighting scheme discussed in text so can't use emergent data to distinguish between 2 families of solutions

note that all solutions have one nodal plane with similar orientation (see Figure 14); use that plane to calculate mean and then take closest actual solution (solution 5)

Preferred solution:

Plane 1:		
	Strike:	95°
	Dip:	79°
	Rake:	44°
Plane 2:		
	Strike:	355°
	Dip:	47°
	Rake:	165°
P-axis:		
	Trend:	218°
	Plunge:	21°
T-axis:		
	Trend:	325°
	Plunge:	38°
B-axis:		
	Trend:	106°
	Plunge:	45°

Quality: B: good azimuthal coverage and redundancy but some uncertainty in strike

Figure Captions:

Figure Captions:

Figure 13a-h. Seismograms from which polarity data were read by the authors.

Figure 14. Focal mechanism solutions. Lower hemisphere projection. The P and T axes are shown on the left and the P nodal planes on the right. Data are also plotted. Solid symbols indicate compressional first motions and open symbols dilatations. S data and nodal planes are plotted at the bottom. The arrows indicate the first motion direction. The solid lines represent the SH nodal planes and the dashed lines the SV nodal planes.

Morin Heights, Quebec: 31 October 1999

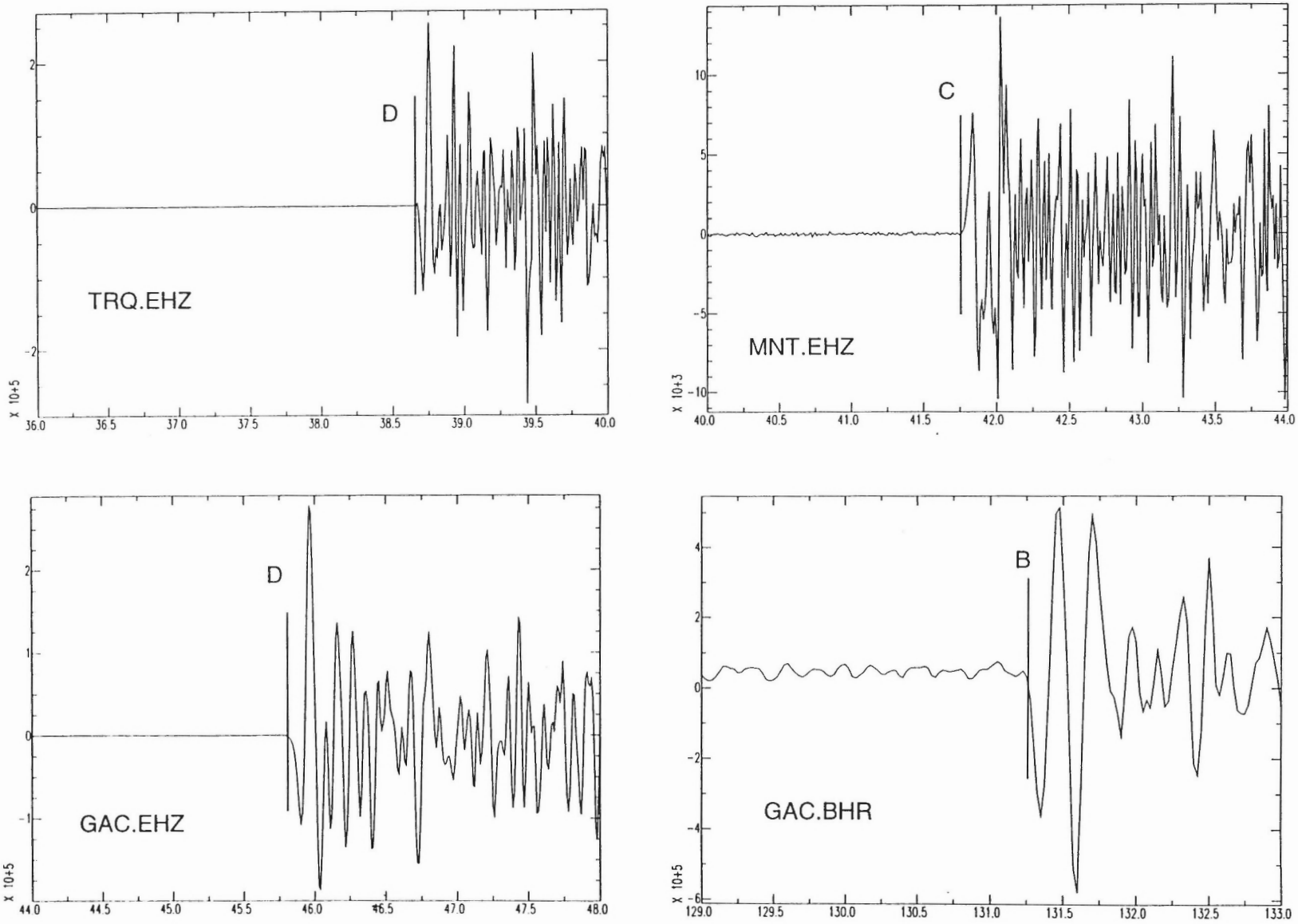

Figure 13a

Morin Heights, Quebec: 31 October 1999

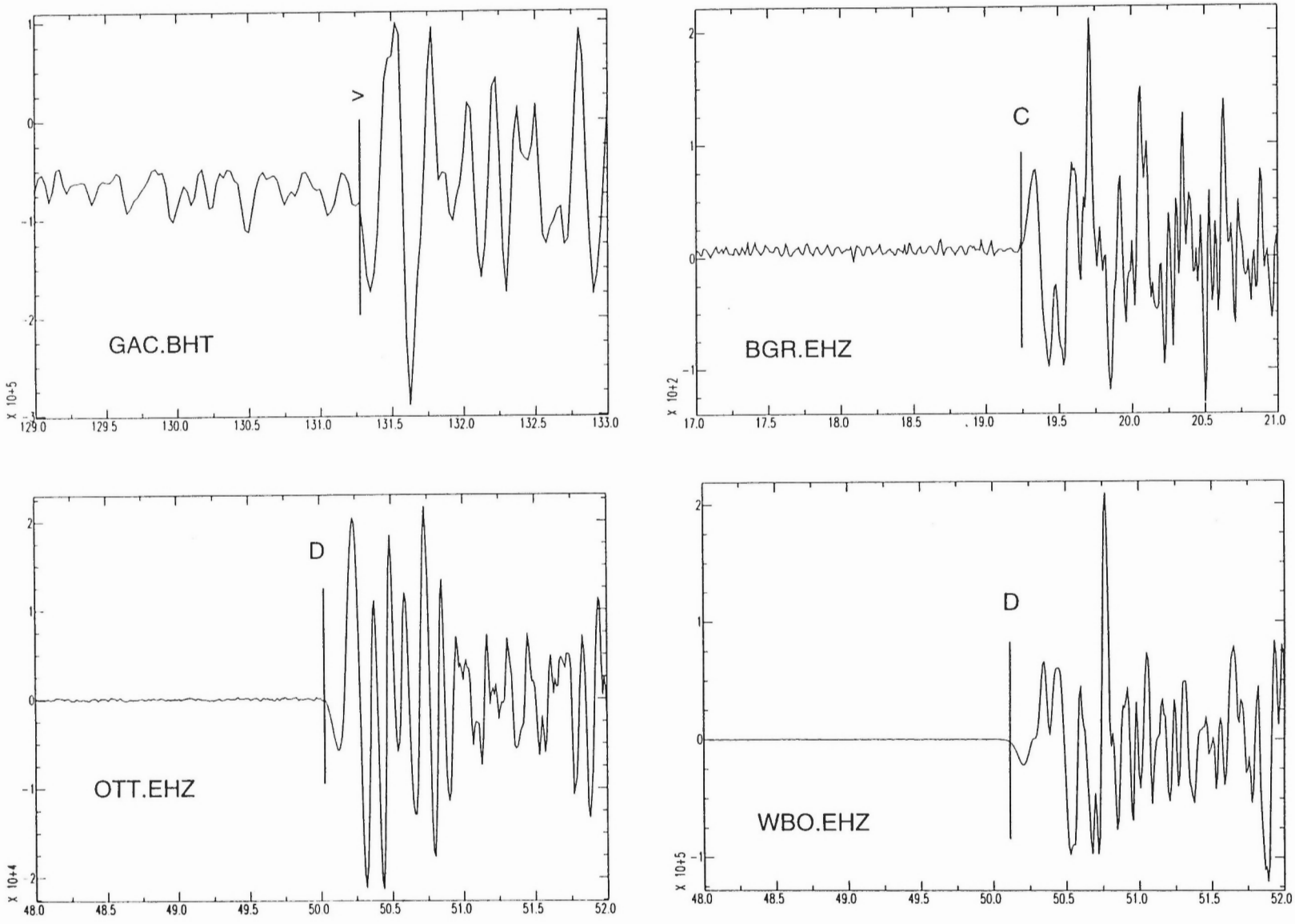

Figure 13b

Morin Heights, Quebec: 31 October 1999

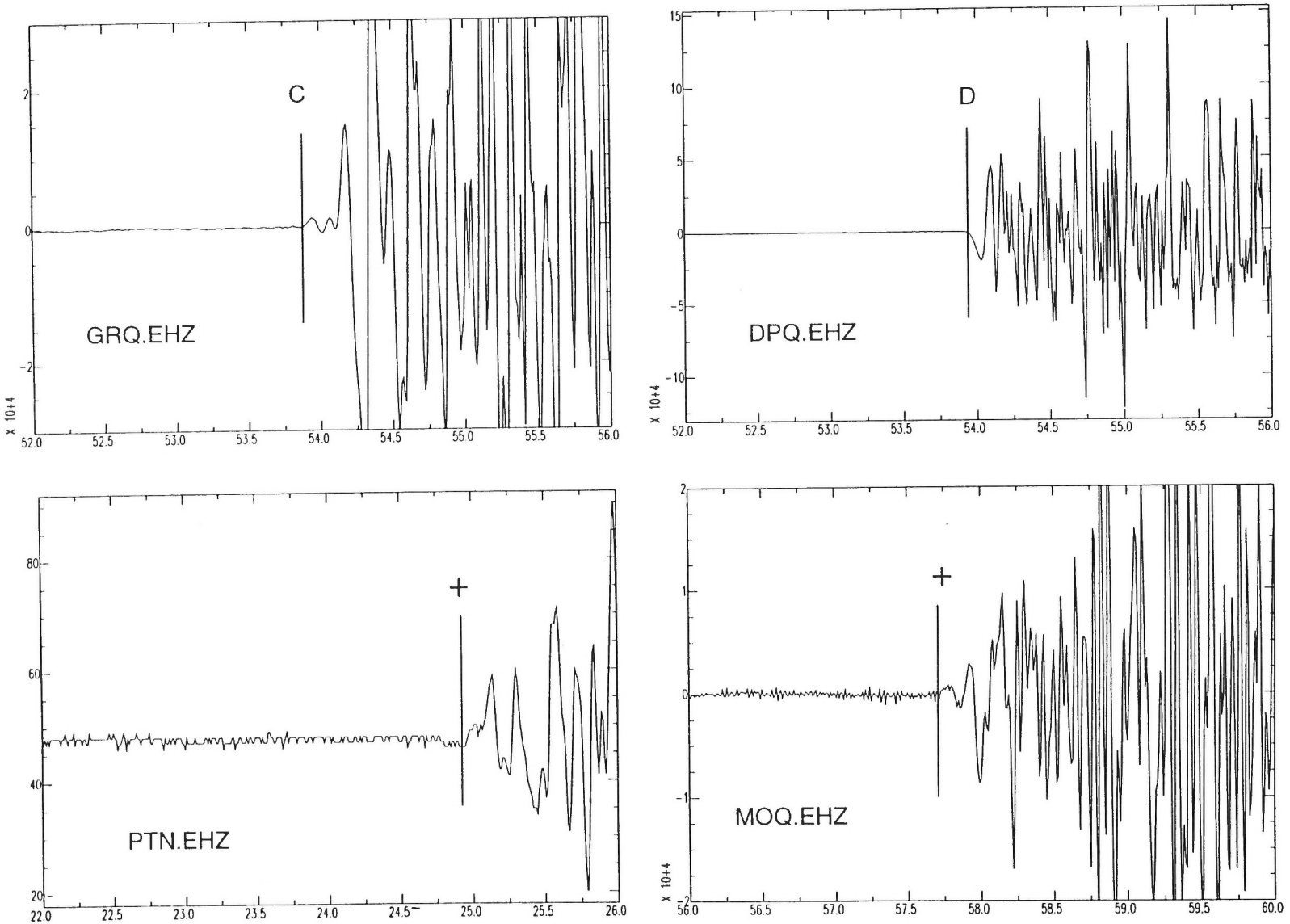

Figure 13c

Morin Heights, Quebec: 31 October 1999

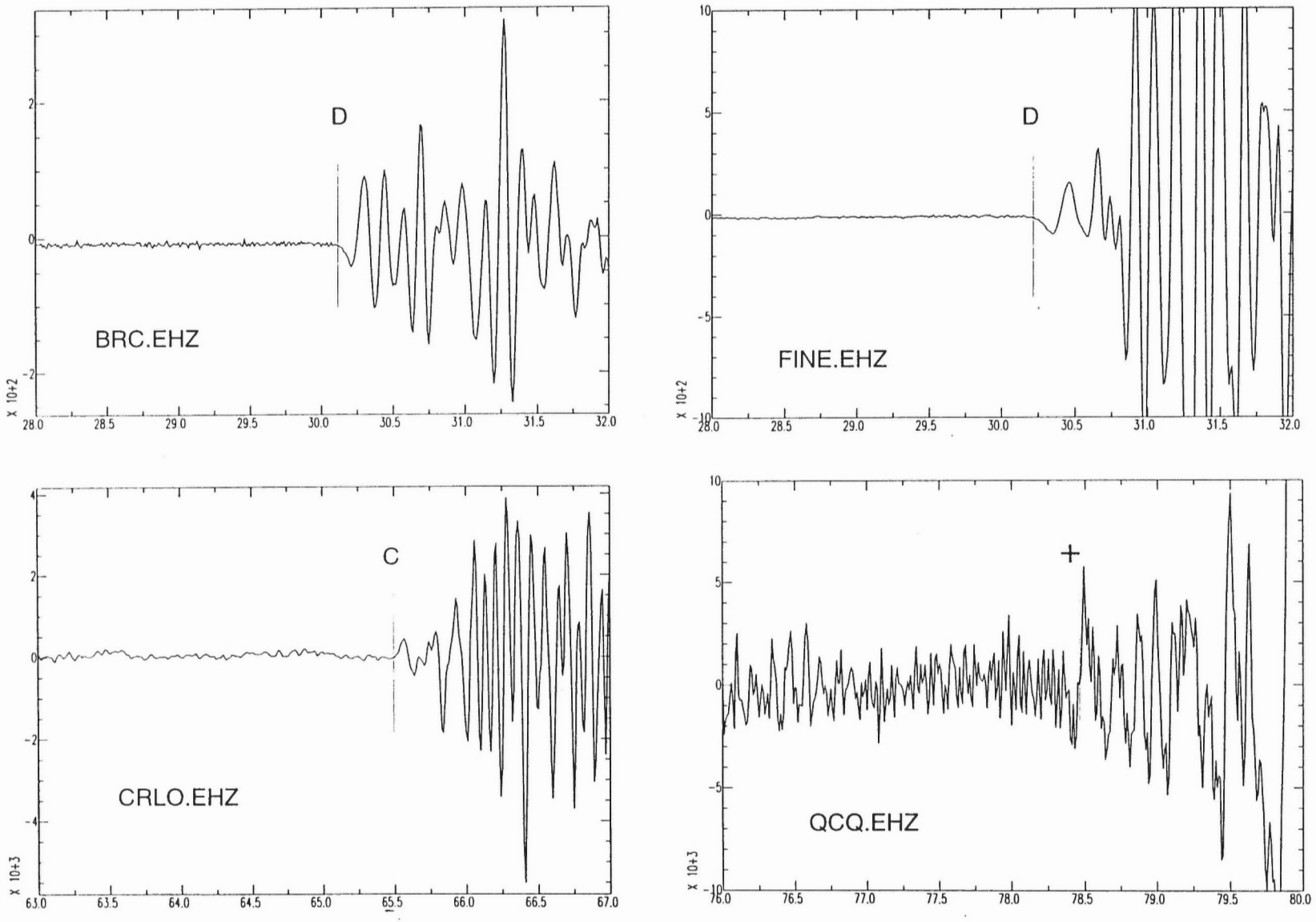

Figure 13d

Morin Heights, Quebec: 31 October 1999

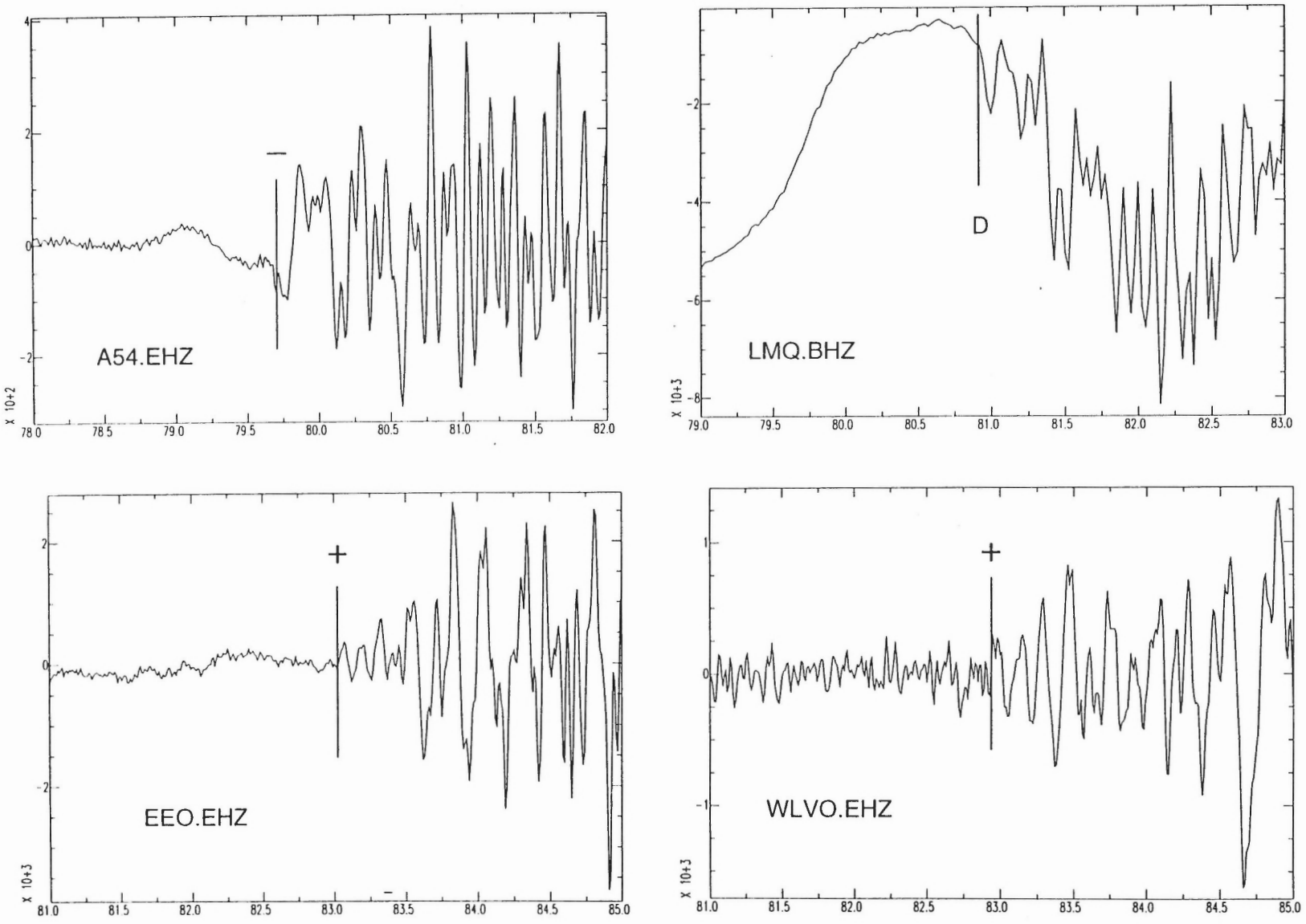

Figure 13e

Morin Heights, Quebec: 31 October 1999

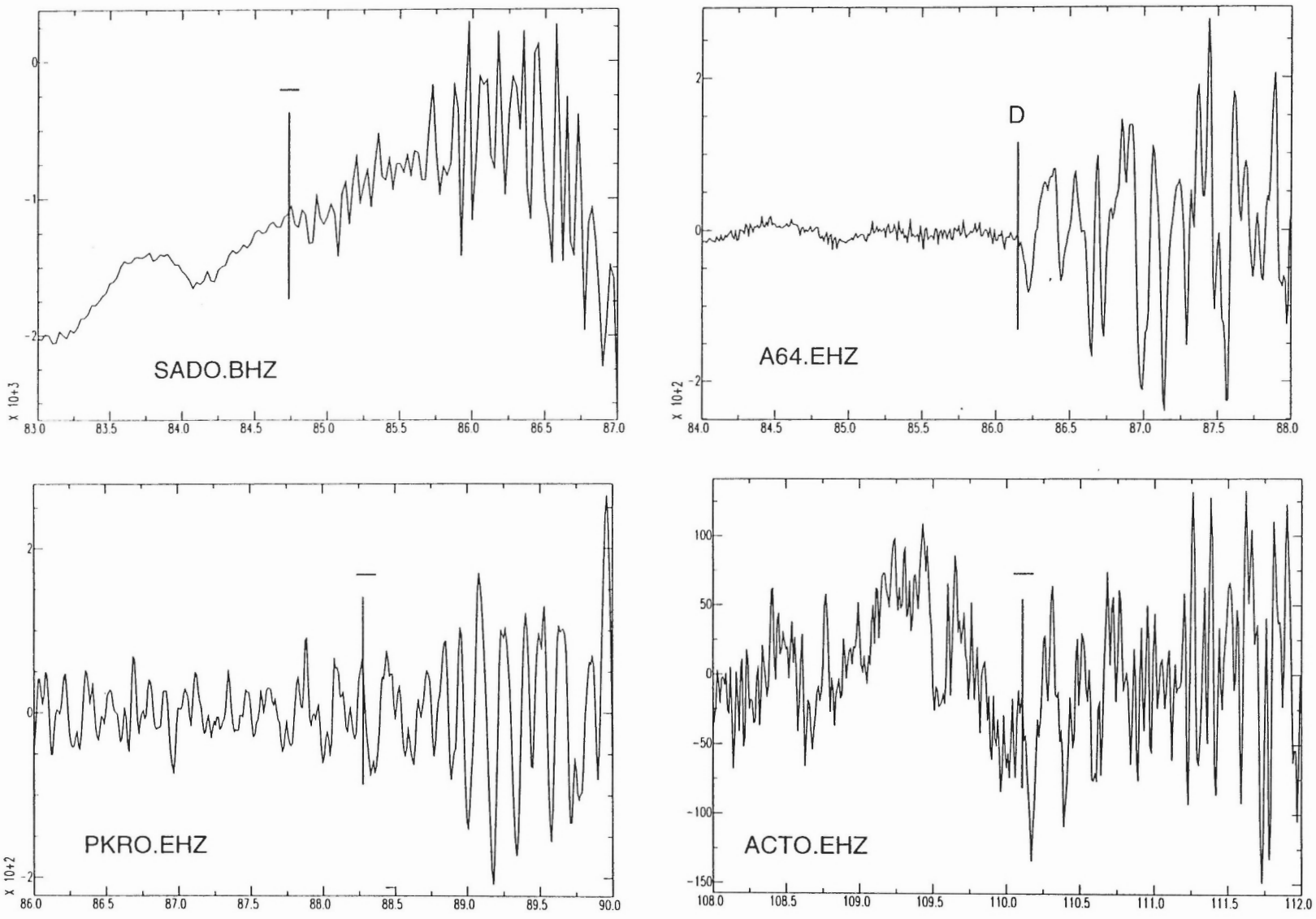

Figure 13f

Morin Heights, Quebec: 31 October 1999

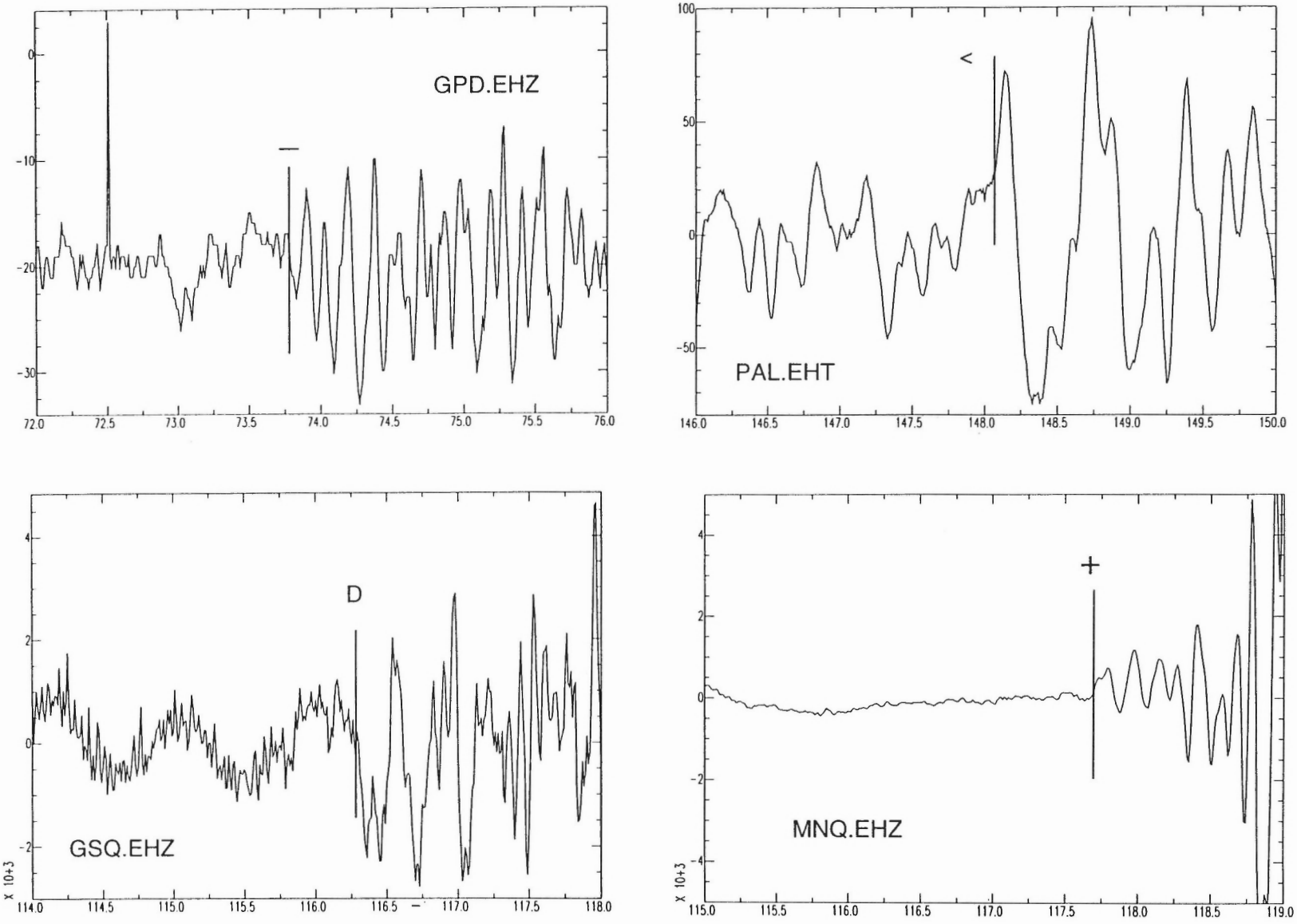

Figure 13g

Morin Heights, Quebec: 31 October 1999

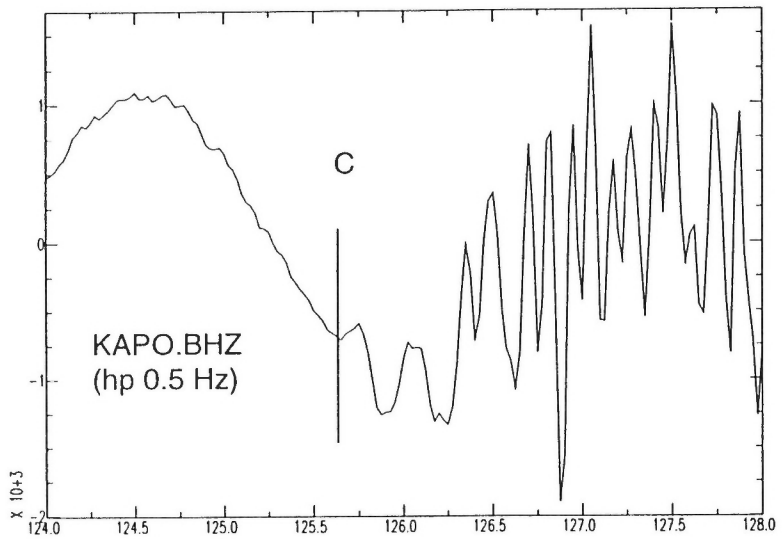

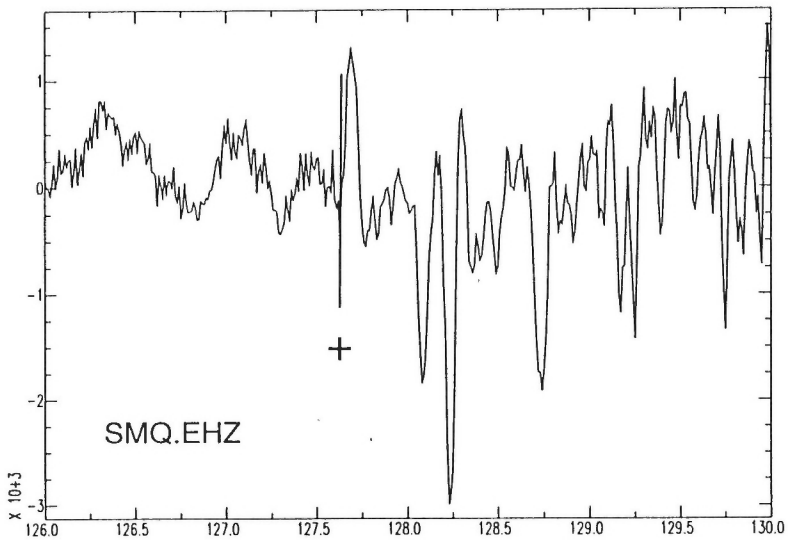

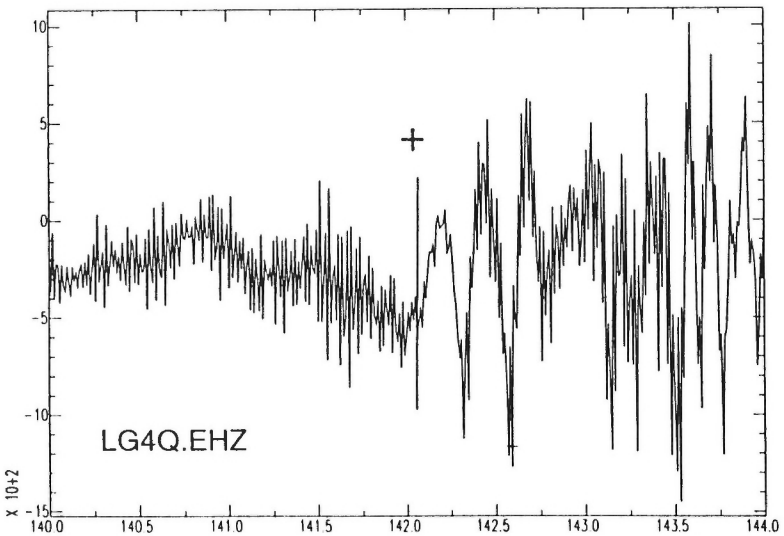

Figure 13h

Morin Heights, Quebec: 31 October 1999

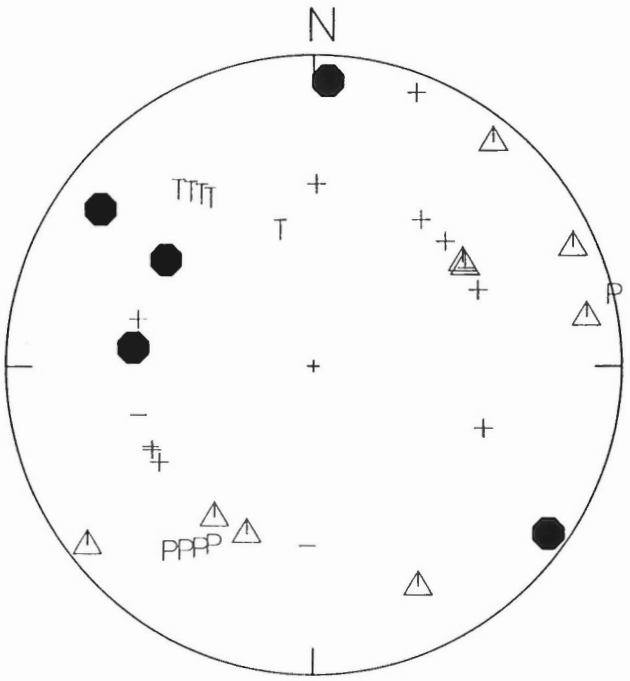

P and T axes

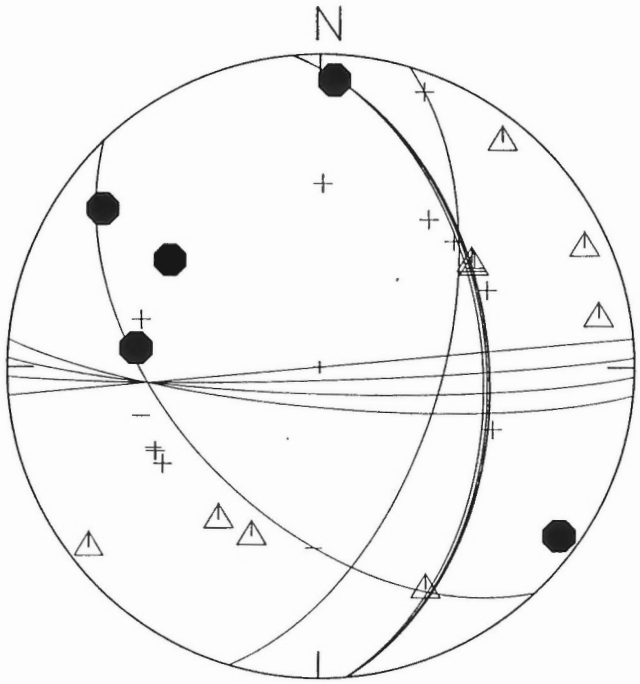

P nodal planes

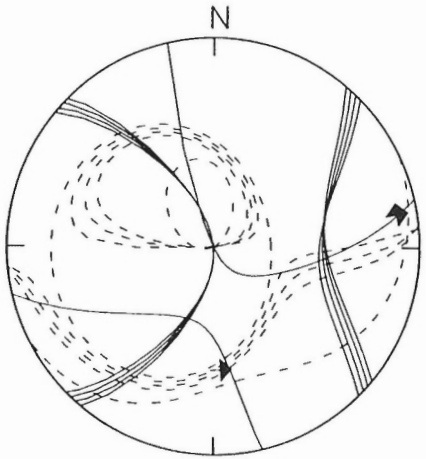

S nodal planes

Figure 14

2 NOVEMBER 1999: LAURENTIAN SLOPE

Seismic Zone: Laurentian Slope
Latitude: 45.20° N
Longitude: 56.08° W
Depth: 18 km (fixed)
Magnitude: 4.5 (M_L)
Origin Time: 08:45:21 (UT)
Comments:

Polarity Data

Station	Distance (km)	Azimuth (°)	Take-off Angle (°)	First Motion
STJN	368	43.1	49.1	C
GBN	427	275.0	49.1	D
DRLN	464	347.1	49.1	C
LMN	686	279.2	49.1	0
ICQ	972	303.6	49.1	+
SMQ	973	308.8	49.1	C
CNQ	1015	301.0	49.1	0
A21	1081	289.8	49.1	C
A64	1099	290.3	49.1	+
A54	1131	287.9	49.1	–
SCHQ	1318	328.3	49.1	+
GAC	1514	279.0	49.1	–

Focal Mechanism Solutions

total number solutions: 950
grid search: 5°
misfits: 0
comments:

Preferred solution:

Fault Planes:	insufficient data to determine
P-axis:	
Trend:	southern hemisphere
Plunge:	undetermined
T-axis:	
Trend:	probably NNW-NNE; anything in the NW to SE hemisphere is possible
Plunge:	undetermined
B-axis:	
Trend:	undetermined
Plunge:	not near vertical; not near horizontal if trend is N-NE or S-SW

Figure Captions:

Figure 15a-c. Digital seismograms from which polarity data were read by the authors.

Figure 16. Focal mechanism solutions. Lower hemisphere projection. The P axes are shown on the left and the T axes on the right. Data are also plotted. Solid symbols indicate compressional first motions and open symbols dilatations.

Laurentian Slope: 2 November 1999

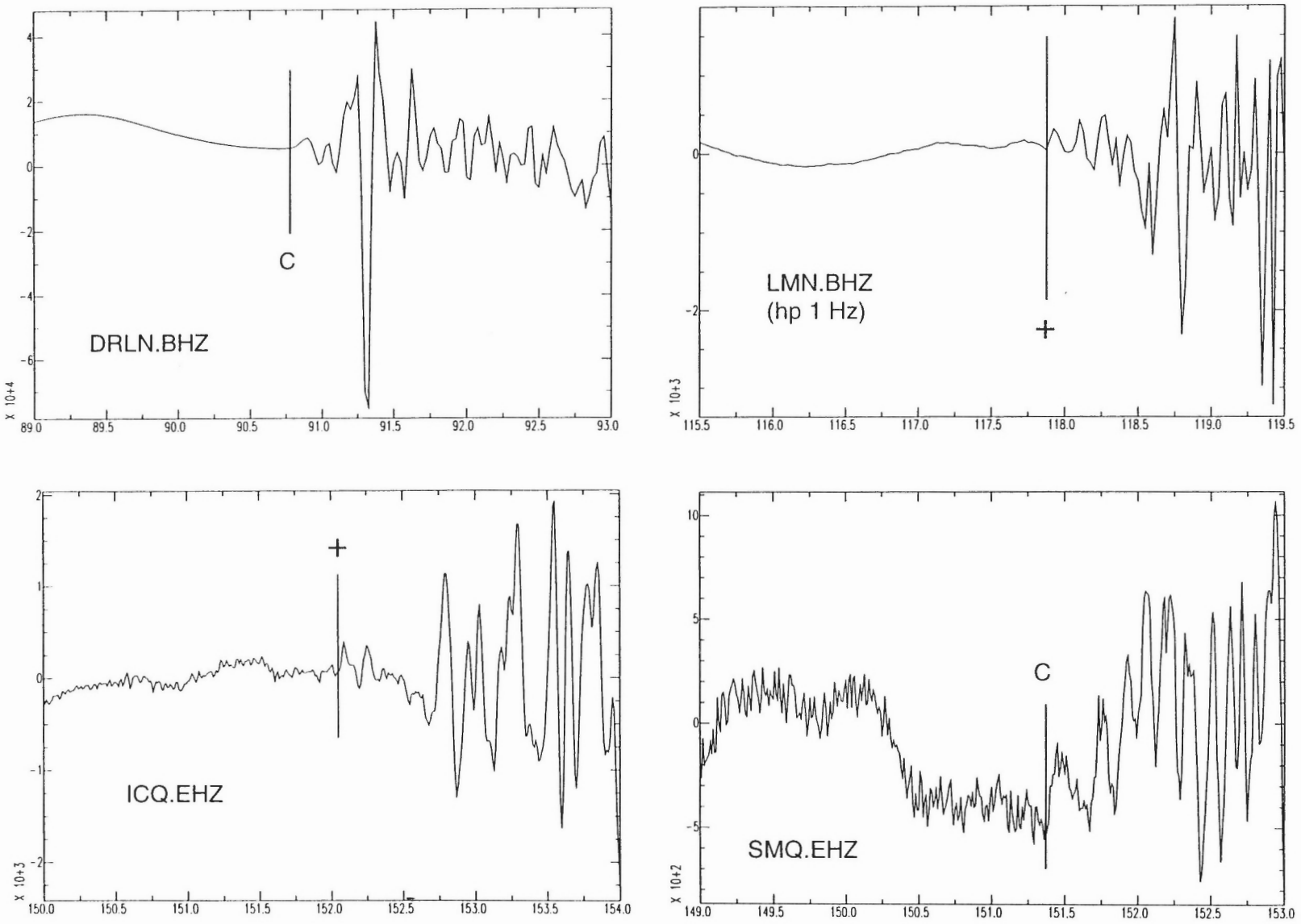

Figure 15a

Laurentian Slope: 2 November 1999

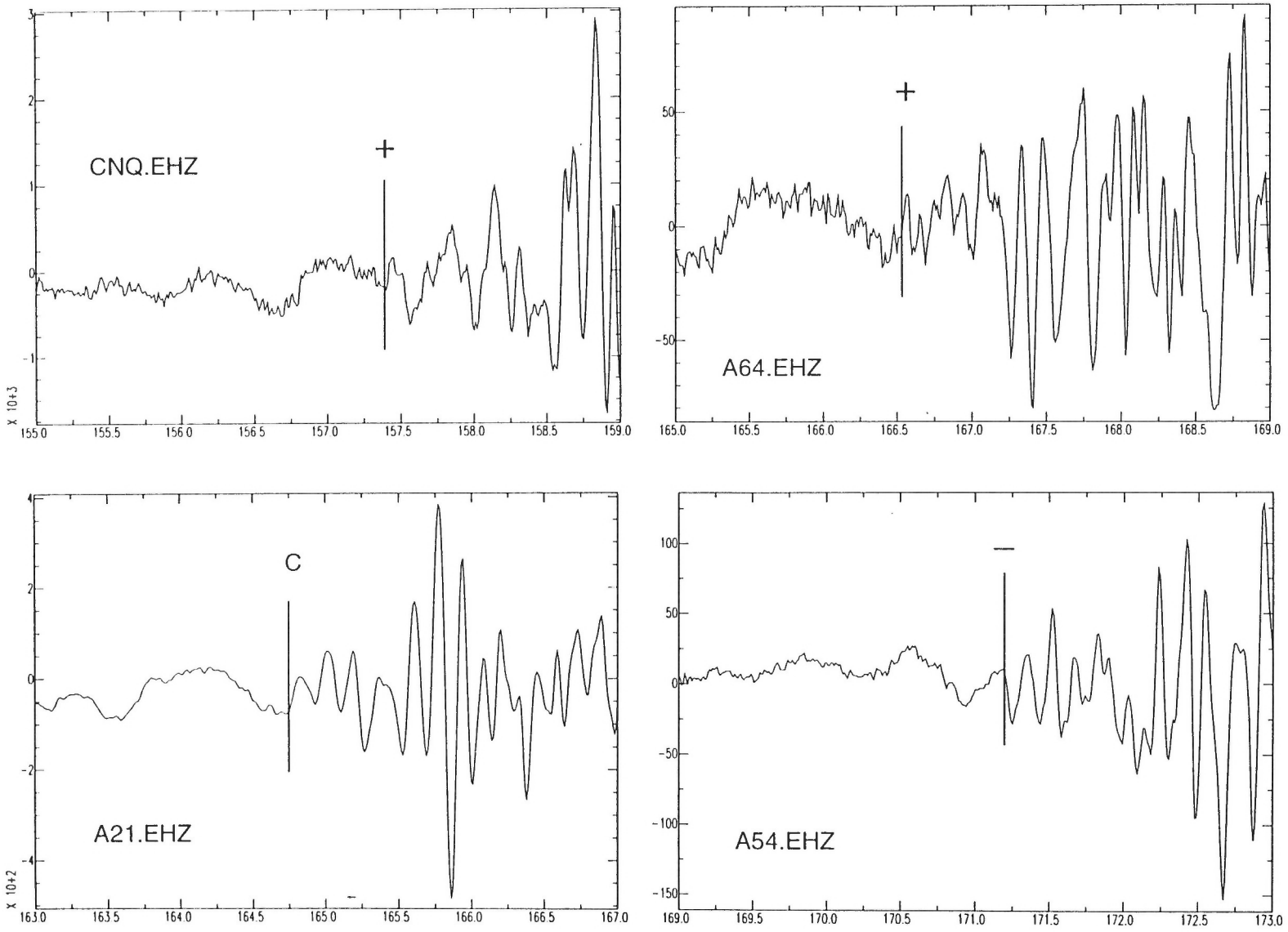

Figure 15b

Laurentian Slope: 2 November 1999

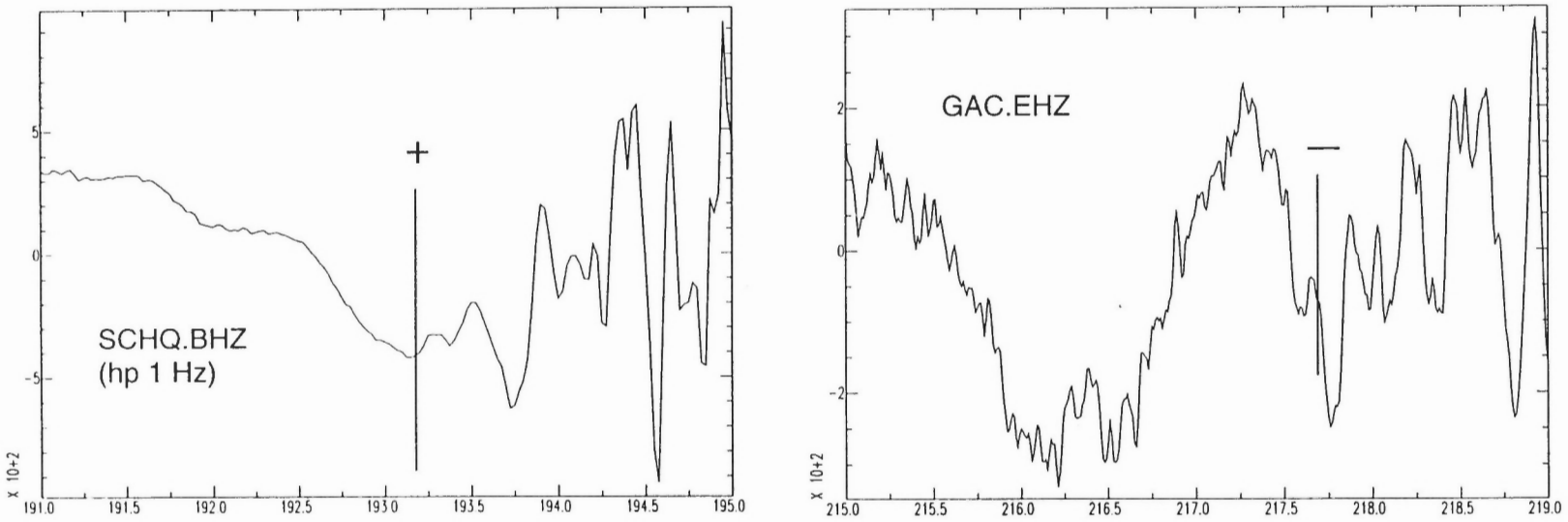

Figure 15c

2 November 1999: Laurentian Slope

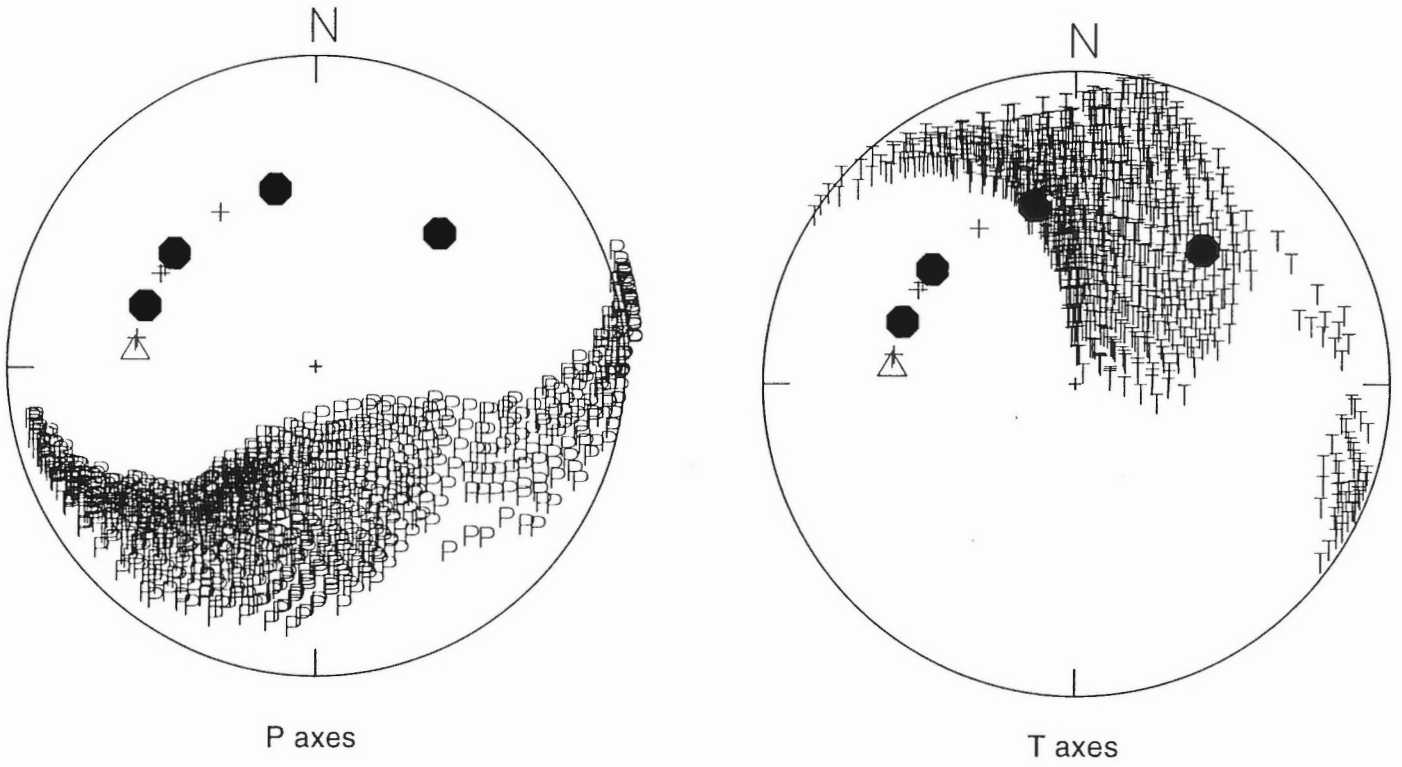

P axes

T axes

Figure 16

26 NOVEMBER 1999: LAKE ONTARIO

Seismic Zone: none
Latitude: 43.71 N
Longitude: 78.99° W
Depth: 10 km
Magnitude: 3.8 (m_N)
Origin Time: 22:33:01 (UT)
Comments: included (despite magnitude < 4) because felt in the Toronto area

Polarity Data

Station	Distance (km)	Azimuth (°)	Take-off Angle (°)	First Motion
PKRO	29	347.5	–71.2	C
WLVO	54	63.0	–79.4	D
EFO	73	200.9	–82.2	C
RD01	76	244.6	–82.5	–
RD02	84	239.0	–83.2	D
RD04	84	223.2	–83.2	D
ACTO	87	263.2	–83.4	D
RD03	97	233.3	–84.1	D
TYNO	98	226.6	–84.2	D
SADO	119	354.3	–85.2	C
SADO	119	354.3	–85.2	F
SADO	119	354.3	–85.2	<
BRCO	206	287.7	49.1	C
CRLO	289	25.6	49.1	D
TRQ	448	49.8	49.1	D

Focal Mechanism Solutions

Strike	Dip	Rake
120.65	60.50	–28.34
122.74	66.07	–26.34

total number solutions:	2
grid search:	5°
# misfits:	0
comments:	looked at data from USGS stations BINY, AAM and LBNH but were unable to pick polarities; examined data from entire SONT network but could pick polarities only from those stations noted in list
	SADO S polarities from rotated horizontal records

Preferred solution: solutions similar; use solution 1

Plane 1:		
	Strike:	120°
	Dip:	61°
	Rake:	–28°
Plane 2:		
	Strike:	226°
	Dip:	66°
	Rake:	–147°
P-axis:		
	Trend:	85°
	Plunge:	40°
T-axis:		
	Trend:	352°
	Plunge:	3°
B-axis:		
	Trend:	258°
	Plunge:	50°

Quality: B good azimuthal coverage but a few gaps; redundancy at some azimuths

Figure Captions:

Figure 17a-d. Seismograms from which polarity data were read by the authors.

Figure 18. Focal mechanism solutions. Lower hemisphere projection. The P and T axes are shown on the left and the P nodal planes on the right. Data are also plotted. Solid symbols indicate compressional first motions and open symbols dilatations. The S data are plotted on the lower figure with the arrows pointing in the direction of the first motion. Solid lines represent SH nodal planes and dashed lines the SV nodal planes.

Lake Ontario: 26 November 1999

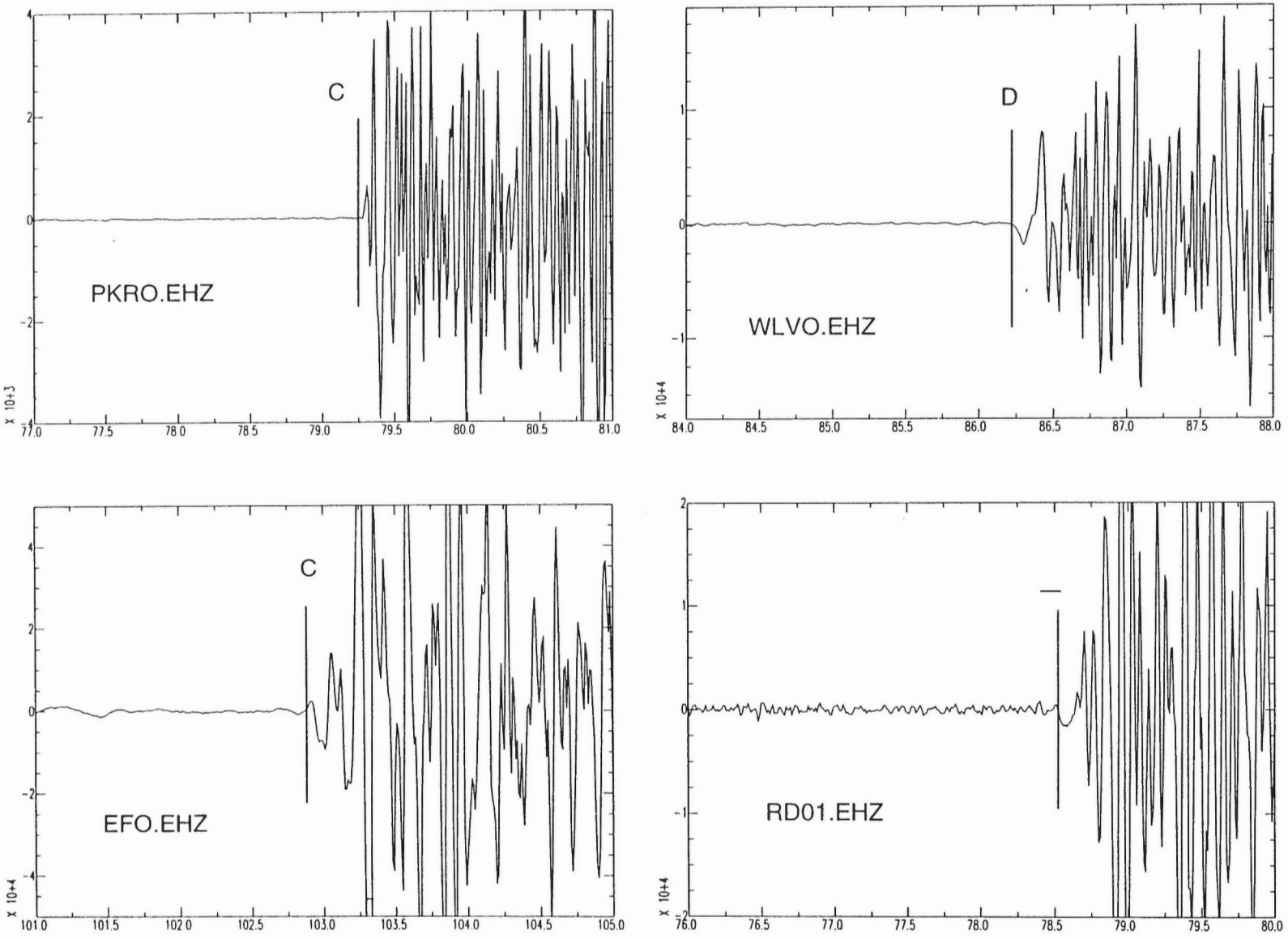

Figure 17a

Lake Ontario: 26 November 1999

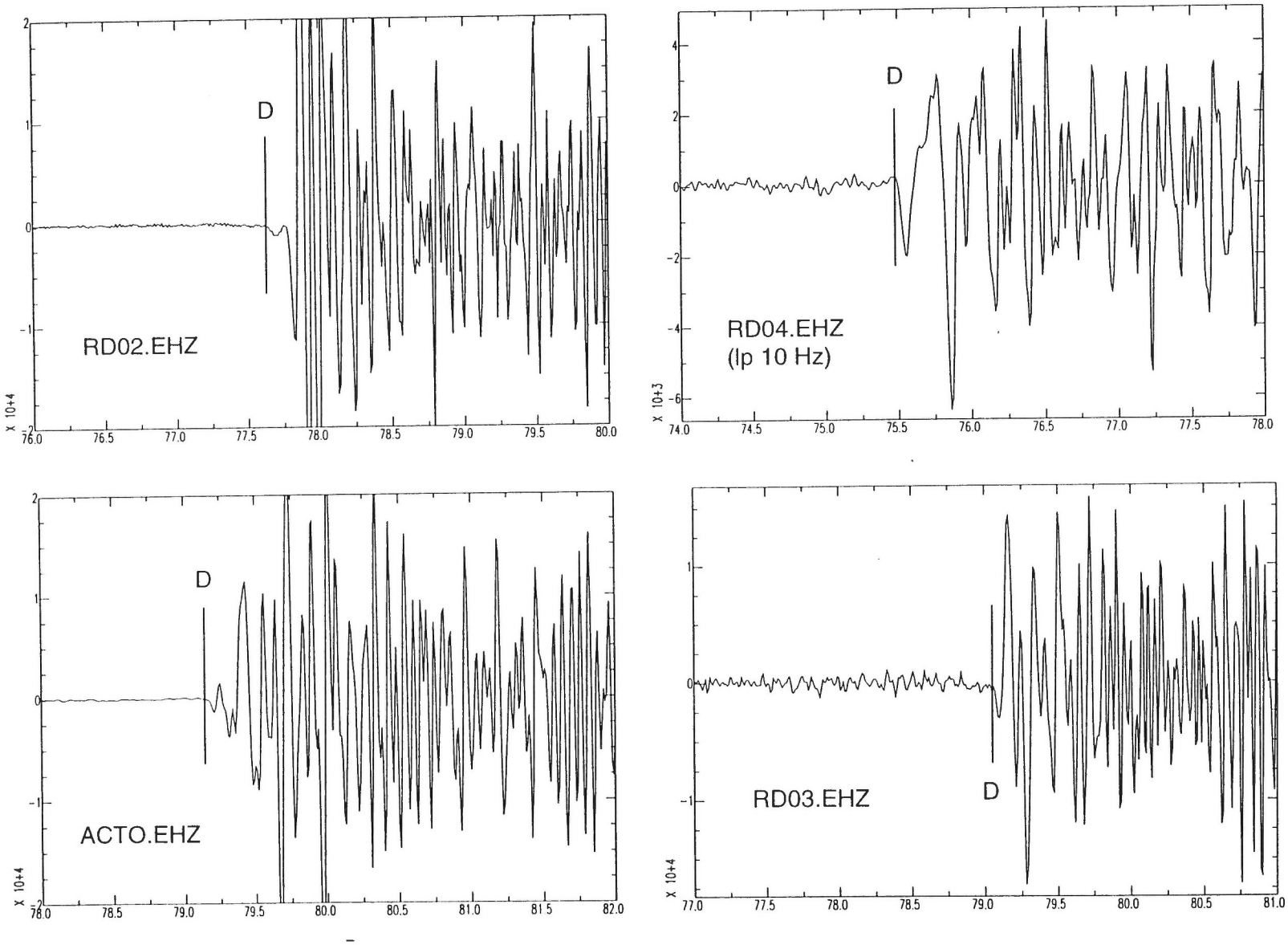

Figure 17b

Lake Ontario: 26 November 1999

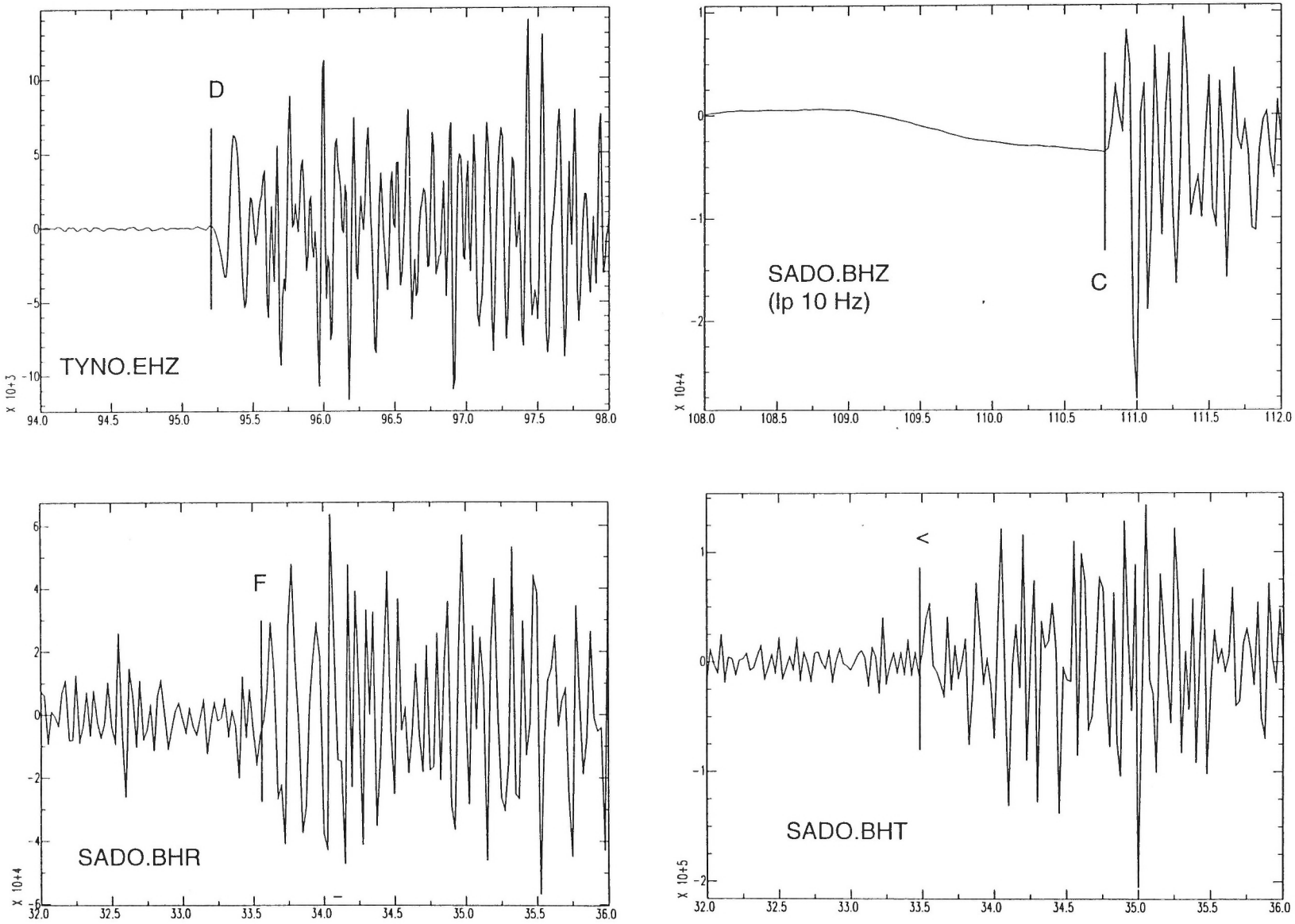

Figure 17c

Lake Ontario: 26 November 1999

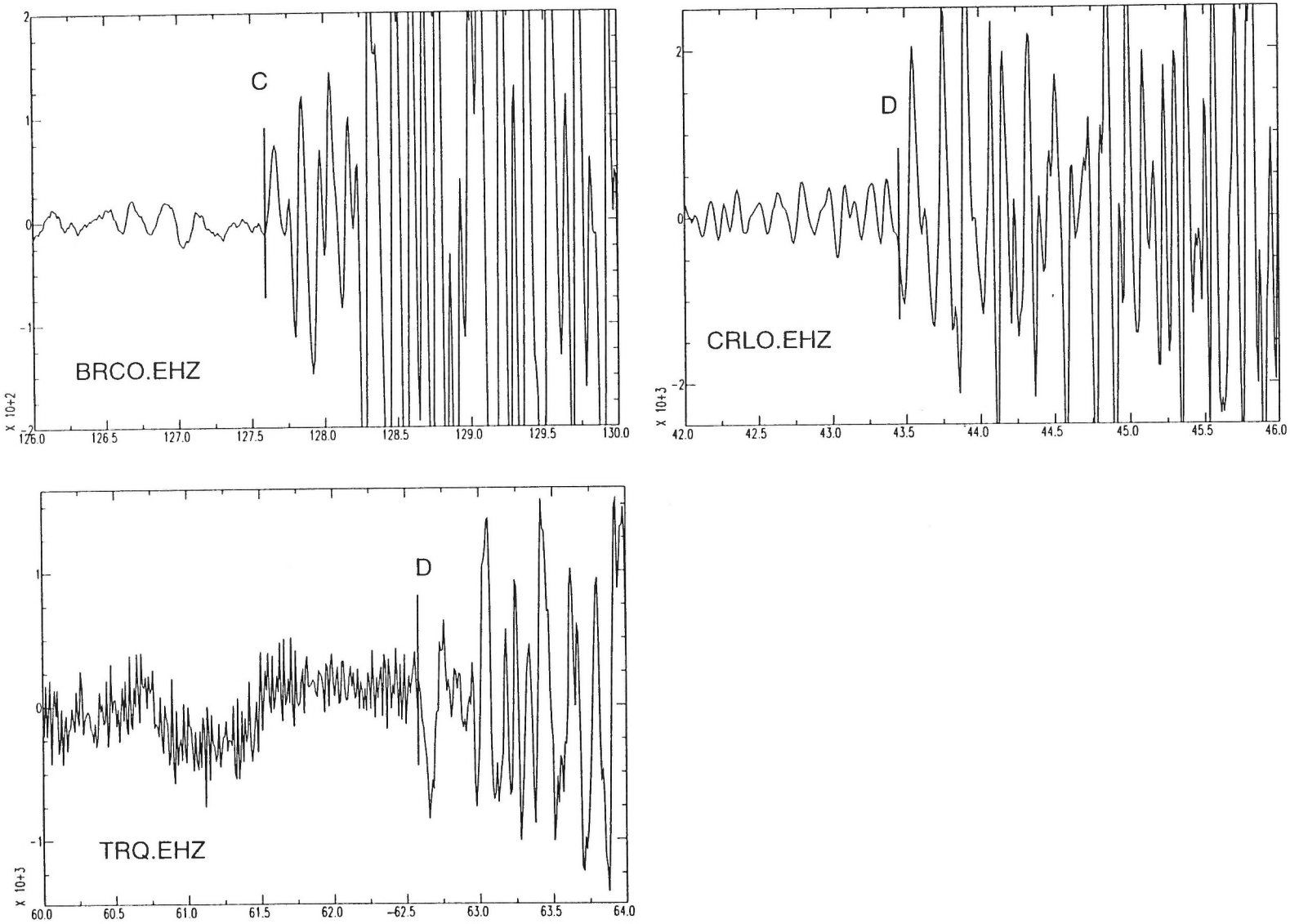

Figure 17d

Lake Ontario: 26 November 1999

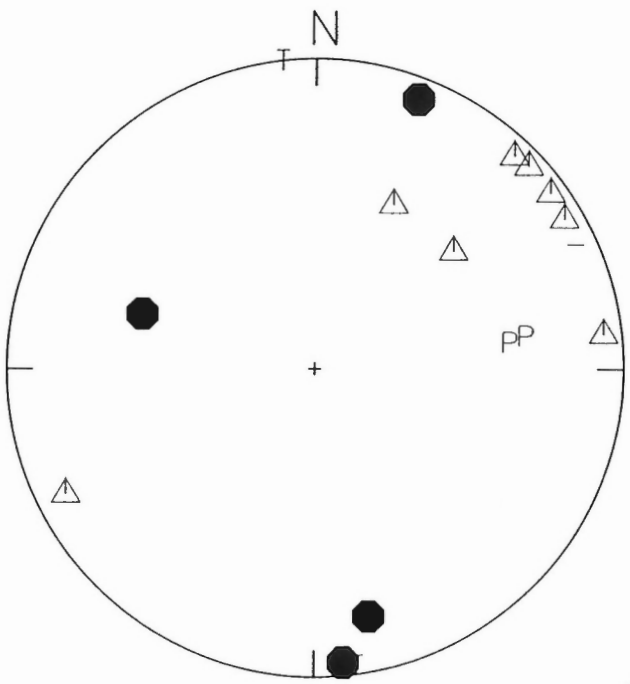

P and T axes

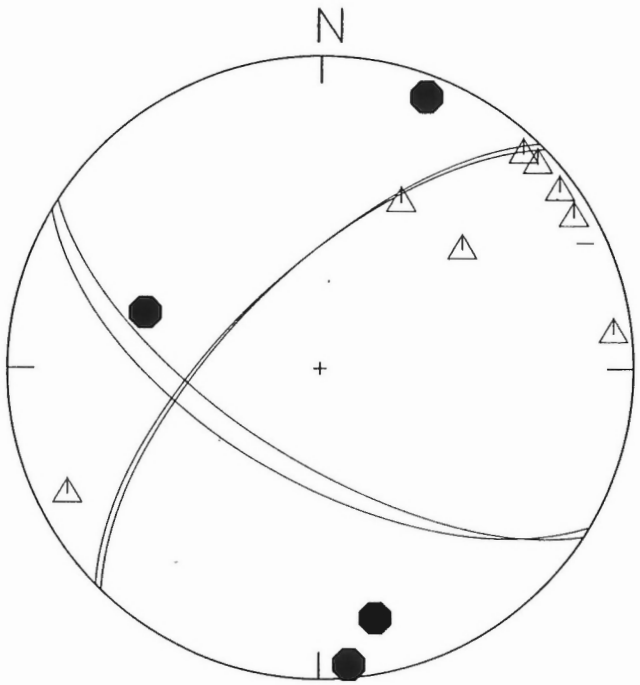

P nodal planes

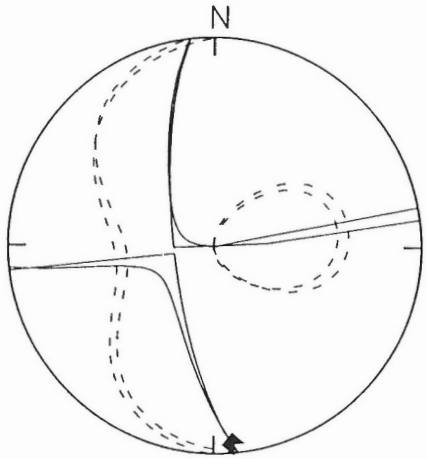

S nodal planes

Figure 18

7 DECEMBER 1999: McCLURE STRAIT, NORTHWEST TERRITORIES

Seismic Zone: none
Latitude: 75.38° N
Longitude: 120.44° W
Depth: 18 km (fixed)
Magnitude: 5.7 (M_L) 4.7 (m_b NEIS)
Origin Time: 05:35:58 (UT)
Comments: a magnitude 4.0 (M_L) aftershock followed at 06:02:49 (UT); focal mechanism not determined for aftershock due to insufficient data; first motion at RES same as mainshock; both are technically outside our area of interest

Polarity Data

Station	Distance (km)	Azimuth (°)	Take-off Angle (°)	First Motion
RES	736	83.6	49.1	C
INK	909	216.3	49.1	D
IGL	1435	97.8	49.1	D
YKW3	1450	168.0	49.1	D
COLA	1539	235.2	49.1	D
WHY	1741	207.1	49.1	D
HYT	1760	211.8	49.1	D
FNBC	1846	184.4	49.1	+
FCC	2141	135.4	45.1	D
FRB	2292	96.2	40.5	C
FFC	2435	150.5	39.0	D
EDM	2494	168.8	38.7	D
KUQ	2835	103.5	34.5	D
WALA	2948	169.6	34.0	–
ULM	3018	144.2	33.2	D
SOLO	3110	139.2	33.0	C

Station	Distance (km)	Azimuth (°)	Take-off Angle (°)	First Motion
LG4Q	3135	114.2	33.0	C
TBO	3303	133.9	33.0	C
SCHQ	3206	150.0	32.9	+
KAPO	3367	127.3	32.7	D
MNQ	3593	110.5	32.4	C
EEO	3738	122.2	29.4	C
CNQ	3761	107.9	29.3	+
DAQ	3790	112.2	29.3	–
GRQ	3817	118.4	29.3	+
A64	3839	110.8	29.2	C
CRLO	3841	120.5	29.2	+
A61	3848	111.1	29.2	C
A21	3857	110.6	29.2	C
A54	3864	111.6	29.2	+
DPQ	3885	114.8	29.1	D
TRQ	3890	117.1	29.1	C
A11	3892	111.5	29.1	C
GAC	3922	118.5	29.1	C
SADO	3935	123.4	29.1	C
DRLN	4025	96.6	28.7	C
MOQ	4042	115.1	28.8	C
LMN	4178	106.6	28.5	C

Focal Mechanism Solutions

Strike	Dip	Rake
168.02	60.50	42.39
130.45	79.45	44.01
134.07	82.95	44.56
164.25	66.07	39.32
141.00	83.59	39.57
148.77	77.30	38.26
156.14	71.25	36.01
160.34	74.24	37.25
163.97	71.25	36.01

total number solutions: 9
grid search: 5°
misfits: 2
comments: ALE not available
misfits for all solutions at KUQ and KAPO

Preferred solution: solutions similar; use closest to mean

Plane 1:
- Strike: 149°
- Dip: 77°
- Rake: 38°

Plane 2:
- Strike: 49°
- Dip: 53°
- Rake: 164°

P-axis:
- Trend: 274°
- Plunge: 16°

T-axis:
- Trend: 16°
- Plunge: 36°

B-axis:
- Trend: 164°
- Plunge: 50°

Quality: B: many observations and good azimuthal redundancy but poor overall azimuthal coverage

Figure Captions:

Figure 19a-j. Seismograms from which polarity data were read by the authors.

Figure 20. Focal mechanism solutions. Lower hemisphere projection. The P and T axes are shown on the left and the P nodal planes on the right. Data are also plotted. Solid symbols indicate compressional first motions and open symbols dilatations.

McClure Strait, NWT: 7 December 1999

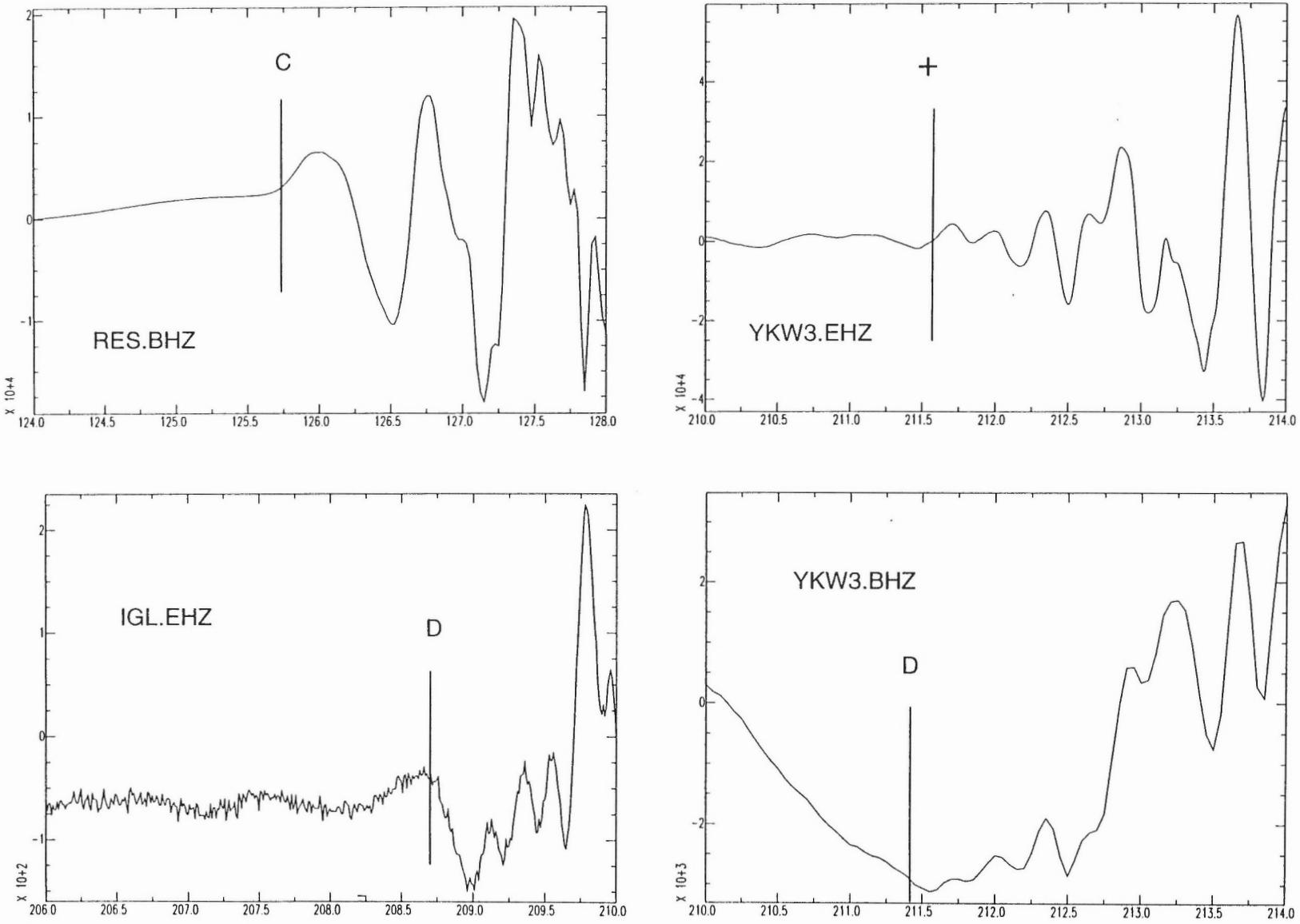

Figure 19a

McClure Strait, NWT: 7 December 1999

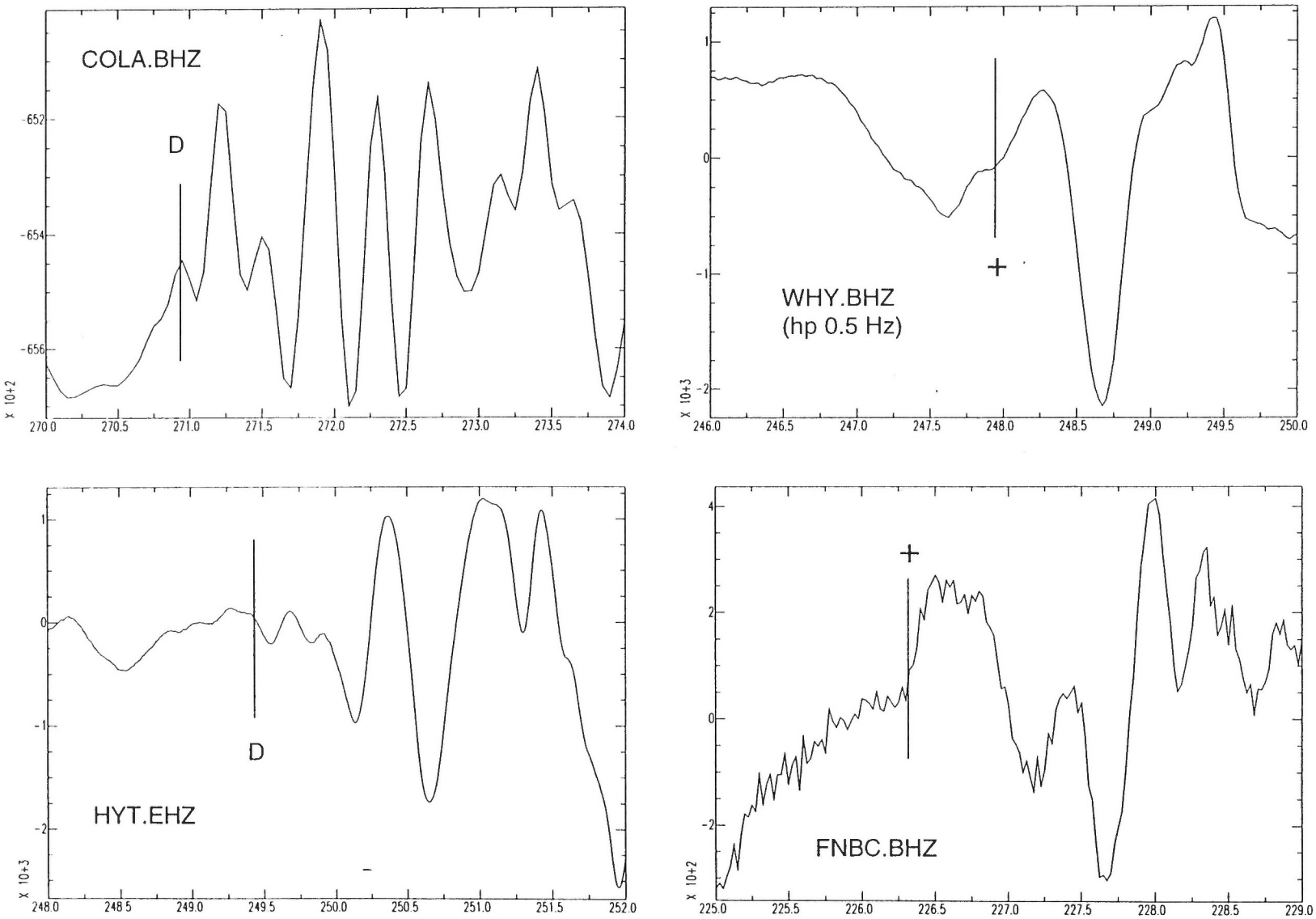

Figure 19b

McClure Strait, NWT: 7 December 1999

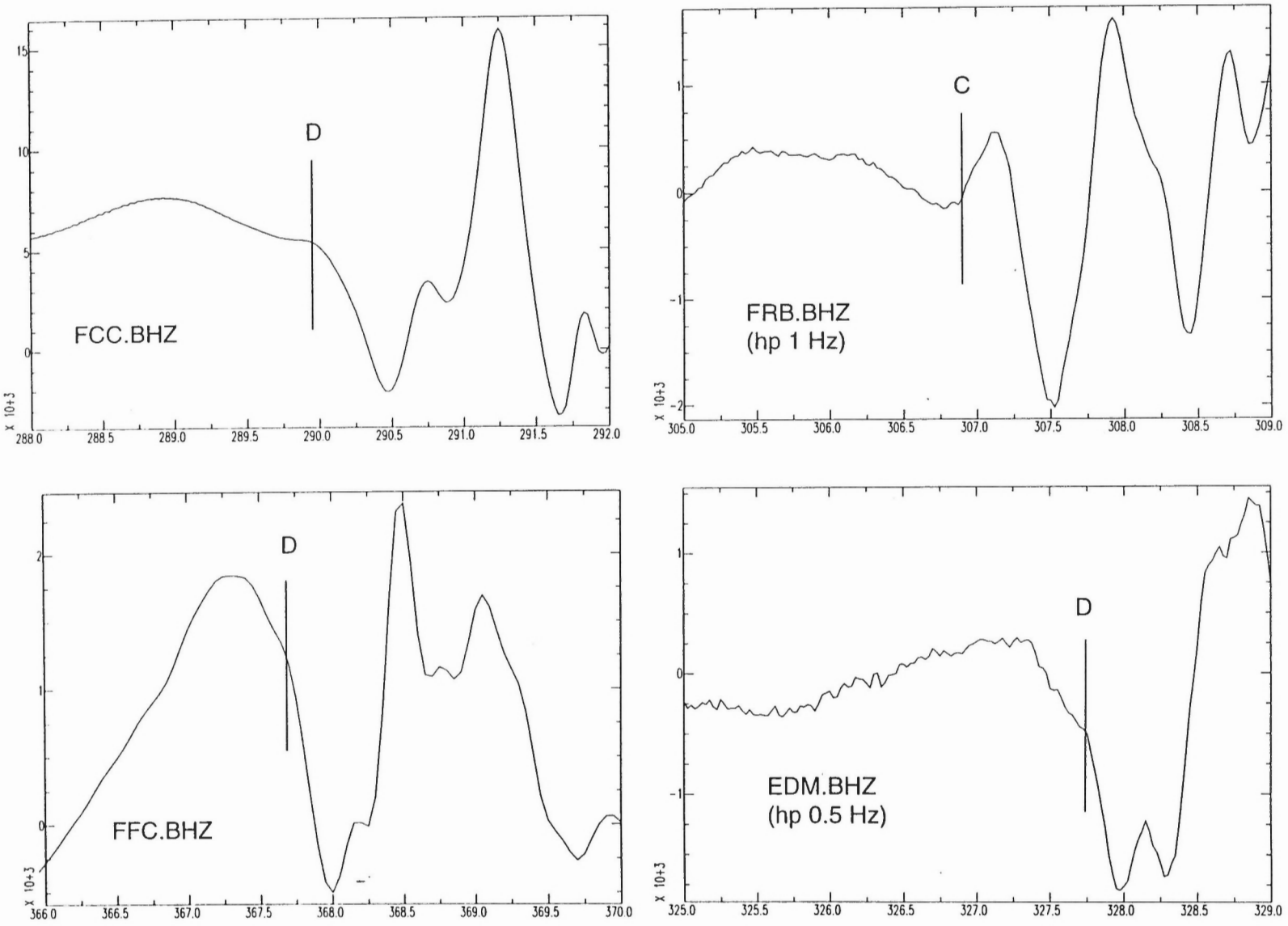

Figure 19c

McClure Strait, NWT: 7 December 1999

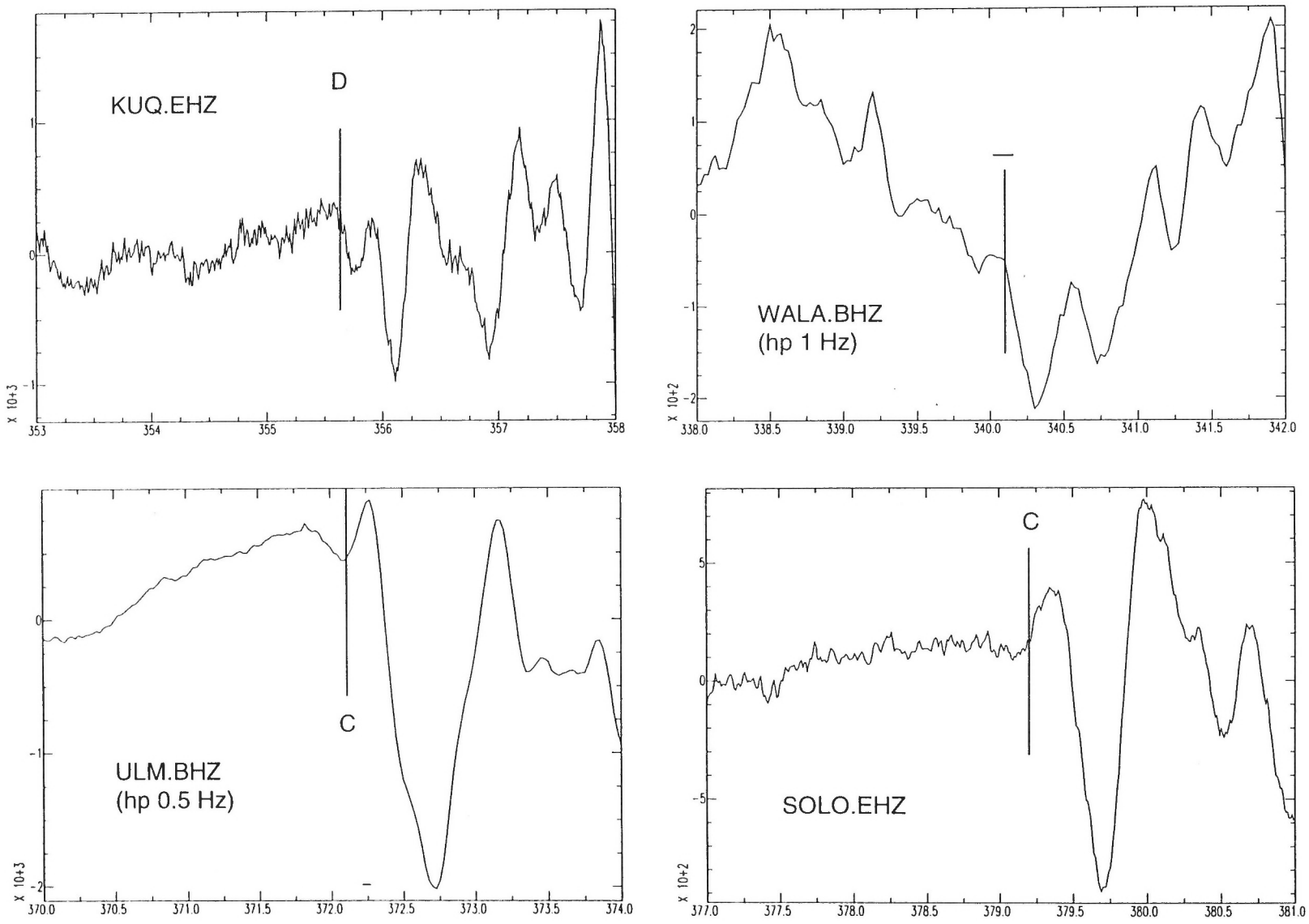

Figure 19d

McClure Strait, NWT: 7 December 1999

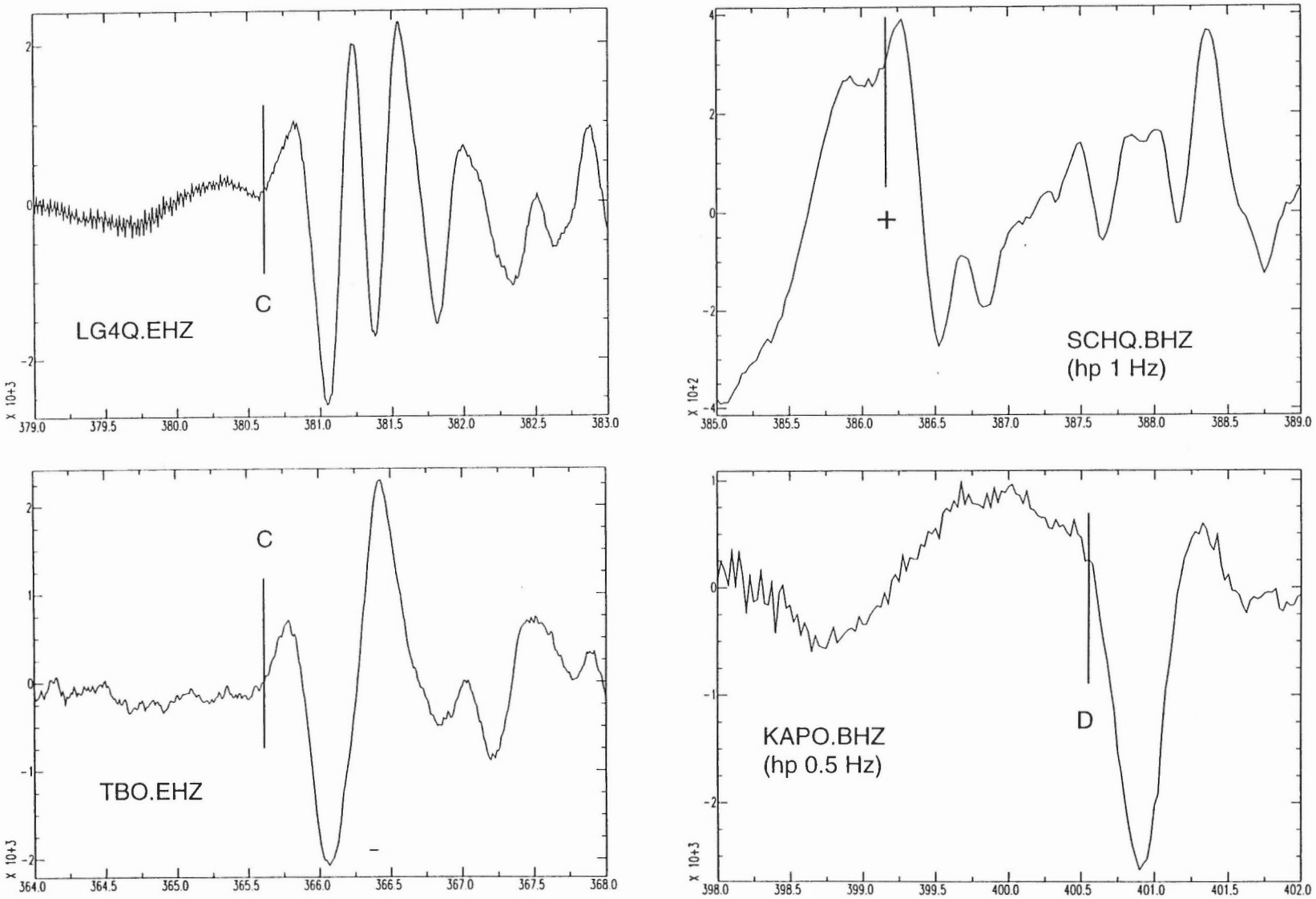

Figure 19e

McClure Strait, NWT: 7 December 1999

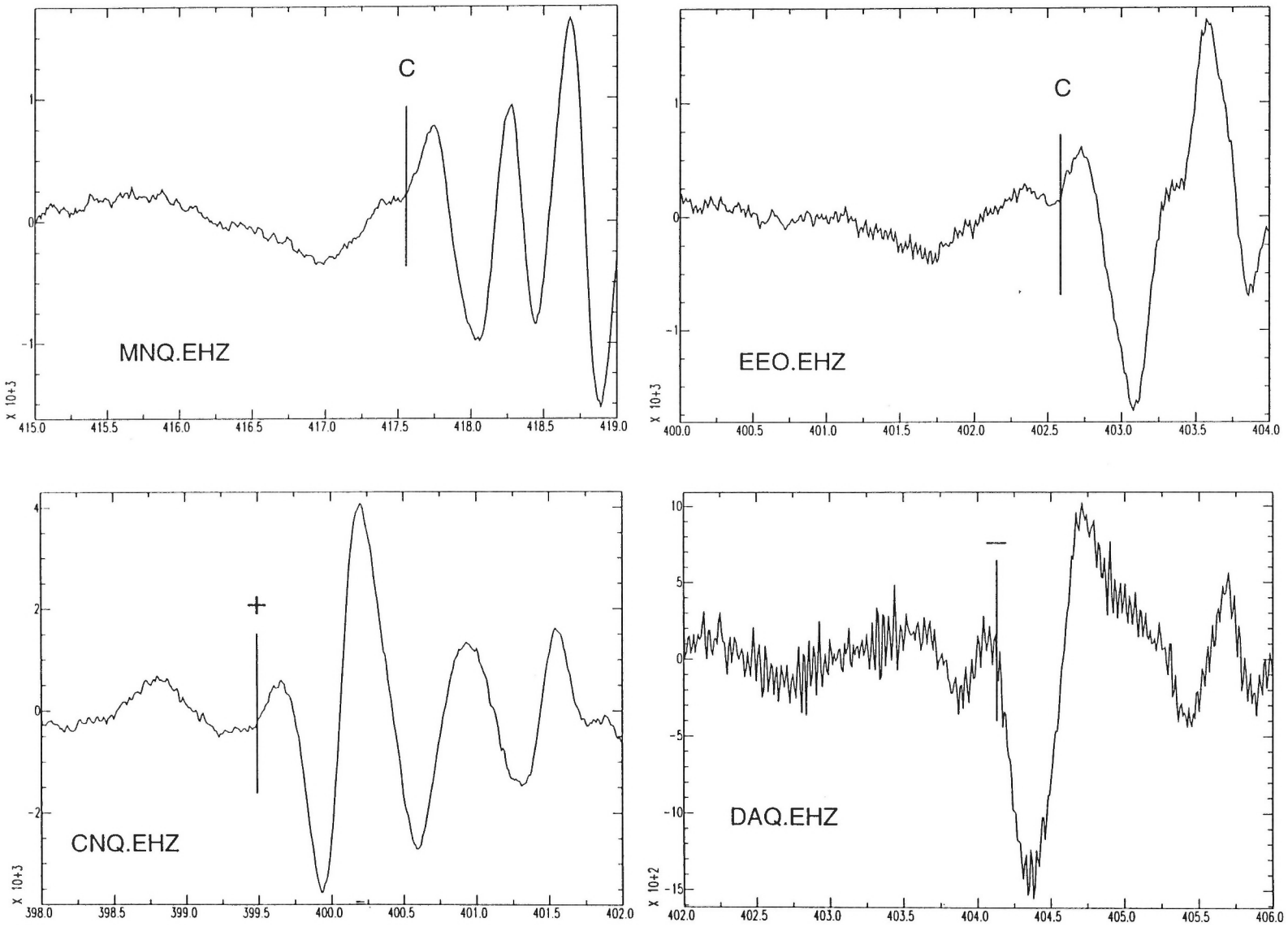

Figure 19f

McClure Strait, NWT: 7 December 1999

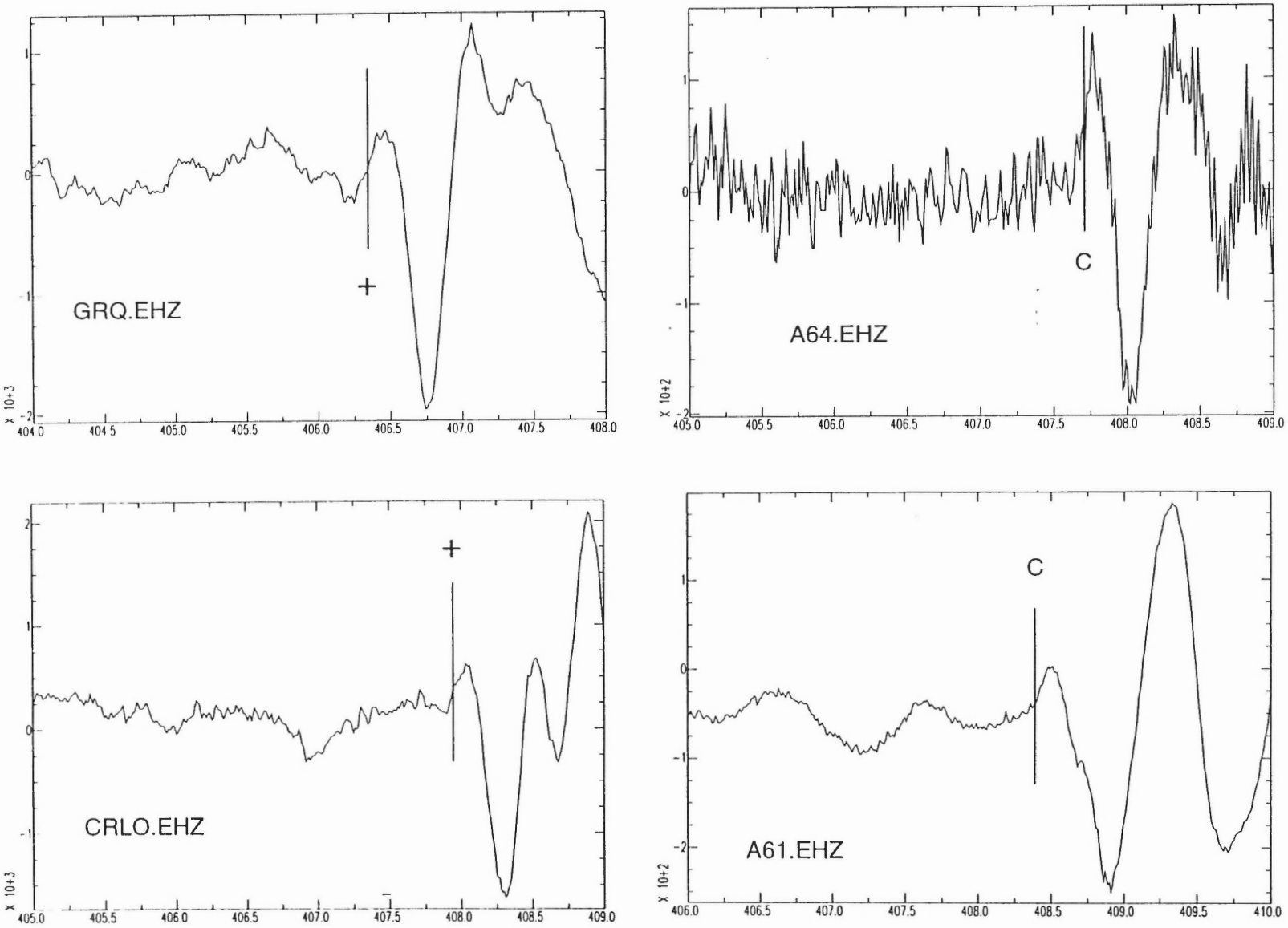

Figure 19g

McClure Strait, NWT: 7 December 1999

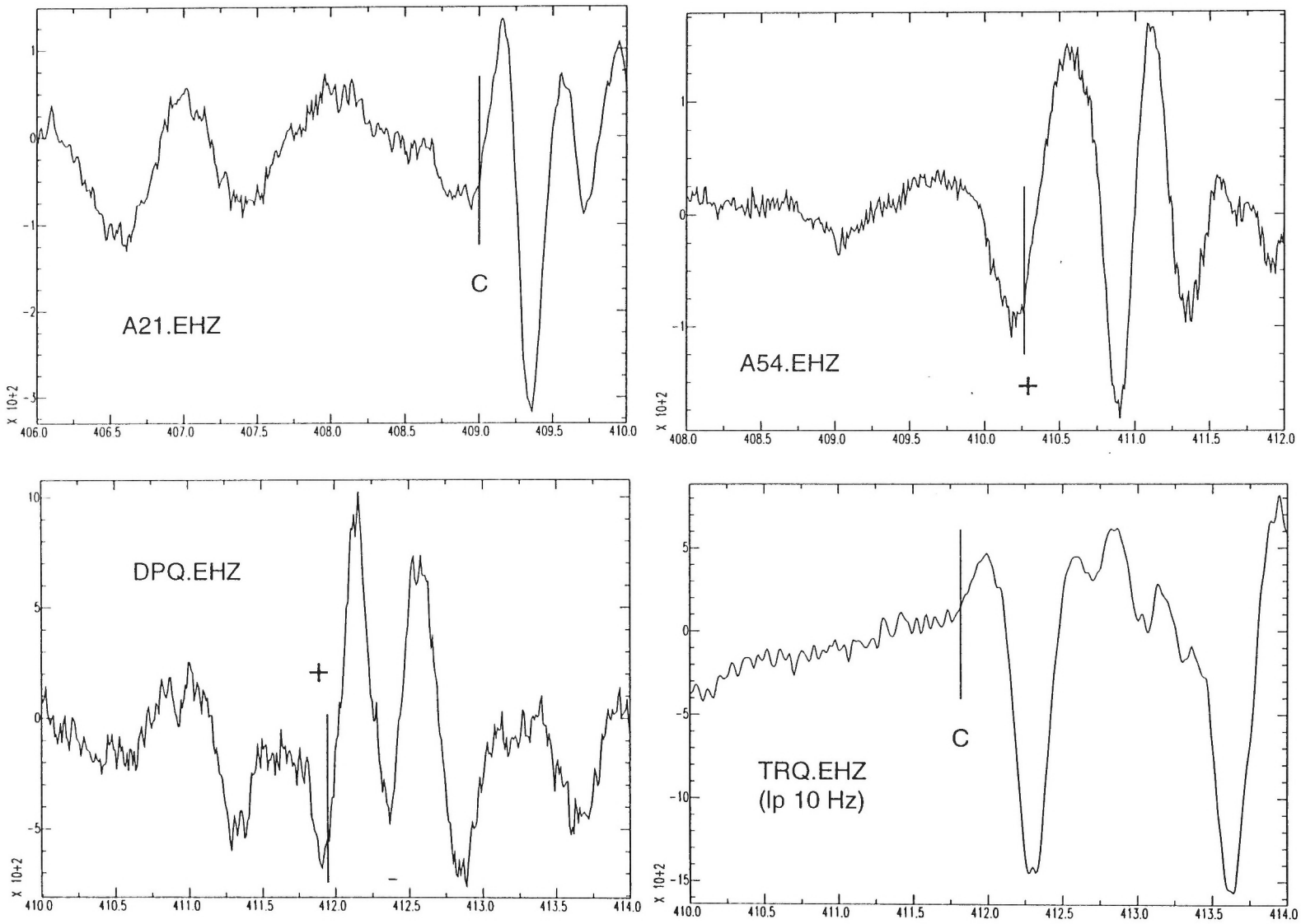

Figure 19h

McClure Strait, NWT: 7 December 1999

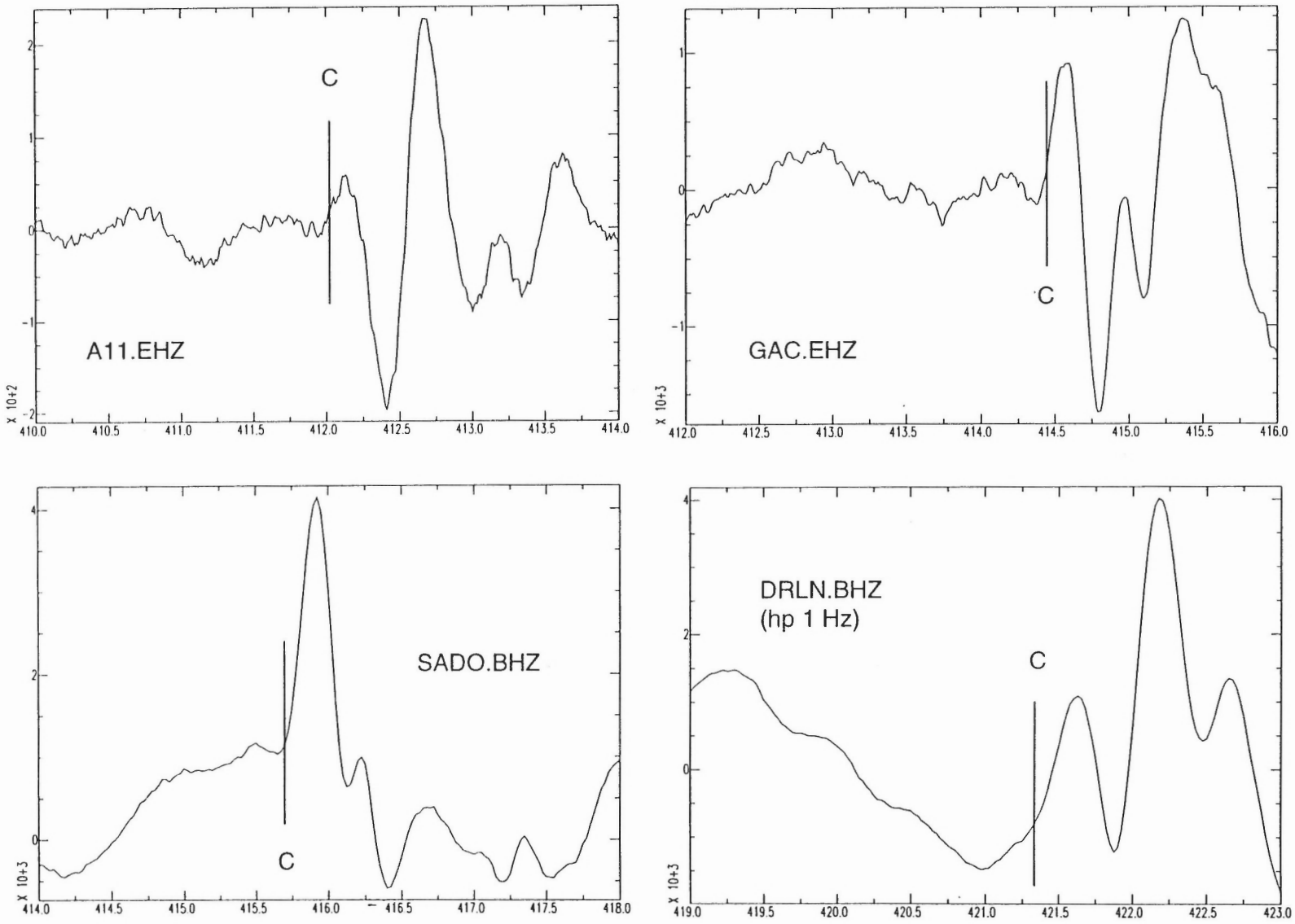

Figure 19i

McClure Strait, NWT: 7 December 1999

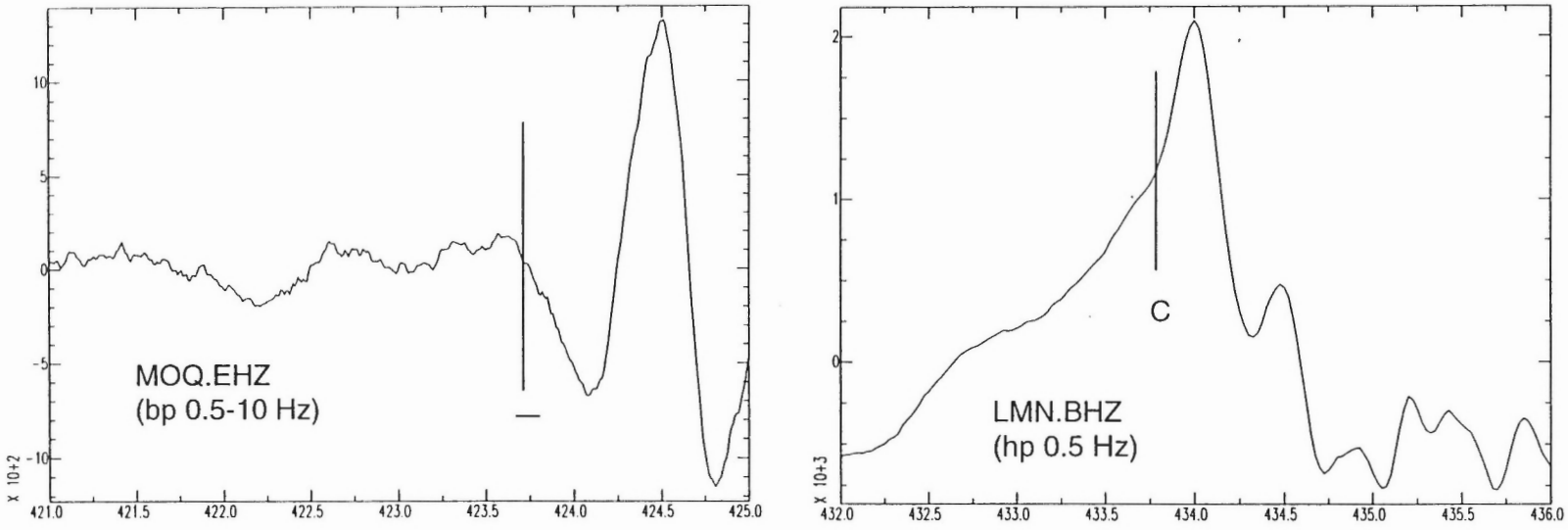

Figure 19j

McClure Strait, NWT: 7 December 1999

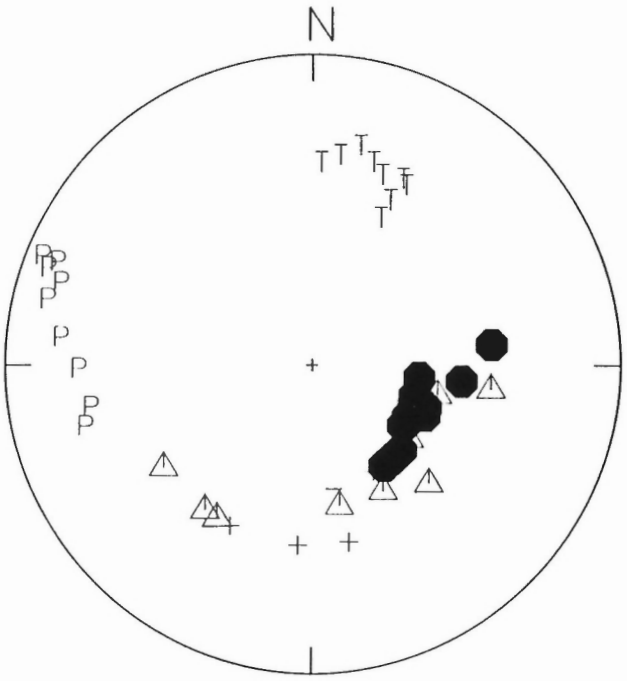

P and T axes

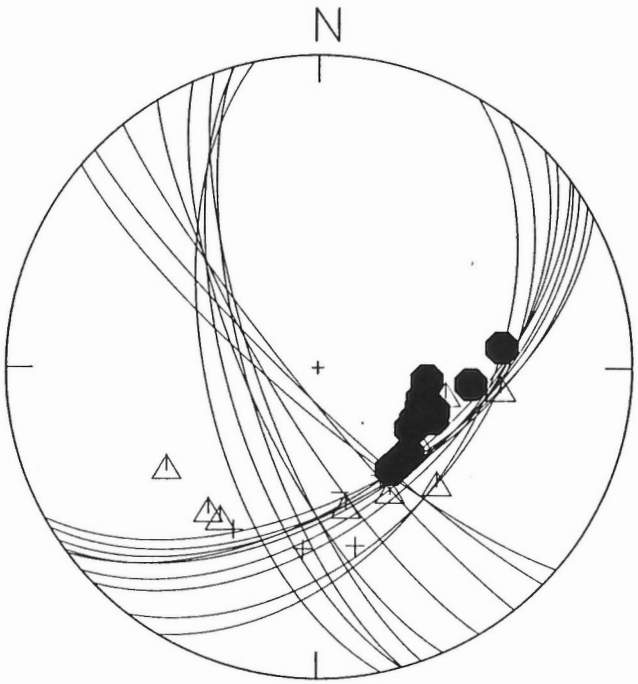

P nodal planes

Figure 20

DISCUSSION

Southeast Mainland: As was the case in previous focal mechanism studies, the southeastern mainland was the region where it was most consistently possible to obtain well constrained focal mechanisms. We obtained solutions for all three events. Event 990316 is one of the few earthquakes in the Lower St. Lawrence seismic zone for which a focal mechanism has been determined. The mechanism implies a combination of strike-slip and thrust motion. One of the nodal planes is roughly parallel to the trend of the St. Lawrence River. The existing mechanisms for lower St. Lawrence earthquakes vary in detail but most have one nodal plane striking approximately parallel to the St. Lawrence River and have a thrust component of slip (Adams *et al.*, 1988, 1989; Bent and Drysdale, 2000).

Event 991031 is typical of western Quebec earthquakes in that it has a primarily thrust mechanism with one nodal plane striking roughly northwest (for example, Wahlström, 1987; Adams *et al.*, 1988, 1989; Adams, 1991; Bent, 1996a, b; Bent and Perry, 1999; Bent *et al.*, 1999; Bent and Drysdale, 2000). This earthquake was of particular interest as it was the fourth earthquake of magnitude greater than 4.0 to occur in the region of Ste-Agathe-des-Monts during the last four years. All have typical western Quebec focal mechanisms but are not identical to each other (Bent *et al.*, 1999). The focal mechanism of 991031 most closely resembles that of 970524, which is also the closest event to it spatially.

Event 991126 beneath Lake Ontario is the smallest of the events studied. We obtained an oblique-normal mechanism with faulting on either a SE-NW or SW-NE striking plane. The normal component of faulting is somewhat unusual for the southeastern mainland, which is dominated by thrust faulting. However, the P axis orientation is within the range expected for southeastern Canada. A preliminary focal mechanism for another event beneath Lake Ontario (20000524, Bent and Drysdale, unpublished data) indicates either thrust motion on a steeply dipping northwest-striking plane or oblique thrust on a shallowly dipping northeast striking plane.

Southeast Offshore: Because of poor azimuthal coverage it is difficult to obtain well constrained first motion focal mechanisms for small earthquakes in the Laurentian Slope region. We were unable to determine a focal mechanism for event 991102. Constraints that could be placed on the stress axes were minimal.

Labrador Sea- Baffin Bay: It is rarely possible to determine focal mechanisms from first motion data for small to moderate Baffin Bay earthquakes due to poor azimuthal coverage. We were not able to obtain a focal mechanism for the Baffin Bay event 990221. Azimuthal coverage for the Labrador Sea is somewhat better although the larger magnitude (5.3) of the Labrador Sea event 990729 was also a factor in being able to obtain a solution. Both nodal planes indicate a combination of strike-slip and normal faulting. Previous studies of Labrador Sea earthquakes have found evidence for all types of faulting (Bent and Hasegawa, 1992; Bent and Perry, 1999, 2000; Bent and Drysdale, 1999). The P-axis trend of 90° is in the range of typical values for eastern Canada.

Far North: We were able to determine focal mechanisms for two of the three events in this region. As was seen in previous studies, the likelihood of obtaining a solution is a combination of earthquake magnitude and location. Not surprisingly, it becomes easier to determine focal mechanisms as the magnitude increases. It is also generally easier to obtain solutions for events in the central and western part of this region than for the

east due to differences in azimuthal coverage. A mechanism could not be determined for the magnitude 4.0 event 990302 on Devon Island.

Event 990101 in the Arctic Ocean was the result of either strike-slip faulting along an east-west striking plane or oblique thrust motion along a near north-south striking plane. There are no focal mechanisms for events very near the epicenter of 990101 but those for events in adjacent regions exhibit many similarities to that of event 990101. Event 96022 of Bent and Perry (1999) near Melville Island (to the south of 990101) also had one nodal plane indicative of strike-slip faulting on an east-west plane. Hasegawa (1977) obtained primarily strike-slip mechanisms for four events in the Byam Martin Channel (southeast of 990101). Similarly, Bent and Perry (2000) found evidence for strike-slip (or oblique thrust) faulting in the Byam Martin Channel.

Our focal mechanism for event 991207 in the McClure Strait is indicative of oblique thrust faulting on a plane striking near east-west or northeast-southwest. This mechanism is similar to those of the events discussed in the previous paragraph, all of which occurred in the regions just to the east of 991207.

Figure 21. Focal mechanism solutions for earthquakes in the southeastern mainland. Lower hemisphere projection with shaded regions representing compressional quadrants. In this and subsequent figures black shading is used for A and B quality solutions, gray shading for C and D quality and a question mark (?) Indicates that a solution could not be determined. Symbol size is scaled to magnitude. Earthquakes are identified by date of occurrence.

Figure 22. Focal mechanism solutions for earthquakes in the southeastern offshore region. Format is the same as for Figure 21.

Figure 23. Focal mechanism solutions for earthquakes in the Labrador Sea to Baffin Bay region. Format is the same as for Figure 21.

Figure 24. Focal mechanism solutions for earthquakes in the far north. Format is the same as for Figure 21.

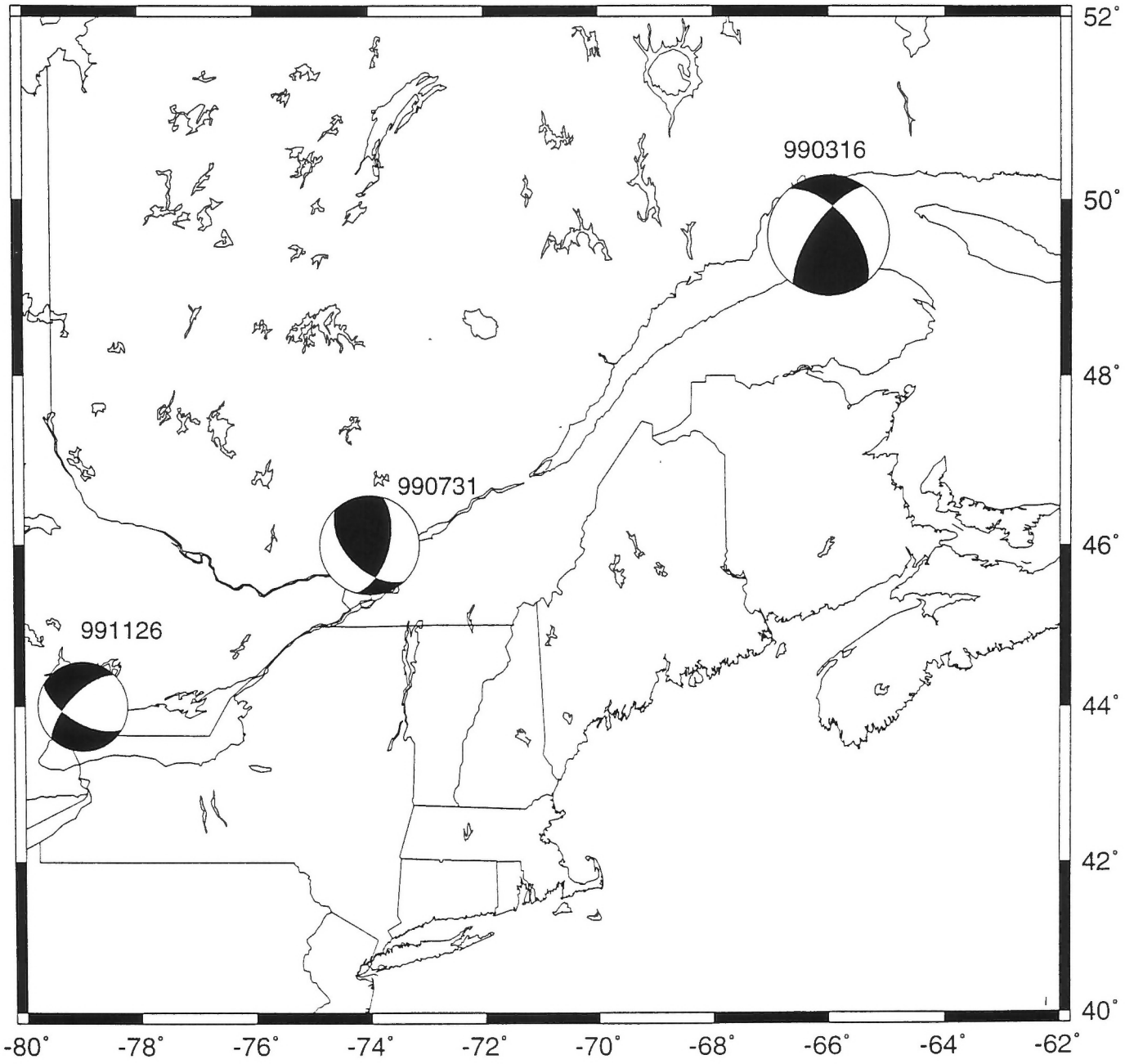
990316
990731
991126
52°
50°
48°
46°
44°
42°
40°
-80°
-78°
-76°
-74°
-72°
-70°
-68°
-66°
-64°
-62°

Figure 21

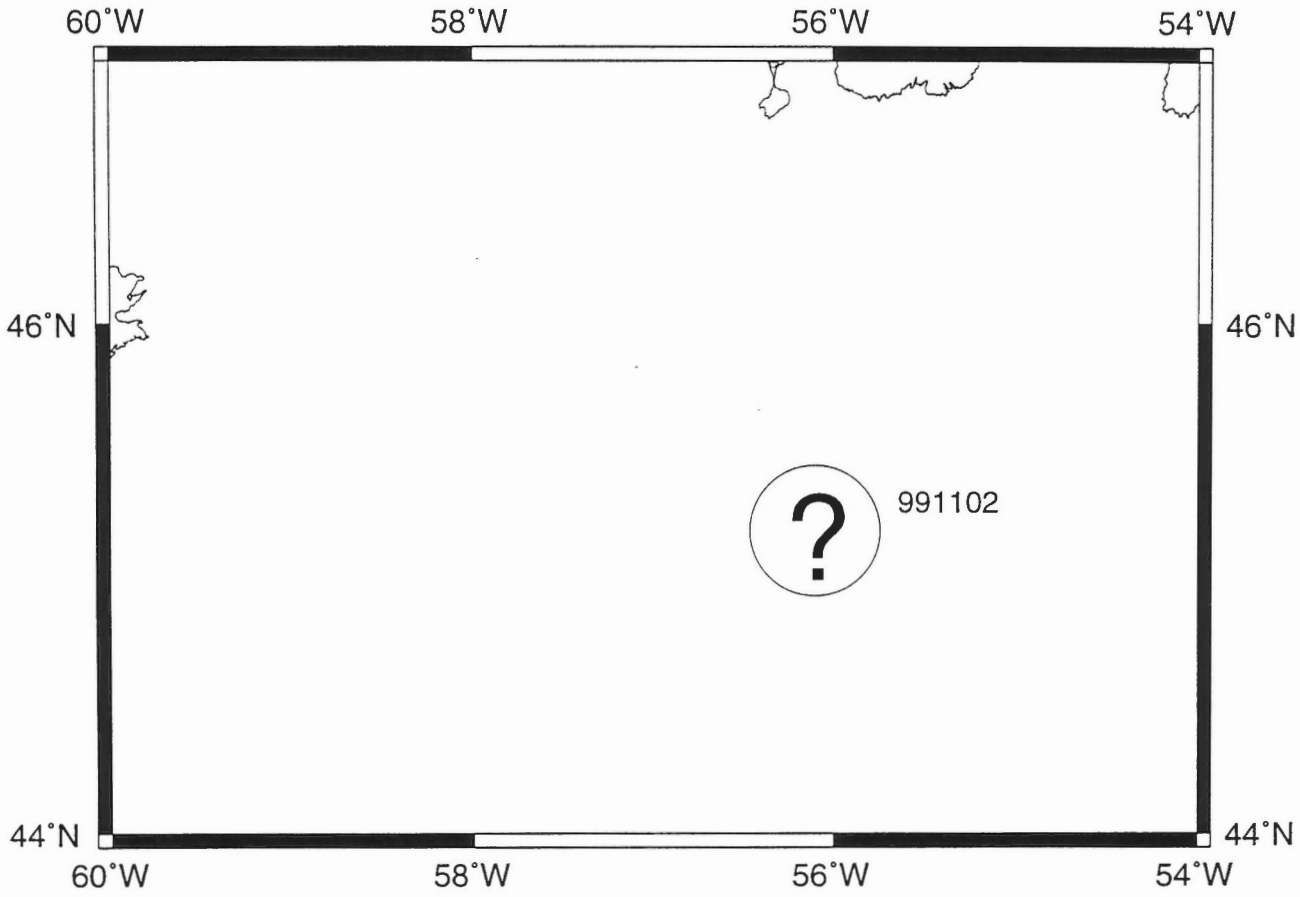

Figure 22

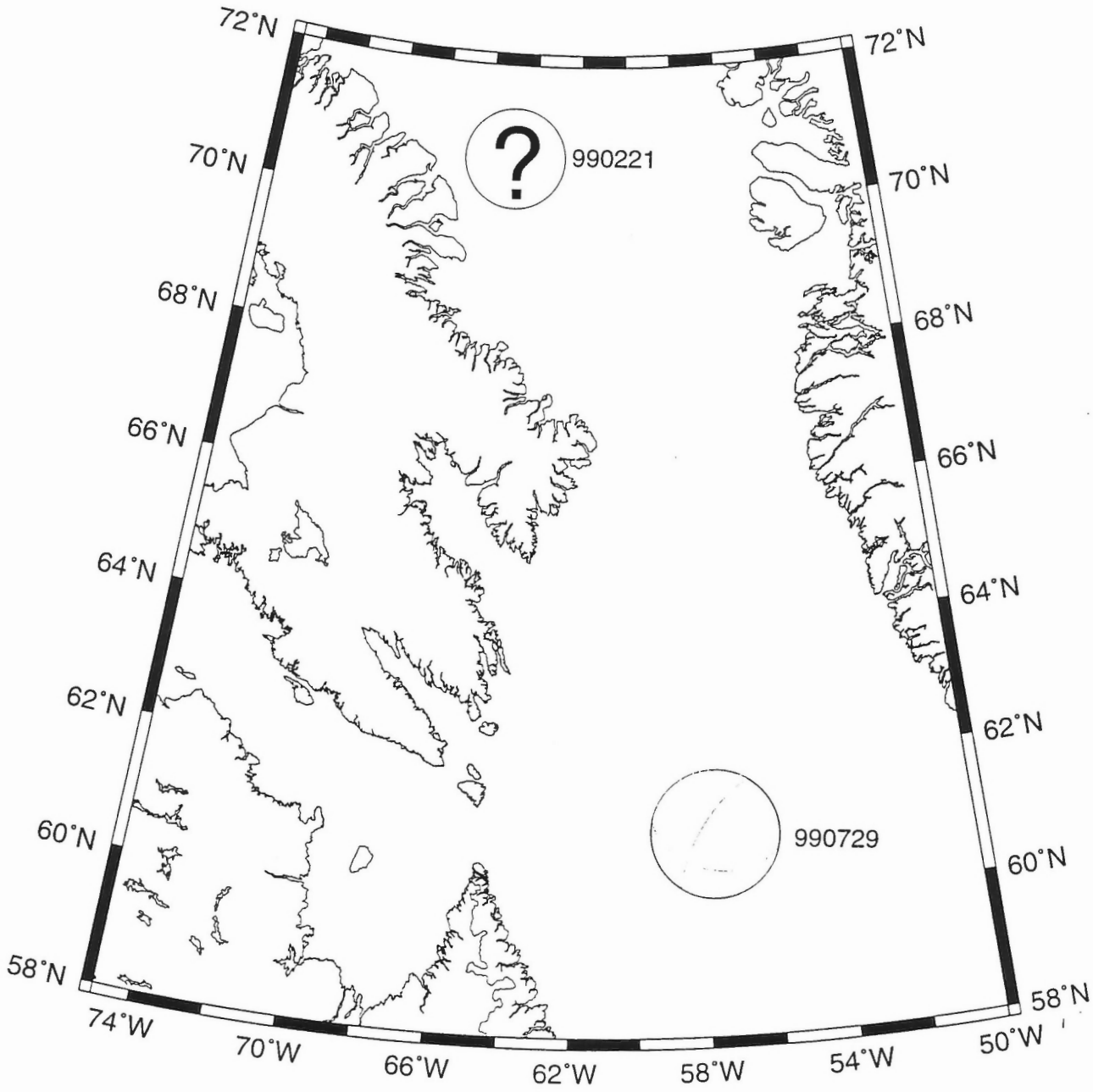
72°N
70°N
68°N
66°N
64°N
62°N
60°N
58°N
74°W
70°W
66°W
62°W
58°W
54°W
50°W
?
990221
990729

Figure 23

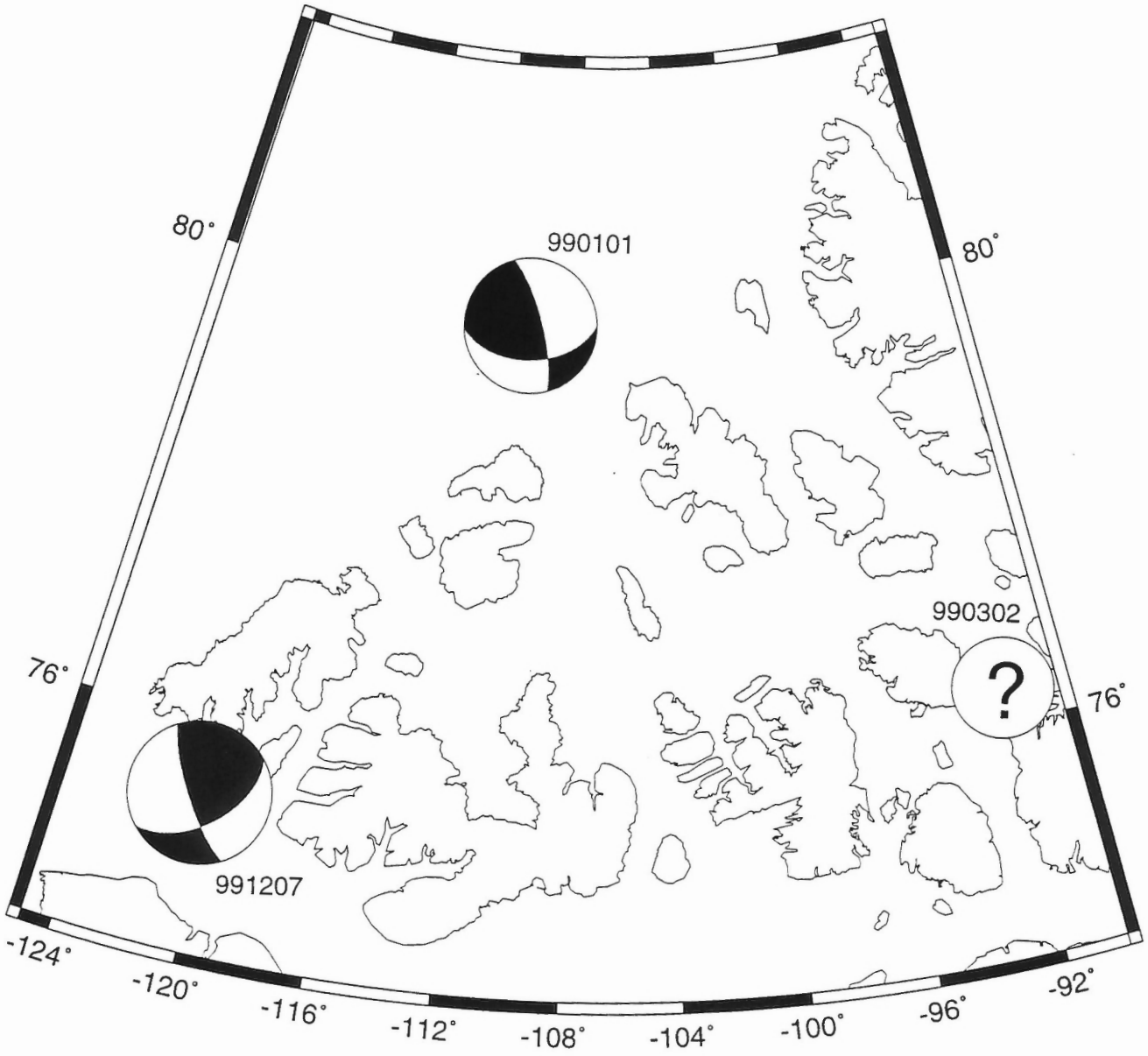
80°
80°
990101
990302
?
76°
76°
991207
-124°
-120°
-116°
-112°
-108°
-104°
-100°
-96°
-92°

Figure 24

CONCLUSIONS

We determined focal mechanism solutions from first motions for six of the nine earthquakes studied. The solutions are summarized in the Table. As was the case in previous such efforts, the events for which we could not obtain solutions occurred in offshore and northern regions where the azimuthal coverage of the CNSN and other seismograph networks is poor and station density is low. Alternate methods of focal mechanism determination, which may prove more useful than first motions in these regions, are under investigation. In contrast, in southeastern Canada both the azimuthal coverage and station density are better and we can obtain solutions for events of magnitude less than 4.0. Focal mechanisms determined in this study are consistent with those of many earlier studies in that we find evidence for primarily thrust faulting in the seismic zones adjacent to the St. Lawrence River, a mix of fault types in the Labrador Sea, and a significant component of strike-slip motion in the western Arctic.

ACKNOWLEDGMENTS

We thank our non-GSC colleagues who supplied us with waveforms and/or polarity information and John Adams for reviewing the manuscript. All maps in this paper were generated using GMT (Wessel and Smith, 1991).

TABLE
SUMMARY OF SOLUTIONS

	Plane 1				Plane 2				
Event	Strike(°)	Dip (°)	Rake (°)	Type*	Strike(°)	Dip (°)	Rake (°)	Type	Quality
990101	85	48	19	SS	343	76	137	OT	B
990221	??	>35	??	not N	??	>35	??	not N	N/A
990302	??	??	??	??	??	??	??	??	N/A
990316	320	58	26	SS	216	68	146	OT	B
990729	117	41	−12	SS	216	41	−130	ON	D
991031	95	79	44	OT	355	47	165	SS	B
991102	??	??	??	??	??	??	??	??	N/A
991126	120	61	−28	N	226	66	−147	ON	B
991207	149	77	38	OT	49	53	164	SS	B

* SS = strike-slip (rake within 30° of pure strike-slip)
T = thrust (rake within 30° of pure thrust)
N = normal (rake within 30° of pure normal)
O = oblique (rake more than 30° from end member; ON = oblique-normal; OT = oblique-thrust)

data (abstract), *Earthquake Notes*, **55 (3)**, 15.

Tapley, W. C. and J. E. Tull (1991). SAC- Seismic Analysis Code Revision 4, Lawrence Livermore National Laboratory, Livermore, California, non-paginated.

Wahlström, R. (1987). Focal mechanisms of earthquakes in southern Quebec, southeastern Ontario and northeastern New York with implications for regional seismotectonics and stress field characteristics, *Bull. Seism. Soc. Am.*, **77**, 891-924.

Wessel, P. and W. H. F. Smith (1991). Free software helps map and display data, *EOS Trans. Am. Geophys. U.*, **72**, 441, 445-446.